Investigation of correlations of precipitation electricity to different receivers

I. Esan Owolabi

INVESTIGATION OF CORRELATIONS OF PRECIPITATION ELECTRICITY TO DIFFERENT RECEIVERS.

by

I. Esan OWOLABI, B.Sc., Grad.Inst.P., F.R.Met.S.

Presented in Candidature for the Degree of Doctor of Philosophy, in the University of Durham.

September 1964

PREFACE

The rationalised M.K.S. system of units has been used throughout in this thesis. As much as possible, standard notations have been used to denote well-known parameters of Atmospheric Electricity, thus:

I (a/m^2 or $a.m^{-2}$) - Current density in amperes per square metre.

σ (C/m^2) - Surface charge density in Coulombs per square metre.

F (V/m) - Potential gradient in Volts per metre.

ϵ_o (Farads/m) - Permittivity of air, (8.854×10^{-12} Farads per metre).

v (m/s) - Wind velocity in metres per second.

m.a. - milliampere or 10^{-3} ampere.

K, M generally represent Kilohm (10^3 ohms) and Megohm (10^6 ohms) respectively, except where otherwise stated in the text.

μF - 10^6 Farad (micro-Farad).

$\mu\mu F$ (or pf) - 10^{-12} Farad (pico-Farad).

r_{xy} - Correlation Coefficient between parameters x and y.

$r_{xy.z}$ - Partial Correlation Coefficient between x and y for a constant value of a third parameter, z, on which x and/or y may depend.

For the graphs of Correlation Coefficient, r_{xy}, drawn against time-lag (or lead) between x and y, it is the lag (or lead) of x on y that is meant.

For the Computer Programme, the Hard-ware representation of Algol 60 on 5-channel tape for the Elliott 803 computer was used. Appropriate changes in the basic symbols and notations would be necessary for use in the 8-channel tape.

ABSTRACT

Measurements were made of the precipitation currents to two identical shielded receivers, constructed according to the design first suggested by Scrase (1938), the earth's electric potential gradient by the Field Mill method, wind speed (using a cup-generator type anemometer), and wind direction (using a rotary potentiometer). The two rain receivers, situated on the flat roof of the Physics building of the Durham University, could be separated horizontally to 30 metres.

Using an Elliott 803 digital computer, and by suitable programming, correlation coefficients between the two currents were calculated for various time lags between one current and the other, both when the receivers were placed side by side and when separated by 30 metres. The conclusion is reached that no significant difference could be obtained between the correlation coefficients calculated when the receivers were side by side and when they were at such a short distance apart, especially under continuous rainfall conditions.

Comparisons were, therefore, made between the precipitation current measured at the Laboratory and that measured 900 metres away. Significant correlation was obtained for instantaneous measurements of the currents when there was no wind, but when the wind was blowing roughly in the direction of the receivers, a definite time lag was found between similar variations of the currents.

By applying the same method of correlation-time lag analysis to the current, I, and the potential gradient, F, the author found

on one occasion, for sleet and snow, that a significant negative correlation existed between the two parameters for a time lag of about 40 seconds of the current on the potential gradient, consistent with the idea that the time of fall of precipitation particles should be considered when fitting the functional relationship $I = a(F + C)$; the discrepancy between the values of constants a and C for Summer and Winter results found by Ramsay (1959) could thus be resolved.

Some of the records, especially those of rain showers, did show that the space charge on the falling precipitation (as pointed out by Magono and Orikasa (1960)) is an important factor in the "Mirror-Image" phenomenon in low potential gradients.

The author's results indicate, also, that the melting process is a plausible mechanism of precipitation charging.

CONTENTS

CHAPTER I

GENERAL INTRODUCTION

1.1 Maintenance of the Earth's Electric Charge

The study of Atmospheric Electricity began early in the eighteenth century when Wall (1708) proposed that a spark and a lightning flash were identical, but this proposal could not be verified for some years because there were no instruments and methods of direct measurement. Later, Benjamin Franklin (1752), Richmann (1753), D'Alibard (1752), Lemonnier (1752) and others were able to show the electric nature of thunderstorm phenomena such as lightning and thunder, and developed the necessary apparatus for such studies.

The three basic elements in atmospheric electricity are, the potential gradient, air-earth current, and conductivity. In fair weather, an electric field exists which is directed from the electrosphere to the earth. The electrosphere - an atmospheric shell characterised by a high ion density, lying in a region of about 50-60 Km. above the earth - could be considered as one plate of a spherical condenser, possessing a net positive charge, and the earth's surface, the other plate of the condenser with a net negative charge. The electrosphere and the earth are both conductors and the charges on both are considered to be evenly distributed over their respective surfaces.

For simplicity, however, the surface of the earth is usually regarded as at zero potential, even though it does possess a surface charge. This is justified by the fact that it is the difference in potential rather than absolute values of potential that is of interest in the study of atmospheric electricity. Measuring potentials relative to the earth, it has been calculated that the potential of the electrosphere is approximately 3×10^5 volts.

As a result of the conductivity of the air, it was estimated that the whole charge would leak away in a period of about 10 minutes, resulting in the destruction of the potential difference between the electrosphere and the earth, unless there are some other sources of replenishment. It is believed that this potential is regenerated by thunderstorm activity all over the earth. It has been estimated that approximately 1800 thunderstorms are in progress at any one minute in different parts of the world, and that the total current in fine weather is about 1800 amperes, giving an average of 1 amp. per storm. These storms carry positive charges back to the electrosphere to compensate for the leakage and thus maintain the potential fairly constant. This process of leakage current and compensation by thunderstorms constitute the world-wide atmospheric electric pattern. Superimposed on this pattern are local disturbances which result from man-made charges, air-pollution, fog, and precipitation; and these local influences make it difficult to determine the undisturbed or uninfluenced nature of the three basic atmospheric electric elements.

1.2 Theories of charge Generation and Separation in Thunderclouds

Several theories have been put forward to account for the generation of charge in thunderclouds. An early theory is that of Simpson (1909), who considered charge to be generated by the breaking ofwater drops. A number of workers, including Simpson, found that when water splashes or is broken up by air currents, the larger portion carries a positive charge and there are produced negative ions in the air. This theory was later abandoned since it gave the wrong polarity to the thundercloud.

Another theory put forward by Elster and Geitel (1885), and Wilson (1929) is that of polarization of a water drop falling in an electric field. A polarized drop has, on its upper surface, a charge of sign opposite to the prevailing field and an opposite charge on the under side. It is therefore capable of selectively capturing ions from the surroundings, depending on the relative motions of the drop and the ions. A separation of charge thus results. An objection to this theory is that it depends on liquid drops, but this has been dispelled by the fact that dielectric polarization of ice crystals would work similarly. Another objection to this theory is that the process depends on ions whereas it is quite unlikely that there is sufficient rate of ion-production in the volume of a thundercloud to account for the measured charges and currents.

Workman and Reynold's theory (1949) is based on observations of charging when small supercooled water droplets impinge on a suspended hailstone. It was found that the droplet partly freezes and partly acquires a negative charge, whilst, the fragments of water splashing off carry positive charges. A difficulty of this theory is that the process would occur only when the temperature is close to $0^{o}C$ for the droplet to freeze only partially; at lower temperatures, there would be complete freezing.

Recently, Latham and Mason (1961) have found that when a supercooled droplet freezes suddenly by impact on a precipitation particle, it freezes first on the outside and then, when the inner liquid freezes, it bursts the skin and sends out splinters which carry away positive charge, leaving the residue on the precipitation particle carrying a negative charge.

The above theories are all based on the connection of electrification with precipitation, liquid or solid, and on gravitation as the agency of separation. To these Grenet (1947) and Moore and Vonnegut (1958) have raised objections. Moore and Vonnegut put forward the view that precipitation might result from the electrification and not the reverse, and gave accounts of experiments showing that high electric fields are built up as a result of the convective movements of the free charges in the atmosphere and that a pronounced increase in the probability of coalescence on collision of

neutral droplets in the presence of these fields occurs. They gave the observations of "warm" thunderstorms as an argument against the connection of electrification with the presence of ice. Several arguments against this theory have also been raised by other workers.

1.3 Origin of Charge on Rain Drops

Repeated attempts have been made to present theoretical explanations of the facts that rain drops from nimbo-stratus clouds carry, on the average, more of positive charges than negative ones, and vice versa when conditions are turbulent or stormy. However, there is still no unanimity of opinion on the basic questions of whether the charges on the drops are those which they have in the cloud or those established in the process of falling. As it has already been mentioned, most theories of charge separation are based on the different falling velocities of the precipitation and the cloud elements which have different weights and different charges and that the separation occurs in the manner that large size precipitation carries charges of one sign down and leaves charges of opposite sign up high.

Simpson (1949) found that when conditions in stormy weather are fairly steady, the rain current is proportional to the point-discharge current but of opposite sign, and that the ratio of the two charges, positive to negative, increases with the rate of rainfall and tends towards a limiting value for high rates of rainfall.

This he explained to be due to the raindrops acquiring the charge by capture of upward-moving ions produced by point-discharge at the earth's surface; the greater the point-discharge current, the greater the number of ions and so the more the charge acquired by the raindrops; the greater the rate of rainfall, the more, and the larger are the raindrops, so that again we get a greater rain current, but this has a limit when the rain can capture all the point-discharge ions. This qualitative picture, given by Simpson, has been worked more precisely by Chalmers (1951) and gives a reasonably good account of the charging of average drops during steady conditions. However, the picture does require that the potential gradient increases quite rapidly with height, but evidence for this is still lacking. Moreover, it is found that precipitation is charged even when the potential gradient is too small to give point-discharge. Wilson's theory gives charging to drops when ions of both signs are present, but calculations show that the observed charging is much greater than could be accounted for this way; since ions of both signs are present, there is no space charge as in the case of the point-discharge ions, therefore, no increase of the potential gradient with height. None of the attempts to explain these results has yet been satisfactory.

1.3.1 Effects of Splashing

Smith (1955), from his work on splashing of raindrops, concluded that the positive charge on rain, and the negative potential gradient might be accounted for by the separation of charge on splashing. This idea was first expressed by Lenard (1892) who found that the splashed drop acquired a positive charge whilst negative charge was released to the air. Adkins's (1959) work was also in support of this idea. This negative charge could move upwards in the air by turbulent diffusion resulting in a potential gradient of opposite sign to that of the drops. However, measurements made on single raindrop charges before the drop could have splashed (Hutchinson and Chalmers, 1951) show that this simple picture could not be true since raindrops were found usually to have positive charge before reaching the ground at all. Simpson (1915) did make the suggestion, though, that gusty winds near the ground, might cause impacts between drops, giving rise to positive charges on the raindrop and negative in the air. An objection to this view is the fact that drops of the size of raindrops are quite stable, and it is unlikely that gusts of wind near the ground would be strong enough to shatter them. Simpson (1942), later, abandoned this idea.

Evidence for the production of a negative space charge within a few metres above the ground had been shown by various workers (Kelvin, 1860; Chauveau, 1900; Collin and Raisbeck, 1962). Both Kelvin and Chauveau found occasions, during rain, when the potential gradient remained positive at the top of a tower but was negative at

the ground, indicating the existence of a negative space charge which might have been produced by splashing at the ground, or by some process such as the Electrode Effect in the lowest regions of the atmosphere.

1.3.2 The Inverse Relation and the Mirror-Image Effect

Among earlier workers, Elster and Geitel (1888), and Benndorf (1910), found that in many cases there was a definite inverse relation between the time variation of the rain current and that of the potential gradient. Ramsay and Chalmers (1959) have found a number of further instances, and have investigated any time intervals between the zeros. Simpson (1909) found a general excess of positive rain current and negative potential gradient. Scrase (1938), Chalmers and Little (1940), also noticed cases of long, continued, positive rain current and negative potential gradient.

There are two main ways of explaining this relation, and there is reason to believe that one is correct in case of high potential gradient, and the other for low values. First, we might consider that there is some process which gives a charge, usually positive, to the rain, the opposite charge remaining in the cloud or in the air below giving rise to the potential gradient at the ground of a sign opposite to that of the rain current. If conditions are reasonably steady, we may apply the principle of the quasi-static state, that is, even though actual charges do not remain static, yet under steady conditions, the flow of charges would be such that

the instantaneous pictures of the distribution of charge taken at different times would be the same. This interpretation leads to a current which is usually positive downwards at all levels. Secondly, Wilson's process of ion-capture, already explained, might be in operation. This process, however, presupposes the existence of point-discharge ions, that is, it could be operative only if the potential gradient is high enough to produce these ions.

In addition to this general inverse relation, many workers have observed that the potential gradient and precipitation current changed sign either simultaneously, or with a short time lag (Simpson, 1949; Sivaramakrishnan, 1961; Ogawa, 1960) sometimes the potential gradient leading the current, and sometimes vice versa. This is usually termed the Mirror-Image Effect; it is an instantaneous relation, whereas the inverse relation, is a statistical one.

Since a drop takes several minutes to fall from the cloud to earth, it would appear that the simultaneous nature of the changes of the potential gradient and rain current indicates that the drops acquire the charges close to the ground, unless, of course, as was explained by Chalmers (1957), the effect could be considered to be due to the motion, over the observer, of the cloud, the rain sheet, and the ions, all of which are moving with approximately the same horizontal velocity, presumably at the wind speed. The mirror-image effect could occur then whatever the height at which the drops acquire their charges. If the wind speed varies vertically, this would result in a time lag between the changes of the potential gradient and the

rain current. If the wind-speed is assumed to increase with height, this would lead to the maximum of the potential gradient coming before that of the rain current, since the latter would take some time to fall through the vertical distance. If the nature of the variation of the wind-speed with height is known, the average height of charge separation could be computed approximately from the terminal velocity of the raindrops.

The above argument disregards the effect of the space charge on the falling raindrops themselves. Magono and Orikasa (1961) have found that this effect could be important. The result of this would be that the maximum of rain current precedes that of the potential gradient.

1.4 Previous Measurements of Precipitation Electricity

Measurements have been made of the charges on individual raindrops by Gschwend (1922), Banerji and Lele (1932), Chalmers and Pasquill (1938), Gunn (1947, 1949, 1950), Hutchinson and Chalmers (1951), Smith (1955); and of the total current reaching an area, comprising of single drops (Scrase, 1938; Chalmers et al., 1959), this being measured either as an actual current or as the charge collected over a certain period of time, giving the mean current.

Most of these observers have made, in addition, simultaneous measurements of other relevant quantities such as the potential gradient, rate of rainfall, size of drops, and the point-discharge current when the potential gradient was sufficiently high. For

single drops, the size of each drop has been measured in a variety of ways. Some (e.g. Gschwend, 1922) measured the size of the strain produced by each drop on prepared paper. Others (e.g. Gunn, 1949) found the time for the drop to fall between two induction rings. For larger drops, Smith (1955) used the variation in the capacity of a parallel-plate condenser as a drop fell through. Arabadji (1959) measured the impulse of the fall of the drop on a piezo-electric crystal.

Results of measurements of these single-drop charges have been very striking in the sense that very wide divergence of values were obtained even for drops of the same size arriving at the same time (e.g. Smith, 1955). However, the differences in the drop charges could be regarded as only statistical, in view of the fact that two receivers, placed closed to one another and receiving rain currents over areas of the order of 10^{-2} m^2, show very nearly the same currents, as has been found by Chalmers et al. (1959) and by the present worker.

It does not appear that much measurements have been carried out of precipitation currents simultaneously at different places. Merry (1959) and Collin and Raisbeck (1962) took simultaneous measurements of rain current and potential gradient at the top and bottom of a 25 metre mast. They observed that the rain current at the top of the mast followed that at the bottom fairly closely but was greater in magnitude by a factor of about six (Merry), and an average of three to four (Collin and Raisbeck). The latter workers found that the

currents at the top and bottom of the mast were often of opposite sign, and the difference appeared to be related to the mirror-image effect which, they found, was much more pronounced for the upper current, where the time lag was rather negligible, than for the lower current where the time lags were often of several minutes. This suggests that the charge of the rain might be due in part to the local potential gradient. Laboratory experiments performed by these two workers indicated that this conventional type rain-current receiver could not be adequately shielded enough to prevent a large potential gradient, such as was encountered on top of the mast, reaching the receiver. With such a high value of Exposure Factor (explained later) of the top of the mast, about 50-100 (Collin, 1963), raindrops splashing at the edge of the conical shield of the receiver were indeed charged.

Similar measurements of rain currents and potential gradient had been made by Chalmers et al. (1959) simultaneously at two places of horizontal distance of some 30 metres apart. They found that minor fluctuations in rain currents to the two receivers were uncorrelated but larger variations appeared on both. The time resolution of their recording camera was insufficient for any certainty as to time intervals between the appearance of a charge at the two receivers.

1.5 Justification for the Choice of the Topic of Research

As it was explained in paragraph 1.3.2, the phase difference between the potential gradient and the rain current might well be due to the fact that the whole cloud system - rain, ions, etc., do move presumably with the wind. In that case, and if the wind speed is not uniform in a vertical direction, any two identical rain-current receivers, separated by a reasonable distance would be expected to collect rain whose charge would not be identical either in magnitude or sign, simultaneously.

A similar phenomenon had been investigated by Whitlock and Chalmers (1956) who found differences in the short-term variations of the potential gradient as measured by two field-mills, displaced 100 metres apart along the direction of the surface wind, and concluded that these variations were caused by the horizontal motion of wind-borne space charge contained within the first few hundred metres of the atmosphere.

The author proposed to continue further the earlier work done by Chalmers and others (1959), already referred to, of measuring rain currents at two places of variable distance apart, but also including a simultaneous record of the wind-speed and wind-direction. He also intended taking a simultaneous record of the potential gradient close to one of the receivers. He could therefore investigate whether the correlation, or otherwise, of the rain currents at the two places could in turn be correlated with the speed of the wind. With the aid of the potential gradient measurement, he could also investigate

17. OCT. 1994

SCRASE	1938	Electricity in rain. Geophys. Mem. Lond. 75.
SIMPSON	1909	On the electricity of rain and its origin in thunderstorms. Phil. Trans. A. 209.
SIMPSON	1915	The electricity of atmospheric precipitation. Phil. Mag. 30.
SIMPSON	1942	The electricity of cloud and rain. Quart. J. R. Met. Soc. 68.
SIMPSON	1949	Atmospheric Electricity during disturbed weather. Geophys. Mem. Lond. 84.
SIMPSON and SCRASE	1937	The distribution of electricity in thunderclouds. Proc. Roy. Soc. A. 161.
SIVARAMAKRISHNAN	1960	Indian J. Met. Geophys. 11.
SIVARAMAKRISHNAN	1961	The origin of electric charge carried by thunderstorm rain. Indian J. Met. Geophys. 12.
SMITH	1955	The electric charge of raindrops. Quart. J. R. Met. Soc. 81.
von KILINSKI	1900	Z. Met. 4.
WALL	1708	Phil. Trans. Roy. Soc. 26.
WHITLOCK and CHALMERS	1956	Short-period variations in the atmospheric electric potential gradient. Quart. J. R. Met. Soc. 82.
WILSON	1929	Some thundercloud problems. J. Franklin Inst. 208.
WILSON	1956	A theory of thundercloud electricity. Proc. Roy. Soc. A. 236.
WORKMAN and REYNOLDS	1949	Electrical activity as related to thunderstorm cell growth. Bull. Amer. Met. Soc. 30.

HUTCHINSON and CHALMERS	1951	The electric charges and masses of single raindrops. Quart.J.R.Met.Soc. 77.
KELVIN	1860	Atmospheric Electricity. Roy. Inst. Lect. and Pap. on Elect. and Mag.
LATHAM and MASON	1961	Electric charge transfer associated with temperature gradients in ice. Proc. Roy. Soc. A. 260.
LEMMONNIER	1752	Observations sur l'electricite de l'air. Mem. Acad. Sci. (2).
LENARD	1892	Uber der Elektrizitat der Wasserfalle. Ann. Phys. Lpz. 46.
MAGONO and ORIKASA	1960	On the surface electric field caused by the space charge of charged raindrops. Journ. Met. Soc. Japan, 38.
MAPLESON and WHITLOCK	1955	Apparatus for theaccurate and continuous measurement of the earth's electric field. J. Atmos. Terr. Phys. 7.
MATHEWS and MASON	1963	Electrification accompanying melting of ice and snow. Quart.J.R.Met.Soc. 89.
MERRY	1959	Durham M.Sc. Thesis.
MOORE, VONNEGUT and BOTKA	1958	Results of an experiment to determine initial precedence of organised electrification and precipitation in thunderstorms. Rev. Adv. in Atmos. Elect. pp. 331 - 360.
MORGAN	1960	Quart.J.R.Met.Soc. 86.
OGAWA	1960	Electricity in rain. Geomag. Geoelect. 1.
RAMSAY	1959	Durham, Ph.D. Thesis.
RANGS	1942	Gerat fur Messung der luftelektrischen Feldstrake. Z.W.B. No. 699. BHF ref. IIB/6022.

CHALMERS and LITTLE	1940	The electricity of continuous rain. Terr.Magn. Atmos.Elect. 45.
CHALMERS and LITTLE	1947	Currents of Atmospheric Electricity. Terr.Magn.Atmos.Elect. 52.
CHALMERS and PASQUILL	1938	The electric charges of single raindrops and snowflakes. Proc.Phys.Soc., London, 50.
CHAUVEAU	1900	Etudes de la variation de l'electricite Atmospherique. Annals de B.C.M. 5.
D'ALIBARD	1752	Letter to Acad. de Sci. (3).
DINES	1912	Advis. Comm. for Aeron. Reports and Mem. 47.
DINGER	1964	Quart.J.R.Met.Soc. 90.
DINGER and GUNN	1946	Electrical Effects associated with a change of state of water. Terr. Magn. Atmos. Elect. 51.
ELSTER and GEITEL	1888	Uber eine Methode die elektrische Natur der atmospharischen Niederschlage zu bestimmen. Met. Z. 5.
FRANKLIN	1752	Phil. Trans. 47.
GERDIEN	1903	Registrierungen der Niederschlagselektrizitat in Gottinger Geophysikalischen Institut. Phys. Z. 4.
GIBLETT	1932	M.O. Geophys. Mem. 54.
GROOM	1963	Durham M.Sc. Thesis.
GSCHWEND	1921	Besbachtungen uber die elektrischen Ladungen einzelner Regentropfen und Schneeflocken. Ib. Radiokt. 17.
GUNN	1947	The electrical charge on precipitation at various altitudes and its relation to thunderstorms. Phys. Rev. 71.
GUNN	1949	The free electrical charge on thunderstorm rain and its relation to droplet size. J. Geophys. Res. 54.
GUNN	1950	The free electrical charge on precipitation inside an active thunderstorm. J. Geophys. Res. 55.

REFERENCES

ADAMSON	1958	Durham Ph.D. Thesis
ADAMSON	1960	Quart.J.R.Met.Soc., 96.
ADKINS	1959	The small-ion concentration and space charge near the ground. Quart.J.R.Met.Soc., 85.
ARABADJI	1959	On the electrical attributes of storm precipitation (Russian) Akad. Nauk. SSSR 127.
BALDIT	1911	Sur les charges electriques de la pluie an Puy-en-Velay. C.R.Acad.Sci. Paris 152, 154.
BANERJI and LELE	1932	Electric charge on raindrops. Nature, 130.
BENNDORF	1910	Luftelektrische Beobachtungen an Graz. S.B. Akad.Wiss.Wien 119.
BEST	1935	M.O. Geophys.Mem. 24.
COLLIN	1962	Sign Discrimination in Field Mills. J. Atmos. Terr. Phys. 24.
COLLIN, RAISBECK and CHALMERS	1963	Measurements of Atmospheric electricity at the top and foot of a 25 m mast. J.Atmos.Terr.Phys. 25.
CHALMERS	1951	The origin of the electric charge on rain. Quart.J.R.Met.Soc. 77.
CHALMERS	1956	The vertical electric current during continuous rain and snow. J.Atmos.Terr.Phys. 9.
CHALMERS	1957	"Atmospheric Electricity", Pergamon Press.
CHALMERS	1959	Modern Theories of Nimbo-status clouds. "Recent Advances in Atmospheric Electricity" Pergamon Press.
CHALMERS et al.	1959	Research on the electricity of rain, U.S.A.F. report Contract No. AF 61 (514 -1072).

ACKNOWLEDGMENTS

The author is whole-heartedly indebted to Dr. J.A. Chalmers, M.A., Ph.D., F.Inst.P., Reader in Physics, the author's supervisor, for suggesting the topic of research; for his incessant guidance and help throughout the course of the research.

And to Professor G.D. Rochester, F.R.S., the Professor of Physics in the University of Durham, for research facilities made available; for his fatherly kindness and his interest in the author's work and well-being.

The author also expresses his gratitudes to all members of the Technical Staff, for their friendliness and readiness to help at all times; particularly to Messrs. Eric Lincoln (Electronics), Denis Jobling (Workshop), and Ron White (Photography); and also Mrs. Patricia Brooke, for the diligence and speed with which she typed this thesis.

And to all his research colleagues, for their friendly attitudes, help and encouragement which the author deeply appreciates; particularly to Mr. H.L. Collin, M.Sc., whose records at the Observatory were made available for comparison with the author's.

And to Dr. J. Hawgood, Ph.D., of the Department of Mathematics, for his help in programming.

Finally, the author registers his gratitudes to the University of Ibadan, Nigeria, for the award of Post-graduate research scholarship throughout the period of this research (October 1961 - September 1964).

I.E.O.

July, 1964.

MODE ..... An integer identifier used as code for data input.

Note: Data tape may be in two different forms:

(1) x_1,y_1; x_2,y_2; x_3,y_3; .... ; x_i,y_i; .... x_n,y_n.
(when MODE is negative)

(2) x_1, x_2, x_3, ..., x_i ...., x_n; y_1, y_2, y_3, ...,
y_i, ..., y_n.
(when MODE is positive). This allows the data to be punched on two separate tapes.

IDENTIFIERS

Parameters x(1:n), y(1:n).

SX ..... Sum of x

SQX ..... Sum of squares of x

SXY ..... Sum of cross-products of x and y

MX ..... Mean x

PX ..... ns_x

VXY ..... Variance ratio, s_x^2/s_y^2

VYX ..... Variance ratio, s_y^2/s_x^2

JXY ..... n^2.covariance (x,y)

RX ..... Regression coefficient, b_{yx}

RY ..... Regression coefficient, b_{xy}

CX ..... Constant a_{yx} in equation $y = a_{yx} + b_{yx}x$

CY ..... Constant a_{xy} in equation $x = a_{xy} + b_{xy}y$

R ..... Correlation coefficient, r

ASQX ..... Mean square relative error from regression equation $y = a_{yx} + b_{yx}x$ $= s_x(1-r^2)/ns_y^2(n-2)$

ECX ..... Error in a_{yx}

ECY ..... Error in a_{xy}

ERX ..... Error in b_{yx}

ERY ..... Error in b_{xy}

GMR ..... Geometric Mean of the slopes of the Regression lines (with respect to the y-x co-ordinate)

APPENDIX

PROGRAMME TO CALCULATE REGRESSION AND CORRELATION COEFFICIENTS BETWEEN TWO SETS OF NUMBERS, FOR VARIOUS LAGS BETWEEN THEM, USING ALGOL 60 ON FIVE-CHANNEL TAPE FOR THE ELLIOTT 803 COMPUTER

```
BEGIN REAL SX,SY,SQX,SQY,SXY,PX,PY,MX,MY,JXY,RX,RY,CX,CY,VXY,VYX,
          R,ASQX,ASQY,ECX,ECY,ERX,ERY,GMR'
      INTEGER N,M,L1,L2,L3,L4,MODE,LAG'
      READ N,L1,L2,L3,L4,MODE'
      WAIT'
    BEGIN ARRAY X,Y(1:N)'
      PROCEDURE SUMS(NMAX,S,T)'
                VALUE NMAX,S,T'
                INTEGER NMAX,S,T'
     BEGIN SX:=SY:=SQX:=SQY:=SXY:=0'
           FOR M:=1 STEP 1 UNTIL NMAX DO
BEGIN SX:=SX+X(M+S)'
      SY:=SY+Y(M+T)'
     SQX:=SQX+X(M+S)**2'
     SQY:=SQY+Y(M+T)**2'
     SXY:=SXY+X(M+S)*Y(M+T)'
           END'
             $
      MX:=SX/NMAX'
      MY:=SY/NMAX'
      PX:=SQRT(NMAX*SQX-SX**2)'
      PY:=SQRT(NMAX*SQY-SY**2)'
     VXY:=CHECKR((PX/PY)**2)'
     VYX:=CHECKR((PY/PX)**2)'
     JXY:=CHECKR((NMAX*SXY)-(SX*SY))'
      RX:=JXY/PX**2'
      RY:=JXY/PY**2'

      CX:=MY-RX*MX'
      CY:=MX-RY*MY'
       R:=JXY/(PX*PY)'
    ASQY:=CHECKR(VYX*(1-R**2)/(NMAX*(NMAX-2)))'
    ASQX:=CHECKR(VXY*(1-R**2)/(NMAX*(NMAX-2)))'
     ECX:=SQRT(SQX*ASQY)'
     ERX:=SQRT(NMAX*ASQY)'
     ECY:=SQRT(SQY*ASQX)'
     ERY:=SQRT(NMAX*ASQX)'
     GMR:=SQRT(RX/RY)'
           $

PRINT DIGITS(1),S, SAMELINE, T, ££S??, ALIGNED(3,3), MY, ££S??,
      MX, ££S??, CX, ££S??, ECX, ££S??, RX, ££S??, ERX, ££L2S5??,
      CY, ££S??, ECY, ££S??, RY, ££S??, ERY, ££S??, PX/NMAX,
      ££S??, PY/NMAX, ££S??, R, ££L2S23??, GMR, ££L2??'
           END OF SUMS'
      FOR M:=1 STEP 1 UNTIL N DO
           BEGIN READ Y(M)'
      IF MODE LESS 0 THEN READ X(M)'
           END'
      IF MODE GR 0 THEN BEGIN WAIT'
      FOR M:=1 STEP 1 UNTIL N DO
      READ X(M)'
           END'
PRINT 2
 S T     MY        MX        CX        ECX        RX        ERX

         CY        ECY       RY        ERY        STX       STY       R

                             GMR
?'
   FOR LAG:=L1 STEP 1 UNTIL L2 DO
      SUMS(N-LAG,LAG,0)'
   FOR LAG:=L3 STEP 1 UNTIL L4 DO
         SUMS(N-LAG,0,LAG)'
              END OF BLOCK'
                 END OF PROGRAMME'
```

and winter results, it would be advisable if the heights of the freezing levels, and the terminal velocities of the precipitation particles are taken into consideration. A method of determining these levels uniquely would be necessary, instead of inferring them from records of nearby stations. The terminal velocity could, of course, be determined merely by keeping a record of the rate of precipitation fall.

Better methods of calculating the exposure factor of the instrument to measure the potential gradient should be devised. The orthodox method of comparison of the fair-weather records at two different places may be erroneous, especially if the criterion of the fairness of the weather is by 'eye-judgement' and the assumption of the non-existence of pockets of space-charge is made.

to the two receivers at 900 metres apart occurred for simultaneous readings of the currents; equally good correlations also occurred for various time-lags between them, but no wind effect as for the snow record was found. Of course, the surface wind speed was very small indeed - mostly less than 1 m/s. The height of freezing level for the four stations mentioned above was everywhere higher than the height of the base of cloud, so that if charging had taken place as a result of the melting process, the height would have been high enough for a fair-size cloud to cover the two places where measurements of currents were being taken, resulting in a good correlation being found between the currents.

8.5 Suggestions for future work.

The number of records analysed in this thesis is not adequate enough to establish conclusively that the melting process is the major mechanism of precipitation charging. It would be worthwhile if more work could be done with the express purpose of establishing this proposition. There would, therefore, be experimental evidence, under natural conditions, to resolve the disagreements between the laboratory experimental results of Dinger and Gunn on the one hand, and Mathews and Mason on the other.

More care should be taken in the analysis of future records which set out to establish the functional relationship between current and potential gradient. Morgan's correction for fitting regression equations is highly recommended. And, to compare summer

8.4 The Melting process as a possible mechanism of precipitation charging

The records analysed quantitatively in this thesis all pointed to the possibility that the charging mechanism of the precipitation was more likely to be due to the melting process. These results are few, however, hence this proposition was not proved conclusively. Other mechanisms, such as splashing, might as well be contributory factors. The record for sleet gave the result that the level of charging was about 250 metres above the ground level, and this coincided roughly with the freezing level recorded by the British Meteorological Office for the four stations (where upper air measurements were made) nearest to Durham. This freezing level was below the base of the lowest cloud in each of the stations. The result for snow suggested that charging must have taken place close to the ground. This conclusion was drawn from the fact that a good correlation was found between the currents to two receivers displaced 900 metres apart when a time-lag of 7 minutes was allowed of the receiver in the down-wind direction on that up-wind. The charge-speed was found to be about the same as the measured surface wind. Since the variation of the wind speed with height follows a power law, the charge speed would be expected to be larger than the surface wind speed if charging had taken place high up. Since the surface air temperature was everywhere above zero, it would be expected that melting of the snow would occur on getting near the surface level. For the continuous rainfall, a good correlation between the currents

above quoted passage had been used synonymously with the 'Inverse relation' and 'potential gradient' respectively. The Mirror-Image effect is an instantaneous one, whereby both the current and potential gradient change signs in opposite senses as if one is a mirror-image of the other, whereas the inverse relation is a phenomenon taking place over a much longer period of time; it is, in fact, a statistical effect.

In the present work, the sign changes of both the current and the potential gradient had not been found to be 'simultaneous' as most earlier workershad reported. The time-lags of one on the other were of varying values - of the order of minutes for the summer results and of seconds in winter. A precipitation particle which gets charged at a height of 250 metres, say, having a terminal velocity of, say, 5 m/s, will take 50 secs. to reach the ground. A time-lag of this magnitude could be easily measured by the author's measuring device where 50 secs. corresponded to about 6 cm of recording chart. In most of earlier workers' records, 50 secs. time-difference might be regarded as simultaneous. However, in many of the author's records, moments of sign changes of currents could not be located precisely because sometimes the current had both positive and negative excursions, though small, about the zero line prior to the incidence of change of sign.

Although the linear equation, $I = a(F + C)$, is the easiest that could be assumed for the relation between I and F, Ramsay's work, supported by the author's own work, did suggest that a 'parabolic' sort of equation would fit the relation better. For rain, Ramsay found that the points lie above the I/F line for all positive and for high negative potential gradients and below for low negative values. For snow, the present worker found the 'parabolic' effect to be of opposite sense, i.e., the points were found to lie below the I/F line for positive current, high negative potential gradient and above for low negative values.

8.3 The Inverse relation and the Mirror-Image Effect

In most of the author's records, the inverse relation between the precipitation current and potential gradient was evident, most especially for continuous precipitation. The results for rain and snow showers did show the same phenomenon, but to a lesser degree; some records were obtained where at the onset of a shower, the precipitation current was of the same sign as the potential gradient. This is in accordance with the theory given by Magono and Orikasa (1960). As a conclusion to their calculations, Magono and Orikasa wrote, "as a rule, the 'Mirror-Image relation' holds in steady rainfall, but when rainfall begins or increases rapidly, a positive space charge due to raindrops brings temporarily a sharp positive field even under the condition of the existence of positive raindrops." The 'Mirror-Image relation' and the word 'field' in the

When a time-lag of 40 seconds was allowed of I on F, a much better I/F scatter diagram was obtained. This gave a narrower range for C, this being between -170 V/m and -340 V/m. The straight line of best fit gave C = -220 V/m, to be compared with Ramsay's result for sleet of -124 V/m. It is not claimed that the author's values were absolutely accurate, since the method of calibration of the field mill was ineffective; nonetheless, this method of analysis does indicate the essence of determining whether the negative correlation between the instantaneous values of I and F is significant enough to justify fitting the linear functional relationship. If the instantaneous values are not strongly correlated, then suitable values of time-lags, consistent with the time that would be required for the precipitation to fall from the charging level to the ground, would need be allowed for. These time-lags would be different for Summer and Winter results since, in general, Summer clouds are much higher than Winter ones. The value of the appropriate time-lag can be determined, as was done by the author, by calculating the correlation coefficients over and over again, each time allowing for a different time-lag, until such time as a maximum value of the coefficient is obtained. This is an easy task if a computer is available. Failing this, a rough method would be to estimate the height of the cloud, or the freezing level, and work out this time-lag from the knowledge of the terminal velocity of the precipitation under consideration.

zero, though by a few degrees. Other mechanisms, such as splashing, could not be ruled out, however.

8.2 The I/F relationship: Discrepancy between Summer and Winter results

What the present work has succeeded to establish is the fact that the discrepancy between the values of the constants a and C of the relationship

$$I = a(F + C)$$

between precipitation current and the potential gradient, obtained by an earlier worker (Ramsay, 1959) for the Summer and Winter results, was not unexpected because of the inadequate method of analysis of his results. The author found, from the results for sleet and snow, that the scatter diagram between the instantaneous values of the current, I, and the potential gradient, F, gave very much scattered points resulting in a very large margin of error in the estimation of the values of a and C. Since both I and F measurements were subject to errors, it is grossly inadequate to determine a and C from the regression line of I on F only. The regression of F on I should also be performed and the straight line of best fit should lie, according to Morgan (1960), between these two regression lines. For instance, the regression line of I on F gave C = -500 V/m whilst the regression line of F on I gave C = 120 V/m for the instantaneous values of I and F for this sleet record.

Much poorer correlation should be expected if the cloud had been otherwise localised. Over a period of one hour, therefore, a good correlation existed between the currents, but shorter time variations, of about fifteen minutes duration, could hardly be correlated.

The second record, of five hours duration, was of snow associated with a belt of low pressure moving across the whole of the British Isles. Only two hours of the five-hour records gave steady values suitable for analysis. It was fairly windy on this occasion, the wind blowing from the South-East direction, whilst the receivers were in the East-West direction. For the two-hour period, averaging the currents over one-minute intervals, the correlation coefficient between the two currents was 0.43. When a time-lag of 7 minutes was allowed for the Observatory record, in the down-wind direction, on that at the Laboratory (up-wind), a better correlation of 0.62 was obtained. Both these values are significant to 0.5%, and give a picture that portions of the precipitation cloud did move across the receivers, superimposed upon a 'background' cloud whose effect was everywhere the same. Calculation of the charge speed, from the knowledge of the distance of separation of the receivers (900 metres), and assuming the cloud to move along the direction of the surface wind, gave the speed to be, within limits of experimental errors, the same as the measured mean value of the surface wind. Thus, the charging process must have taken place quite close to the ground on this occasion. The melting process is a plausible mechanism since the precipitation was of snow but the surface temperature was above

correlation coefficients of 0.57, 0.39, 0.39 when the receivers were 30 metres apart. These values were insignificant statistically. Another record, typical of showers, analysed for a six-minute shower gave a value of correlation coefficient of 0.46, averaging over 5-sec. intervals. This is statistically significant, but much poorer than for continuous rainfall. Conclusion is therefore reached that 30 metres separation is rather too short a distance to displace the receivers in order to detect a break-down of the correlation between the currents.

Attempts were therefore made to correlate the records taken at the Laboratory with other records, taken by a colleague of the author, some 900 metres away. Two interesting records were analysed quantitatively, the others being unsuitable for such analysis because of the rapid variations of the parameters. The first one was an hour's recording of continuous rainfall current. There was hardly any wind - mostly below the limit of measurement (1 m/s). Even for such a distance, and averaging over $\frac{1}{2}$-minute intervals for the whole hour period, a correlation of 0.69 was found for the two currents. Dividing the record into four $\frac{1}{4}$-hour sections gave values of 0.08, 0.58, 0.00, 0.55 respectively. The second and fourth values above are, statistically, not as significant as the values might suggest because of the small numbers of pairs of values involved in the calculation. Such a good correlation as was found here could only be expected if the two places of measurements were under the same massive wind-spread cloud, giving similarly charged precipitation.

CHAPTER VIII

CONCLUSIONS

8.1 Correlations of Precipitation Electricity to Different Receivers displaced horizontally apart

For most of the recordings made throughout the period of this investigation, the two receivers constructed by the author were either stood side by side or displaced by about 30 metres apart. Cursory inspection of the records for periods of time of about 5 mins. or more, showed that when the receivers were placed side by side, there was a strong correlation between the currents received by them for all types of precipitation - continuous rainfall, snow, rain- or snow-showers. When the receivers were displaced 30 metres, good correlation still existed between the currents, this being stronger for continuous rainfall than for showers. Short-time variations of the order of seconds were usually not correlated, however. This was because the speed of recording (7.5 cm of recording chart per minute) was high enough to make the effects of single drops or of small numbers of drops noticeable. Most of these records were not subjected to quantitative analysis, but a typical record, taken with the receivers close together, and later on separated by about 30 metres, during a continuous rainfall, gave values of correlation coefficients of 0.90 and 0.84 respectively when averaged at 10-sec. time intervals for a period of 10 minutes. Taking 5-sec. averages of three 2-minute sections of the same record gave values of

The graphs shown in Fig. 43 illustrate the sort of correlations between the potential gradients at the laboratory and those measured at the research hut and the observatory respectively, allowing for various time lags between them. The negative correlations found between the observatory and laboratory records (900 m apart), even if statistically significant, are of no physical meaning, and may be put down to the very local effects at the places of measurements.

Other records taken on 31st January 1964, are shown in Fig. 44 which is the graph of the actual half-hour records of the potential gradients again at the laboratory and observatory. Fig. 45 is also the correlation coefficient - time lag graph. This record was taken on a day visually similar to that of 21st January. A good correlation was found between the two potential gradients on this day, however, and so it was decided to determine the exposure factor of the laboratory field-mill from this pair of records. The straight line of best fit of the scatter diagram was drawn, taking the errors in both quantities into consideration, as usual. The exposure factor was deduced from this line, and was found to be 2.5.

31.1.64. Correlation coefficients between fine-weather potential gradients measured at the Laboratory and Observatory against time-lag (and lead) of the former on the latter.

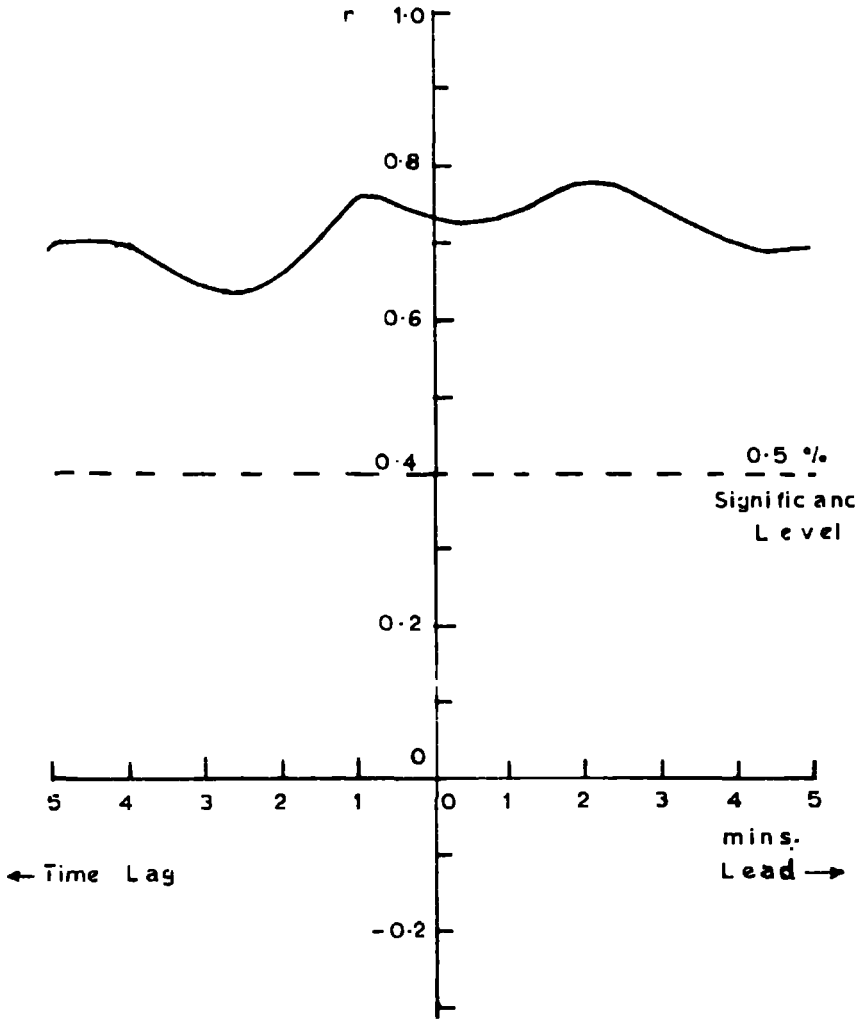

Fig.45.

Fine-weather records of Potential Gradients at two places 900m apart

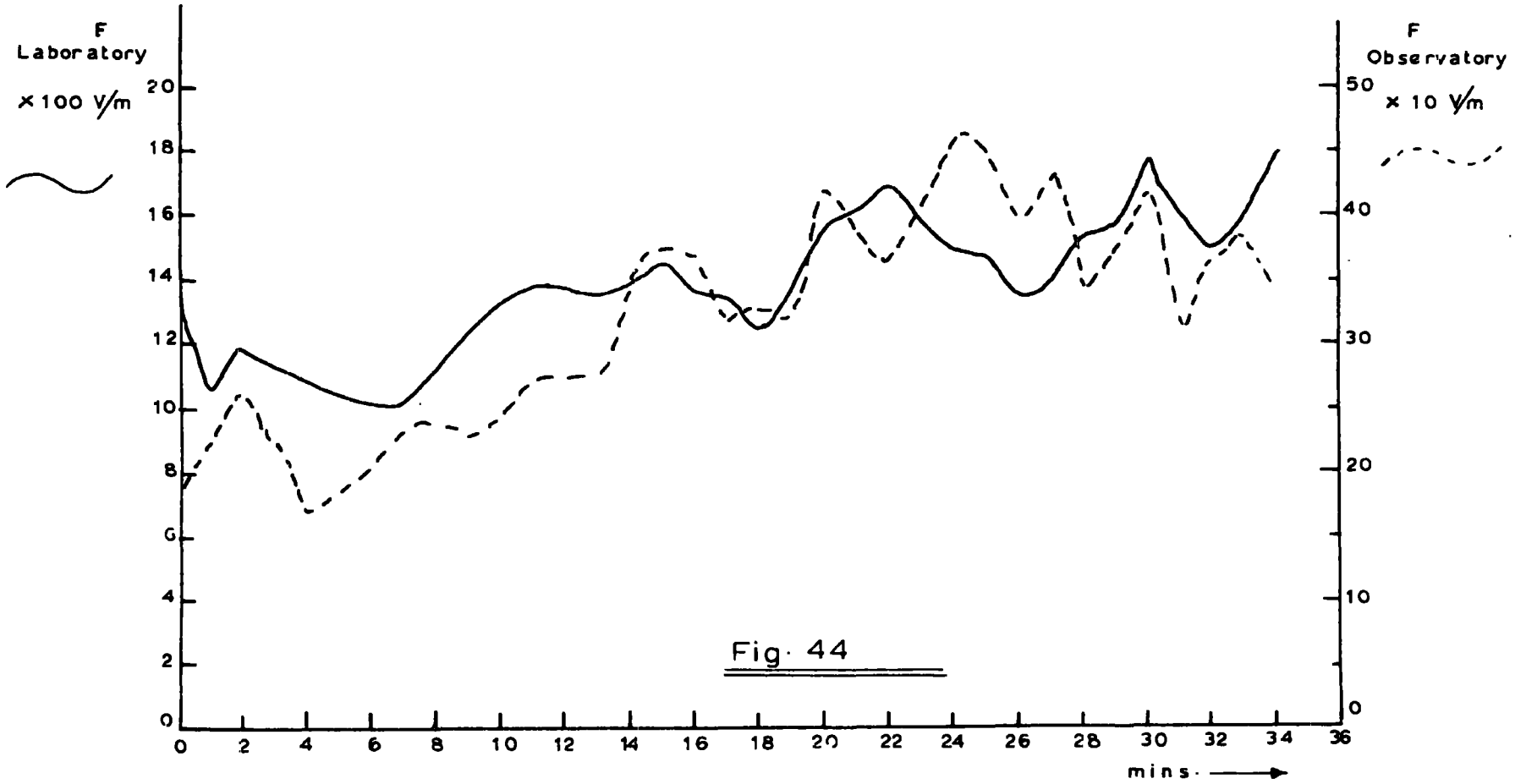

Fig. 44

7.2 The Exposure Factor of the Field Mill

In paragraph 3.3, it was stated that the exposure factor of the field mill was determined by comparing two records taken at 900 m apart on a day when the weather was such that the potential gradient could be assumed to be the same at both places. The criterion was merely by visual observation, and deciding whether the sky was cloudless and fair enough for the records to be taken. The actual results recorded indicated to what extent this judgement could be erroneous. A record taken on 21st January, 1964, showed that there was no correlation between the two potential gradients. A third record of the potential gradient was taken simultaneously at the research hut about 80 metres East of the laboratory, by another worker. These latter two records showed strong correlation. A correlation coefficient of 0.80 was obtained for the simultaneous readings of the two records, as against a value of -0.07 between the records at the observatory and the laboratory, Fig. 43.

There was a higher correlation coefficient, 0.91, between the former pair, if there was a time lag of two minutes between them, indicating that some space charges in motion, of a speed somewhat less than 1 m/s, contributed to the potential gradient variations. This is consistent with Whitlock and Chalmers' (1956) results already referred to. The records of the wind speed and wind-direction taken on this occasion showed that the surface wind velocity in the direction of the field-mills was indeed less than 1 m/s.

21.1.54. Correlation coefficients between potential gradients measured at (a) the Laboratory and (b) at the Research Hut (I), (c) at the Observatory (II), against time-lags (or leads) of r (a) on (b) and (c).

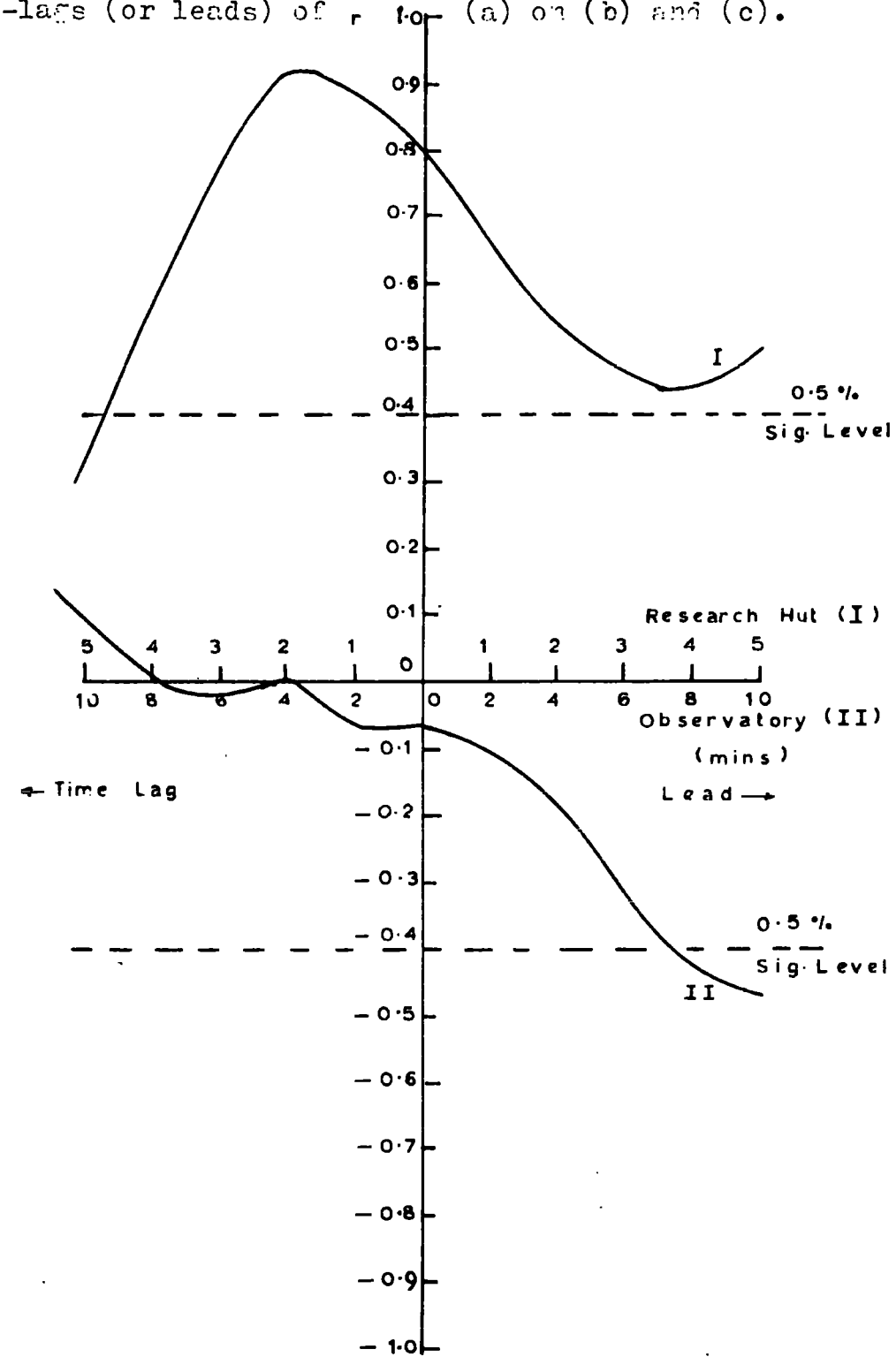

Fig. 43.

The potential gradient, F, was measured by the field mill, close to the receiver. This value, as already explained, was not the same as the atmospheric potential gradient, since the site had its own exposure factor, which does not come into the present calculation. What is being calculated is the factor by which the receiver cuts down the surrounding potential gradient.

The mean value of e_r was determined from the record by calculating

$$e_r = i_d/(\epsilon_o \Delta F/\Delta t) \qquad \text{..... } 7.3$$

where ΔF is the change in the potential gradient during time, Δt, of the order of 5 secs. This value was found to be

$1/e_r = 26 \pm 3$, and 25 ± 3, for the first and second receivers respectively. These values are in fair agreement with Scrase's value of 30. It would be recalled that the author's two receivers were constructed in accordance with the specifications of Scrase's (1938) model. The error in this measurement is not unexpected, because of the contribution of the conduction current which had been neglected. Moreover, the potential gradient record was not sensitive enough to make an accurate estimate of the small changes occurring within a 5-sec. time interval possible. Taking longer time intervals would further vitiate the accuracy especially if the potential gradient was changing rapidly.

At first, the phenomenon proved elusive because the V.R.E. was switched, most of the time, to the 10^{10} ohm range, this being the most favourable input resistor for precipitation currents, and the displacement current appeared merely as 'bumps' on the record trace.

Some records of this displacement current, using the 10^{12} ohm input resistor, as well as simultaneous records of the potential gradient were taken, under non-raining cumulus clouds. There was a striking similarity between the two traces. The sign of the current depended not on the sign of the potential gradient, but on the sign of the potential gradient changes. This was expected, since the displacement current, i_d, is given by

$$i_d = \epsilon_o dF/dt \qquad \ldots\ldots 7.1$$

where dF/dt is the rate of change of the potential gradient and ϵ_o ($=8.854 \times 10^{-12}$ Farads/metre) is the permittivity of the air.

However, the value of the potential gradient, inside the receiver, giving rise to the measured current, was not the same as the value of the potential gradient outside the receiver because of the shielding. Hence, i_d can appropriately be expressed as

$$i_d = \epsilon_o e_r dF/dt \qquad \ldots\ldots 7.2$$

where e_r is the "exposure factor" of the receiver. Since e_r is essentially less than unity, however, it is perhaps better to refer to $1/e_r$ as the "shielding factor" of the receiver.

CHAPTER VII

AUXILIARY WORK

7.1 Displacement Current - The Shielding Factor of the Receivers

It has been explained that the major argument in favour of using a shielded receiver in the measurement of precipitation current is the factthat the interfering effects of conduction and displacement currents are cut down to a minimum. These effects are by no means completely eliminated, however, especially under conditions of high potential gradients and rapid potential gradient changes. The work of Raisbeck and Collin (1962) on the measurement of rain currents at the top and bottom of a 25-metre mast gave a serious pointer to the unreliability of the shielded receiver when the ambient potential gradient is high. They found that the magnitude of the current at the top of the mast was about 3 to 4 times that at the bottom, and concluded that this might have been due to the fact that the potential gradient at the top of the mast was magnified by a factor - the exposure factor of the mast, of about 100. Kirkman (1956) found the exposure factor of a mast of this type to be about 125.

Under fair weather conditions, with cumulus clouds drifting across the receivers, giving rise to varying potential gradients, the author found that by using the 10^{12} ohm input resistor of the V.R.E., appreciable deflections occurred on the recording chart.

One other factor that needs to be considered is the effect of the wind. Most frequently, it would be expected that the wind speed would increase with height, so that the potential gradient maximum would occur before the current maximum. The two maxima are in anti-phase, of course, due to the general inverse relation between current and potential gradient. This effect would be enhanced if, with the type of shielded receivers used in precipitation charge measurements, small drops are blown across the receiver rather than inside. Smith (1955) found that the smallest drops did carry charges opposite in sign to the potential gradient, whilst the larger ones carry charges of the same sign. Most of the results in light rain, obtained by the author, were under conditions of very little or no winds. Where the wind-speed was not below the lower limit of measurement (1 m/s), no correlation was found between the magnitude of the current measured and the wind-speed.

For a light rain, however, say, R = 2 mm/hr, τ = 28 mins., indicating clearly that the splashing effect on the rate of change of the existing potential gradient is very slight.

If the space charge on the falling precipitation is to be taken into consideration, then a third term, which is a function of the charge density ρ, the height, h, from which charging takes place and the terminal velocity, v, or the rate of rainfall, R, should be included in equation 6.9. Hence, equation 6.9 may be written as

$$dE/dt = dX/dt - 0.015R^{1.29} - f(\rho, h, R) \quad \ldots\ldots \text{6.11}$$

For light rainfall, the third term on the R.H.S. willbe more important than the second term, and whether or not the potential gradient on the ground changes sign before, after, or simultaneously with the change of sign of the current would depend on h and R.

The present worker has not got sufficient data to be able to give a quantitative expression for the function, f, introduced into equation 6.11. This would involve keeping a good record on the various phase lags between the current and potential gradient, as well as a simultaneous record of the rate of rainfall. The only thing evident throughout the period of the author's work was that frequent sign changes of current and potential gradient occurred as the rainfall became heavier, and this, as already mentioned, might, in addition, be due to splashing.

were 0.72 and 0.79 respectively. This is consistent with the idea that portions of the cloud do move across the receivers with the wind-speed. Thus the relative effects of vertical as well as horizontal displacements of charges are demonstrated. As might be expected, the correlation between the potential gradients were better than that between the currents.

From Fig. 34b, it could be seen that the slope of the straight line of best fit is 0.7, again suggesting that the value of the current measured at the laboratory was about $\frac{3}{4}$ that on top of the mast, the same as was found for steady rainfall.

6.6 The Mirror-Image Effect

In discussing the mirror-image effect, it sounds reasonable to bring in terms depending on splashing effects as well as the space charge on the precipitation in order to investigate qualitatively the phase relations between current and potential gradient.

In heavy rain, the current due to splashing becomes large, and the consequent rate of change of the potential gradient, dE/dt, near the ground has been expressed by Adkins (1959) as

$$dE/dt = dX/dt - 0.015R^{1.23} \text{ E V.m.}^{-1} \text{ min}^{-1} \quad \ldots\ldots 6.9$$

where dX/dt is the rate of change of the free potential gradient. Any potential gradient will therefore be reduced towards zero with a time constant

$$\tau = 66.7R^{-1.23} \text{ minutes} \quad \ldots\ldots 6.10$$

If R = 10 mm/hr, τ = 4 mins., and

if R = 15 mm/hr, typical of a heavy shower, τ = 2.5 mins.

space charge. The potential gradient caused by the positive raindrops would first increase rapidly, then become steady after the first arrival of raindrops whilst that caused by the negative space charge would fall rapidly at first but gradually reach steady values also. The resultant picture would be that at the approach of rain, the potential gradient would increase rapidly and decrease exponentially towards steady values. Figs. 21, 22, taken during periods of short showers seem to justify this claim.

The effect of the wind was neglected in the argument above. This would affect both the downward velocity of the falling precipitation as well as the rate of dispersal of the ionic space charges. Thus, the overall behaviour of the potential gradient at the ground would be a combination of the vertical as well as horizontal displacements of the charges above the measuring instrument.

The correlation coefficients between the current measured at the laboratory and those at the bottom and top of the mast, on 19th March, 1964, for instantaneous readings of these, were 0.42, 0.43 (Figs. 33, 34a). The corresponding values for the potential gradients were 0.37, 0.39 respectively. These values were significant to 0.5%, considering the number of pairs of values compared. This might be due to the fact that the snow cloud was widespread such that the receivers were under the same mass of precipitating cloud. Allowing a time lag of about 7 minutes of the readings on the mast on those at the laboratory, the correlation coefficients were again 0.52, 0.62 respectively, Fig. 34b. The corresponding values for the potential gradients

$$= 2\rho \int_{H_1}^{H_2} h\,dh \int_{0}^{2\pi} d\theta \int_{0}^{R} r\,dr/(h^2 + r^2)^{3/2} \quad \ldots\ldots 6.6$$

where H_2, H_1 are the heights of the top and bottom of the cylindrical space charge respectively, R is the radius of the cylindrical space, and θ is the azimuthal angle around the axis of the cylinder.

Integrating equation 6.6 gives

$$F = 4\pi\rho(H_2 - H_1 + (H_1^2 + R^2)^{\frac{1}{2}} - (H_2^2 + R^2)^{\frac{1}{2}}) \quad \ldots\ldots 6.7$$

When the charge separation takes place, both the positive space charge and the equal negative space charge resulting from the process would combine to affect the surface potential gradient, so that

$$F = F_+ + F_- \quad \ldots\ldots 6.8$$

The relative importance of F_+ and F_- therefore depends upon the heights of the positive and negative charges above the ground as well as their densities ρ_+ and ρ_-.

Magono and Orikasa (1960) applied this theoretical consideration to the space charge on falling raindrops. (The same applied to snow but with opposite signs). Using mean experimental values for the number of drops per unit volume, the charge on individual raindrops, rate of rainfall, terminal velocity of raindrops, and assuming 1 Km for the cloud thickness, $\frac{1}{2}$Km radius, and about 500-1000 m for the height of the cloud base, they illustrated the nature of the variation of the potential gradient at the ground as the raindrops fall. The negative space-charge left behind by the falling raindrops would however be expected to diffuse into surrounding regions, hence a diffusion term was brought into the rate of increase of the negative

ratio, from Fig. 18, ought to be about 1.5 to 1.8. The result obtained, that the two speeds are more or less the same, indicates that the charging takes place quite close to the ground; that is, well below the cloud base. This may be compared with the result for sleet of 17th February, 1964, where the precipitation would have fallen some distance from the cloud base before crossing the freezing level, at and below which melting would occur. Since the surface temperature was above zero, charging might well be due to the melting near the ground or to some other process such as splashing.

For the relation between the current and the potential gradient, we may consider the picture that the charge separation takes place at a certain height above the ground, and that a uniform space-charge occurs in a space of cylindrical form. The vertical component of the surface potential gradient, F, caused by a charge Q at a distance h from the ground and a horizontal displacement r from an observation point, is given by

$$F = 2hQ/(h^2 + r^2)^{3/2} \qquad \ldots\ldots 6.5$$

If the charge is not concentrated at a point, but distributed uniformly with a space charge density, ρ, in a cylindrical volume, then the vertical component of the potential gradient caused by the space charge is

$$F = \int 2h\rho dV/(h^2 + r^2)^{3/2},$$

where dV is an element of volume.

measurements with two field-mills, 100 m apart, along the direction of the surface wind, and concluded that the variations in the potential gradient over periods of the order of minutes were caused by the horizontal motion of wind-borne space charge contained within the first few hundred metres of the atmosphere. In the present work, a good correlation was found between the two records of potential gradients measured at both places mentioned above, both for instantaneous readings, and also when a time-lag of about 7 minutes was allowed between them. This gives a picture that the observed potential gradient was well bound-up with the process of charging.

The daily aerological records for the four stations shown on the map of Fig. 42 for 19th March, 1964, gave the values shown in the following table as the height of the base of cloud, the approximate height of the freezing level and the surface temperature.

	Height of base of cloud (metres)	Approx. height of freezing level (metres)	Surface Temp. (°C).
Shanwell	200 - 300	350	3
Long Kesh	200 - 300	250	2
Aughton	200 - 300	120	2
Hemsby	300 - 600	390	3

On this occasion, the freezing level was within (Long Kesh, Hemsby) or quite close to (Shanwell, Aughton) the range of the base of the cloud. If charging is assumed to take place within this range of level of cloud base, the charge speed to surface wind speed

When averaged over a long period of time, and if the potential gradient is changing rapidly, the effects due to splashing would probably cancel out. The overall effect would be that the standard deviation of the individual values from the mean value would be large. The mean values of the currents measured at the laboratory and on top of the mast, for each quarter-hour, are as shown in Table (7), from which it can be seen that the errors of the mean values of the current at the laboratory were fairly constant, whilst those of the mast were steadily increasing, consistent with the fact that as the potential gradient increased, the effects of splashing became more appreciable, resulting in a wider scatter of the points.

The slope, 0.75, of the straight line of best fit of Fig. 29 indicates that on the average, the current measured at the laboratory at a height of 12 metres, was $\frac{3}{4}$ that on top of the 25-metre mast, 900 m away.

6.5 Effects of the wind

That the charge falling from a portion of the cloud moves with the wind as the cloud moves over is well borne out by the results shown in Fig. 36. Here, the variations of the currents to the two receivers, 900 m apart, followed quite closely but with a time-lag of some 5 to 7 minutes. The mean wind direction was South-East, and the two receivers were along the E-W direction. The charge-speed to surface wind-speed ratio of 0.9 indicates, within limits of experimental errors, that the charge was moving with the surface wind. It would be recalled that Whitlock and Chalmers (1956) made

gradient was less than 1000 $V.m^{-1}$. Moreover, the flat roof of the Physics building, and the top of the mast were not similar surfaces over which identical splashing effects could be assumed to occur.

The effect of splashing of rain can therefore be reckoned with only when the rain is heavy, for it is under such a condition that the potential gradient is also high. Under such a turbulent condition, however, there would be point-discharge and the capture of ions by Wilson's process would be more important. Hence, the problem of charging of raindrops of quiet rainfall still remains unsolved.

If measurements are made of rain current in a region of highly magnified potential gradient, then charging effect of raindrops, even for light rainfall, would become considerable. Such was the case with Collin and Raisbeck's measurements on top of the 25-metre mast, where the existing potential gradient was expected to have been magnified about 100 times. The record of Fig. 25, shows that for the rain-current on top of the mast, there are sharp peaks which become more pronounced on the second half of the record where the negative potential gradient was between -400 $V.m^{-1}$ to -1000 $V.m^{-1}$. This, with an exposure factor of 100 means a range 40,000 $V.m^{-1}$ to 100,000 $V.m^{-1}$! Even though there was found a good correlation of 0.69 (Fig. 27) between the current measured on top of the mast and that measured 900 m away, it could be seen from Fig. 25 that the individual peaks resulting from splashing on top of the mast, were uncorrelated with the record at the laboratory.

6.4 Effects of Splashing

The negative potential gradient and positive rain charge in continuous rain with low potential gradients had been explained by Smith (1955) to be due to the effects of splashing. While this mechanism could be accepted as a contributory factor to the variations of the current and potential gradient at the ground, it could not account for the relation between rain charges and potential gradient. Hutchinson and Chalmers (1951), measured single drops before they had time to splash and these were found to have charges on them.

Adkins (1959) found that the amount of splashing depended upon the surface concerned, the rate of rainfall and the magnitude of the prevailing potential gradient. He derived the relation

$$I_s = 0.13R^{1.23} E \ \mu\mu C \ m^{-2} \ min^{-1}$$

where R, the rate of rainfall, is in $mm.hr^{-1}$, and E $V.m^{-1}$ is the potential gradient existing when splashing takes place. For a light rain, falling at 2 $mm.hr^{-1}$, for instance,

$$\begin{aligned} I_s &= 0.304E \ \mu\mu C \ m^{-2} \ min^{-1} \\ &= 0.005E \times 10^{-12} \ a.m^{-2} \end{aligned} \qquad \ldots\ldots \ 6.4$$

It can be seen, therefore, that E must be greater than 1000 $V.m^{-1}$ before the contribution of charging due to splashing could be appreciable. For quiet rainfall, the potential gradient is hardly near this value. The author's result of 23rd February, 1964, for quiet rainfall, showed that for the one-hour period, the rate of rainfall was less than 1 $mm.hr^{-1}$, and the magnitude of the potential

depends on the magnitude of the potential gradient".

The value F_o = 147 V/m was substituted for F in Ogawa's equation to find the value of F_h and was found to be 495 V/m.

The degree of agreement between the two values of F_h using the two different formulae is striking. Since the two equations were derived purely from theory rather than experimental results, the agreement, perhaps, is not fortuitous. It may well be that Ogawa's equation is no less fundamental than Chalmers's. However, it makes valid the interpretation that t, which was the time lag between the current and potential gradient necessary to give a good negative correlation between i and F, was the time of fall of the precipitation particles from the charging level. For, if the values i_o = -47×10^{-12} a/m^2, F_o = 229 V/m obtained from the author's result for instantaneous readings of i and F Fig. (40) are used in equations 6.2 and 6.3 respectively, the values of F_h obtained are 441 V/m, 880 V/m respectively. Here, there is a large discrepancy which can be attributed only to i and F not being strongly negatively correlated for instantaneous values.

The above considerations disregard the effect of ionic space charge. It is not envisaged that the charging of the melting snow being considered above could be by capture of ions according to Wilson's process. The potential gradient was too small to effect the release of copious ions by point-discharge. The charging effect due to the melting process appears to be a more plausible cause.

The potential gradient at the charging region, F_h, is given by

$$F_h = F_o - \int \frac{idh}{\epsilon_o v}$$

$$= F_o - 4\pi \frac{i_o h}{\epsilon_o v}$$

$$= F_o - 4\pi \frac{i_o t}{\epsilon_o} \quad \text{(since } v = \frac{h}{t}\text{)} \quad \ldots\ldots 6.2$$

where F_o is the mean potential gradient measured at the ground, and i_o is the mean current.

Equation 6.2 is independent of the value of the terminal velocity of the particles. Its accuracy depends on the accuracy with which t, the time of fall of the charged particles from the charging level, can be estimated.

The above formula was applied to the result of 17th February, 1964 for sleet and snow, where t = 40 secs., $i_o = -64 \times 10^{-12}$ a/m^2, $F_o = 147$ V/m, $\epsilon_o = 8.854 \times 10^{-12}$ Farads/m.
F_h was calculated to be 437 V/m.

Ogawa (1960) gave a relation

$$F_h = 3F^{1.3} \quad \ldots\ldots 6.3$$

between the potential gradients, F and F_h at the ground and charging region of raindrops respectively. F and F_h are in volts/cm. He derived this expression from the consideration of the rate of rainfall and the charging of raindrops according to Wilson's theory of ion-capture. He found that the relation satisfied his experimental results, and maintained also that the relation should hold for all values of potential gradient since "there is no characteristics which

	Height of base of cloud (metres)	Approx. height of freezing level (metres)	Surface Temp. (°C).
Shanwell	600 - 1000	820	4
Long Kesh	200 - 300	450	8
Aughton	0 - 50	450	7
Hemsby	200 - 300	2100	1

The freezing level was everywhere higher than the height of the base of cloud. If the charging of the falling raindrops was due to the melting process, this would have taken place at heights high enough for a fair-size cloud to cover the two places where measurements of currents were being taken, such that a good correlation, as was found between the currents, might not be unexpected.

6.3 Space Charge on Precipitation Particles

Chalmers (1957) stated that, if conditions are steady, the potential gradient due to the space charge on precipitation particles could be estimated from a measurement of the current flowing through a unit area in space and the terminal velocity of the particles. Thus, if i a/m^2 is the current density and v m/s is the terminal velocity of the particles, the charge density will be i/v C/m^3. The rate of change of the potential gradient with height, $\frac{dF}{dh}$, is then given by

$$\frac{dF}{dh} = - \frac{i}{\epsilon_o v} \qquad \ldots\ldots 6.1$$

where ϵ_o is the permittivity of the air.

	Height of base of cloud	Approx. height of freezing level	Surface Temp.
Shanwell	600-1000 m	250 m	$3^{o}C$
Long Kesh	600-1000 m	390 m	$4^{o}C$
Aughton	300-600 m	160 m	$2^{o}C$
Hemsby	200-300 m	320 m	$2^{o}C$

It would be seen that the cloud base was well above the freezing level for the two stations Aughton and Long Kesh, the nearest two stations to Durham.

If a value of 4 or 5 m/s is assumed for the terminal velocity of the sleet, then for the time t = 40 secs., the precipitation would have fallen through a distance 160 m or 200 m. This would correspond with the freezing level below the cloud base, and since the temperatures on the ground at these stations were $4^{o}C$, and $2^{o}C$ respectively, it would be expected melting would occur around this freezing region. The charging of the sleet could then be assumed to be due to this melting process.

On 23rd February, 1964, when the one hour's recording of continuous rainfall was made, the table below gives the values of the heights of bases of lowest clouds and the heights of the freezing levels for the four stations.

On the other hand, Mathews and Mason (1963) failed to detect separation of charge and indicated that any charge produced was less than 0.01 e.s.u./gm. or two orders of magnitude smaller than reported by Dinger and Gunn.

Dinger (1964) has stated that Mathews and Mason's result was probably due to the nature of the snow and water specimen they used for their experiment, for Dinger and Gunn (1946) found that the exposure of water, prior to the experiment, to CO_2 would completely eliminate any charging effects on gas bubbles released during melting of the ice. No agreement has been reached on this mechanism up to the time of writing of this thesis. But the work of the present worker tends to support (not conclusive evidence!) that electrification might occur under natural conditions when snow melts.

The daily aerological record of the British Meteorological Office was consulted to check the value of the freezing level of the atmosphere on 17th February, 1964. No upper air observation was made in Durham, but judging from the general atmospheric condition prevailing throughout the British Isles on this particular day, a reasonable inference could be made from reports given for certain stations shown on the map of Fig. 42, to give a reasonable value for the freezing level and the height of the base of clouds in Durham on 17th February. The following table gives the values for the four stations shown on the map.

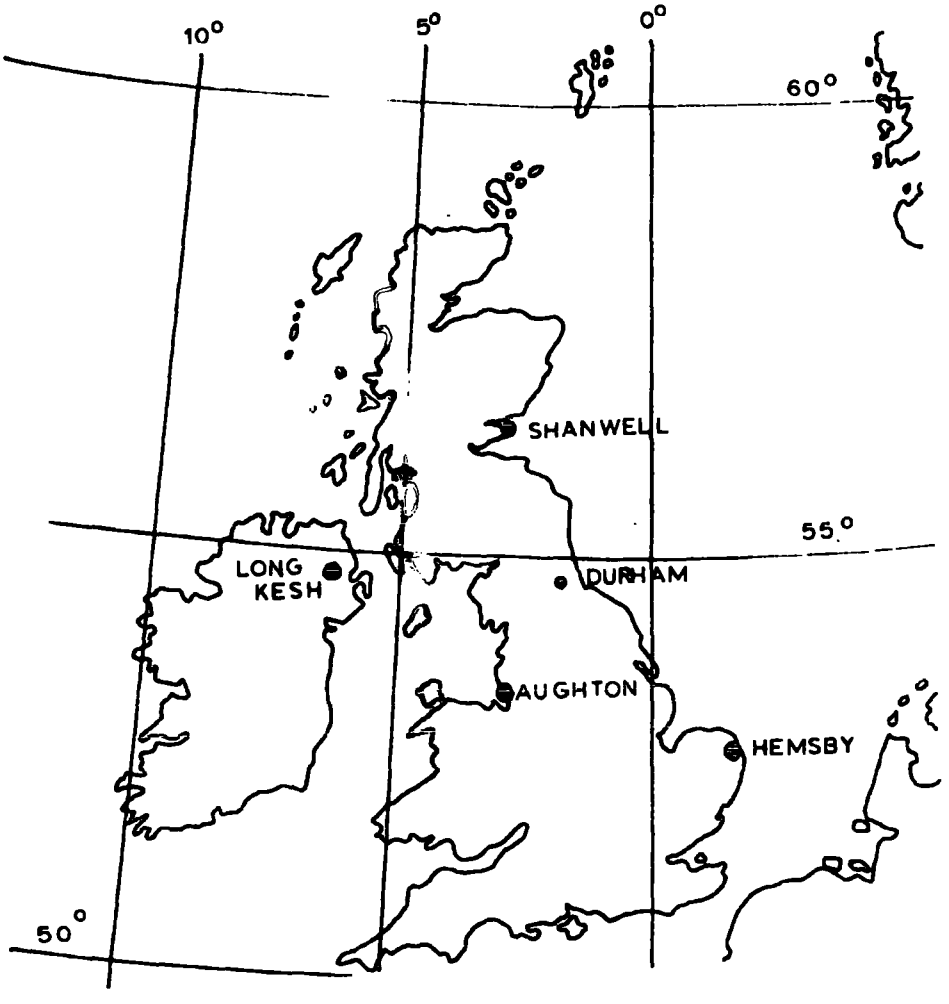

Fig. 42.

coefficient and other relevant statistical parameters for about 200 pairs of numbers, and repeating the same process about 20 times, allowing a specified number of lags between the numbers each time, all within 10 minutes!

Where the arduous task cannot be performed, it is very desirable that Morgan's method of analysis be adopted; this assumes that both quantities which are being compared are subject to errors, as indeed they would be in Atmospheric Electricity. A pair of regression lines would need be drawn, and the straight line of best fit lies between these two, as can be seen in the scatter diagrams drawn in chapter V.

6.2 Electrification accompanying melting of ice and snow

Dinger and Gunn (1946), from the results of their laboratory experiments with ice, found that a positive charge was acquired by melting ice. This charge was of the order of 1.25 e.s.u. per c.c. of melted ice. The presence of impurities such as weak concentration of NaCl, NaOH, and KCl greatly reduced and, with sufficient concentrations, completely prohibited the charging-effect of the melting ice. The presence of dissolved gases in the water before freezing was found necessary to produce electrification, the dissolved gases being forced out of solution during freezing and entrapped in the ice in the form of small negatively charged bubbles which were ultimately released during melting.

A comparison of Figs. 40 and 41 indicates clearly the need to determine whether the negative correlation between I and F is significant enough to justify fitting the functional relation to the observed values. The instantaneous values of I and F, especially if the space charge on the falling precipitation particles has a large disturbing influence on the surface potential gradient, would produce a very widely scattered points on an I/F scatter diagram. If reasonable time lag is allowed between I and F, it appears that a better negative correlation between I and F would be obtained than for the instantaneous values. The value of this time lag would depend on how far up the charging level is, and the rate of rainfall. In general, Summer clouds are much higher than Winter ones, indicating that time lags of up to 5 mins. would have to be allowed for. It is not surprising, therefore, that a discrepancy should occur between Summer and Winter results.

It is appreciated by the author that the volume of work entailed in calculating the correlation coefficient between any pair of readings, if individual values have to be considered, is a large one. If this same process of calculating sum of squares, sum of cross-products, has to be repeated for each unit of time lag until the point of maximum correlation is reached, then it is not a job for a desk-calculating machine! A computer, where available, is well suited for this kind of repetitive work. The computer (Elliott 803) used by the author was capable of calculating the correlation

CHAPTER VI

DISCUSSION OF RESULTS

6.1 The Importance of the determination of Correlation Coefficient

Ramsay (1959) reported a discrepancy between the results he obtained in Winter 1957-58 and Summer of 1958. In fitting a relation

$$I = a(F + C)$$

to his current and potential gradient values, he found that the values obtained for constants a and C for his Winter results agreed more with Chalmers's (1959) results than his Summer results. When a large amount of data is to be handled, earlier workers had found it necessary to group the data into 'class intervals' in order to reduce the volume of work entailed in the calculations, and had determined the gradients and intercepts of the 'straight line of best fit' by the method of least squares. This short-cut method of analysis was found by Ramsay, for instance, to be less than 2% less accurate than when individual values were considered. It is usual also to draw only a regression line of one quantity against the other with the tacit assumption that the other quantity is not subject to error. The analyses performed in the course of this work have demonstrated the futility of the methods of analysis outlined above especially if a definite functional relationship between I and F is being sought.

between I and F when only a regression line is drawn. This becomes worse still if, for a large number of readings, the data are grouped to escape the arduous task of dealing with individual values!

Fig. 41, however, gives a value of F lying between -170 V/m and -340 V/m when I = 0. The straight line of best fit gives -220 V/m. This may be compared with Ramsay's (1959) value for sleet of -124 V/m.

gradient was significant to 2.5%, but not to 0.5%. That between the second current and the potential gradient (-0.12) was not significant even to 2.5%; but both of them gave strong negative correlations of -0.82 and -0.88 respectively for a time-lag of 40 seconds of the currents on the potential gradient. This would mean that the charging of precipitation particles occurred at such a level from which it would take the particles about 40 secs. to fall to the ground. A further discussion on this is done later on.

A scatter diagram of I/F is given in Fig. 40 for the instantaneous values of I and F. The wide scatter resulting in the poor negative correlation of -0.38 should be noted. Another I/F scatter diagram is drawn in Fig. 41, allowing for the 40 sec. time-lag of the current on the potential gradient. That the negative correlation of -0.82 obtained is much better in this latter case than the former is quite obvious. If, from Fig. 40, a functional relation is to be found between I and F, as is usually the case, by drawing the regression line of I on F, then a value of about -500 V/m would be obtained for the value of F when I = 0. If, on the other hand, the regression of F on I had been performed, this would give 120 V/m as the value of F when I = 0. This means the true value of F lies between 120 V/m and -500 V/m - a large margin of error! This indicates what an error could result when finding a function of the form

$$I = a(F + C)$$

17.2.64 : Sleet and Snow.

I/F Scatter diagram : 40-sec. lag of I on F.

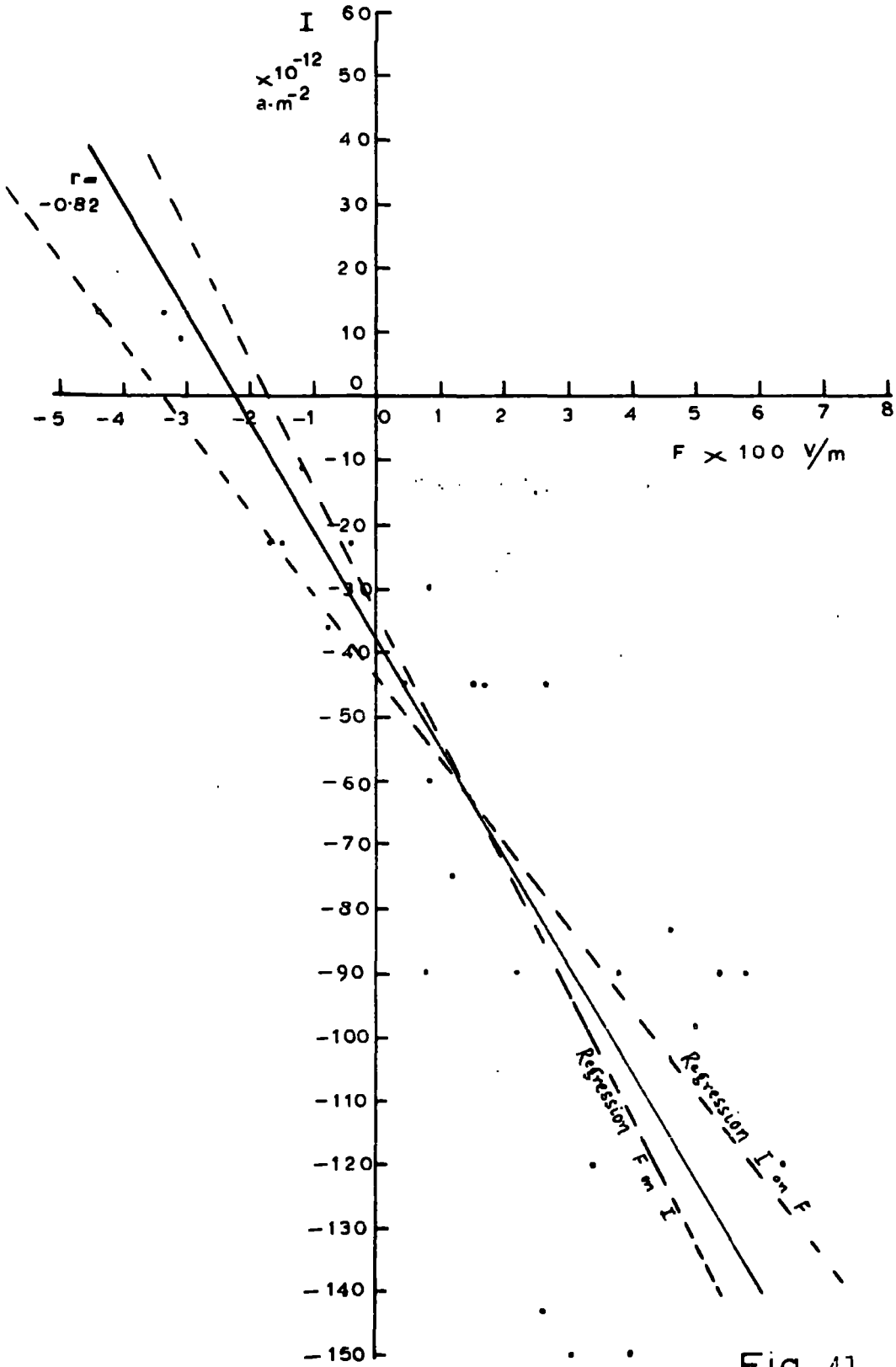

Fig 41.

17.2.64 : Sleet and Snow.

I/F Scatter diagram : Simultaneous readings.

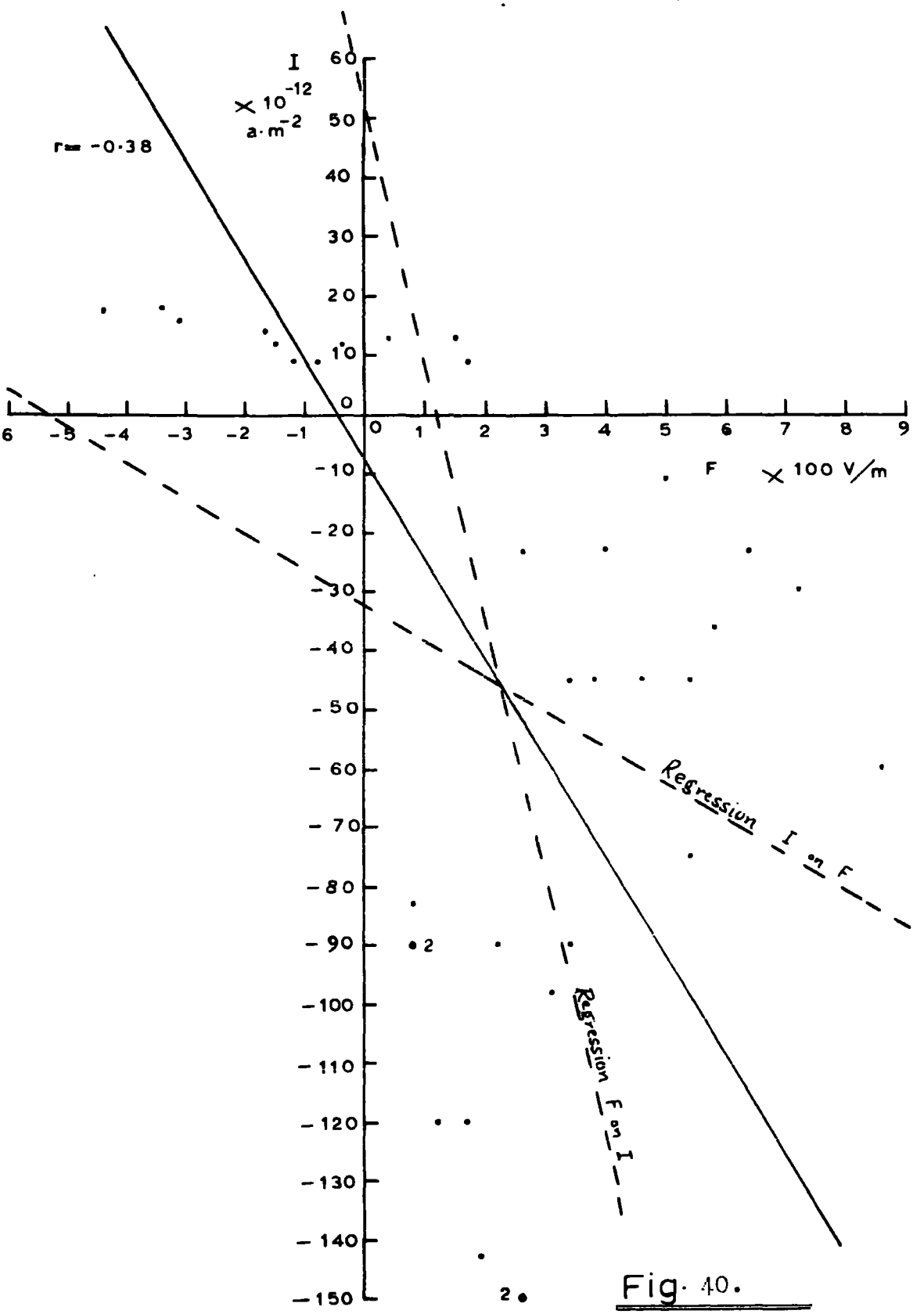

Fig. 40.

5.4 Sleet and Snow

Fig. 38 is an actual record taken when there was a shower of sleet and snow on 17th February, 1964. The part of the record analysed was quite small, lasting for just over 3 minutes, the rest being unsuitable for analysis. The fast speed of 7.5 cm per min. was used for recording. Records were taken of the two rain currents to the receivers displaced 30 metres apart, and of the potential gradient close to one of the receivers (here called receiver I). The wind was blowing from the South-East, and the average value of the wind speed was 2.7 m/s. Five-second averages of the values were taken for analysis.

Fig. 39 shows r_{12}, r_{13}, and r_{23}, plotted against time-lag of parameter 1 on 2, 1 on 3, and 2 on 3 respectively; 1, 2, 3, being the currents to the first receiver (1), second receiver (2), and the potential gradient respectively. r_{12} shows a high correlation coefficient of 0.79 between instantaneous values of the currents 1 and 2, even for such a short time. A slightly higher value of 0.82 was obtained if a time-lag of 10 sec. was allowed between the two sets of readings. This indicates an average charge speed of 2.1 m/s, again assuming the charge moves in the direction of the surface wind. The two values of correlation coefficients are not statistically significantly different, however.

A point of interest in Fig. 39 is the fact that if the instantaneous readings are considered, then the negative correlation of -0.38 between the current to the first receiver and the potential

17.2.64 : Sleet and Snow.

Correlation coefficient, r_{xy}, against time-lag (or lead) of x on y.

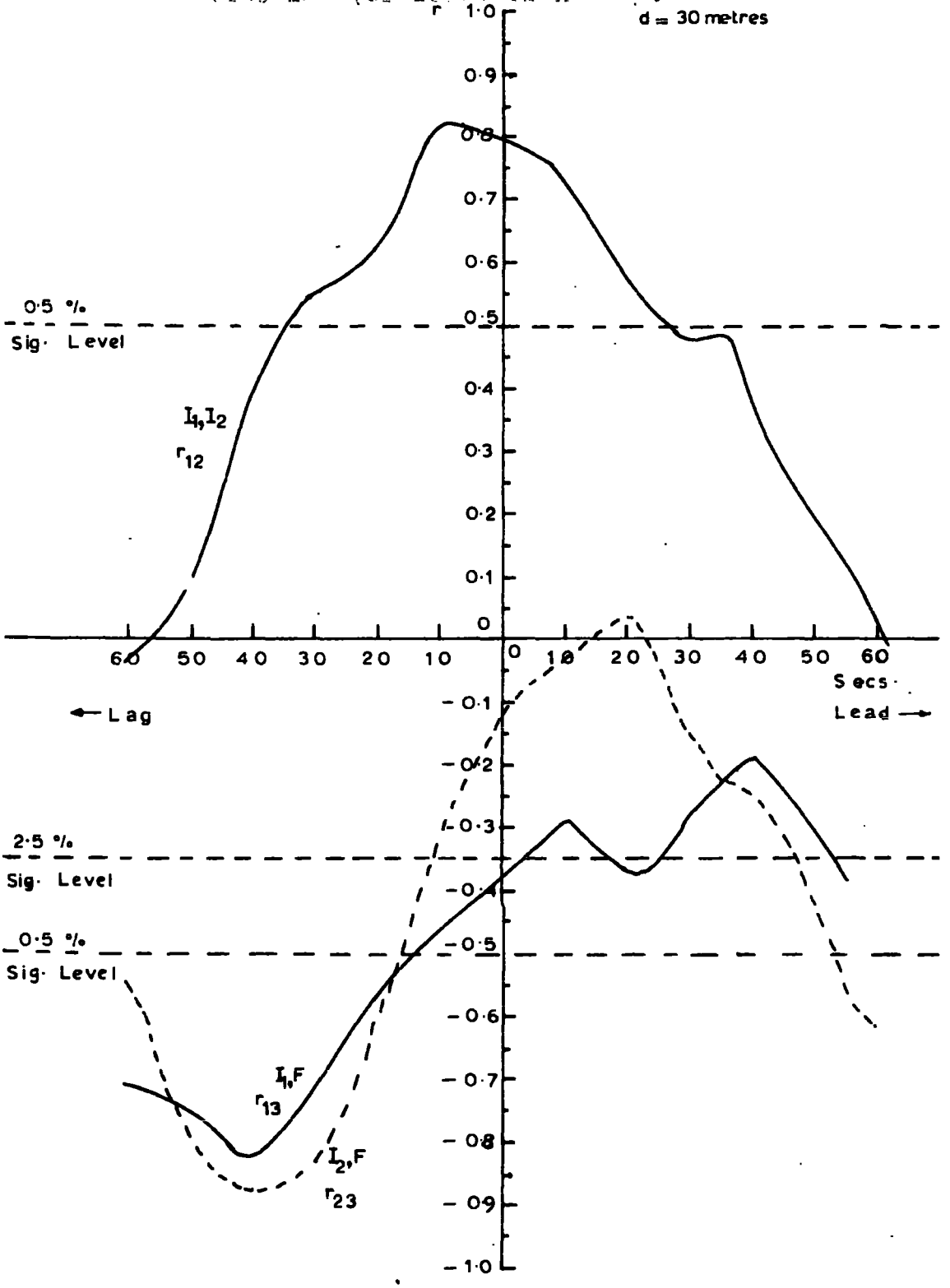

Fig 39.

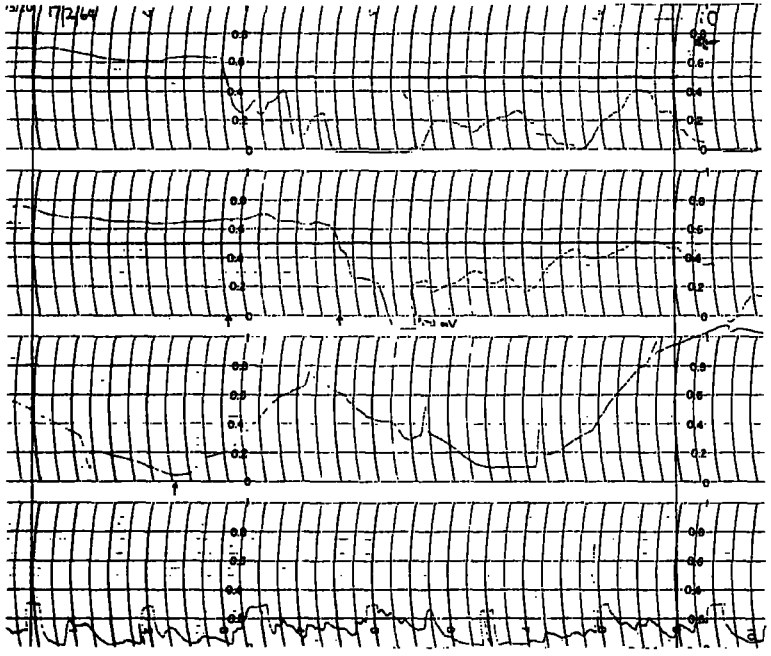

reasonably well and give an average of 0.90 which, within limits of experimental errors in the measurements of the surface wind-speed, could be regarded as unity; that is, the cloud speed was nearly the same as, or slightly less than the surface wind speed. This, of course, rests on the assumption that the precipitation cloud was moving in the same direction as the surface wind, and that the cloud 'front' was at right angles to this direction as shown diagrammatically below.

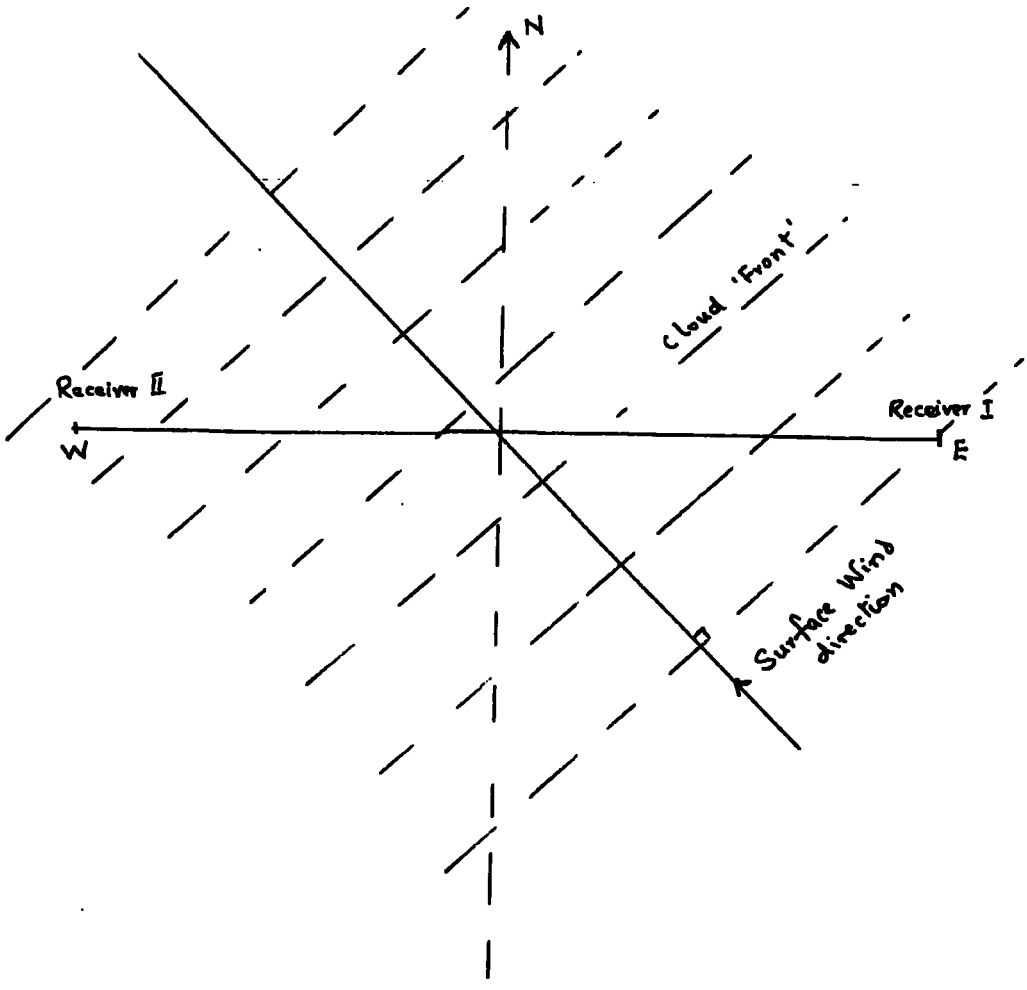

The record was divided into four half-hour sections, and the correlation coefficients between the currents at the laboratory and observatory, 900 m apart, were calculated for the various time lags between them. The wind direction was South-East. Fig. 36 shows that significant correlations did occur between the currents at some time-lags of the observatory record on that at the laboratory. The mean cloud speeds calculated from the knowledge of the distance between the receivers and these time-lags, and the mean surface wind velocity measured, are as indicated at the bottom of the graphs. It can be seen that in every case except the first $\frac{1}{2}$-hour, the cloud (or charge) speed was close to that of the surface wind.

For the two-hour period, Fig. 37 shows the correlation coefficient against time-lag curves for r_{12}, r_{13}, and r_{14} where 1, 2, 3 and 4 stand for currents at the laboratory (1 & 2), current at the top of the mast (3), and the potential gradient at the top of the mast respectively. It can be seen also that these values are significant to 0.5% both for instantaneous readings as well as for a time-lag of about 7 mins. of the observatory records on those of the laboratory. This time-lag gives a charge speed of about 1.4 m/s. The average value of the surface wind speed ratio of 0.67. Perhaps, it would be more justifiable to average the wind speed over the half-hour periods because of its gustiness. The ratio would then be 1.8, 0.84, 0.88 and 0.93 for the first, second, third and fourth half-hour periods respectively. The last three values agree

any changes in the phase relationship of the potential gradient and rain current. If results favoured the propositions already cited, there might well be further clues which could help to the solution of the major problem of where the rain gets its charge from.

He proposed to take his readings under various conditions of weather and types of precipitation and hoped his results might help further to elucidate upon the mechanism already proposed for the charging of rain drops under conditions of low potential gradient and quiet rainfall when it could not be assumed that Wilson's process of ion capture would take place. It would be recalled that Smith (1955) proposed that the charge is produced by the splashing of the rain drops at or close to the earth's surface, presumably in gusts of wind near the surface. However, Chalmers (1961) has considered that the charging process might be due to the melting of snow at the lower levels of the atmosphere.

1.6 The Site and Recording Room

The site chosen was the flat roof of the Physics building, at a height of 12 metres above the general surroundings. It was quite open, except for the little building housing the lift, boiler and fan systems for the whole building (Fig. 1). Next to the lift operation room was another room almost completely empty but for the fan exhaust pipe. This room was used for the recording. The cables, from the instruments outside, were led in through the wall, along railings, on to the Vibrating Reed Electrometer (V.R.E.), for each of the two receivers, amplifiers for the field mill and

The Site

Fig. 1.

Recording Instruments

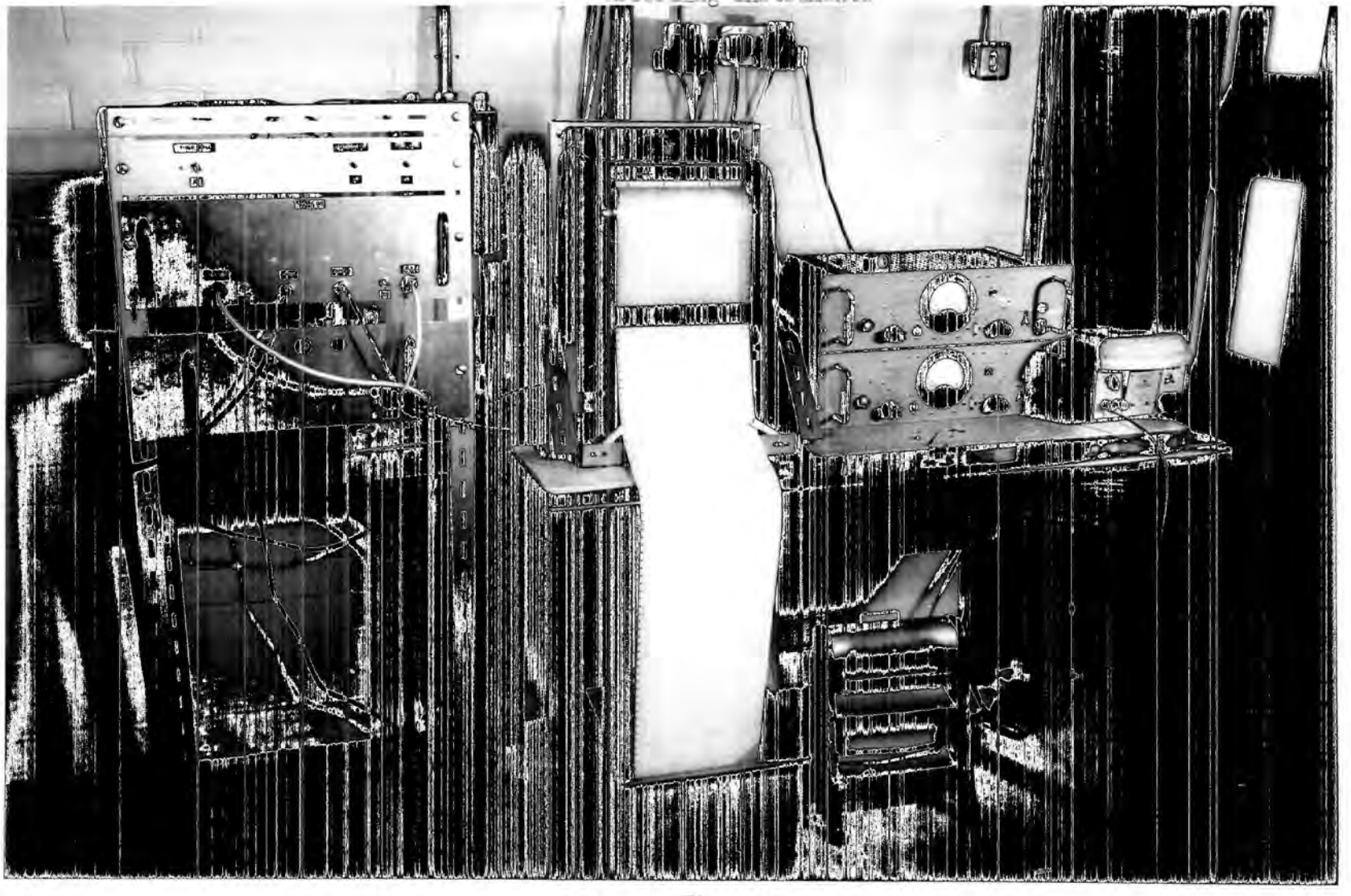

Fig. 2.

anemometer and thence to the pen recorder. The recorder was a sizeable, portable instrument and so was stood comfortably on the same table as the V.R.E.'s. Alongside stood the monitoring panel on which were mounted the power pack, amplifiers, and switches for the field mill and anemometer (Fig. 2). The pulse generating circuit used for the sign discrimination mechanism of the field mill was also mounted on this panel.

CHAPTER II

APPARATUS - DESIGN AND CONSTRUCTION

2.1 The Vibrating Reed Electrometer, (V.R.E.)

The V.R.E. is a standard electrometer supplied by the firm of ECKO Electronics Ltd., for measuring small direct currents in the range 10^{-8} to 10^{-14} amps., from sources which have a resistance to earth of about 100 times the value of the chosen input resistor.

The current to be measured is applied to the selected input resistor and the voltage developed across the resistor is applied via a hold-off resistor to a dynamic capacitor, the capacity of which is changed cyclically at a frequency of about 450 c/s, thus giving an a.c. signal of a magnitude proportional to the d.c. in the input resistor. This a.c. voltage is amplified, subsequently rectified, and displayed on a panel meter. It employs a negative feed-back from the output voltage back to the 'earthy' end of the input resistor. This gives the instrument a good zero stability.

Three input resistors, 10^{8}, 10^{10} and 10^{12} ohms respectively were supplied with the instrument used by the author; and the meter had four ranges, 0 to 30, 100, 300 and 1000 millivolts respectively, so that the instrument gave a full scale reading of 3×10^{-14} amp. in its most sensitive range.

The instrument was arranged to provide either a voltage or a current output. With a recording milliammeter connected to the appropriate plug, the instrument gave 1 m.a. full scale whatever the input resistor or voltage range was selected, thus saving one the trouble of providing an Ayrton shunt externally to the recording meter.

The rapid fluctuations of the rain current being measured necessitated the author altering the time constant of the instrument, by replacing the 10 pf. condenser across the 10^{10} ohm (the resistor most often used throughout) by one of a high insulation, 470 pf. The time constant was therefore about 5 seconds.

2.2 The Rain-current Receivers

For the measurement of rain currents, various workers have used either the open or the shielded receiver. Either of these methods has got its advantages and disadvantages. The major objection to using an open receiver is the fact that the effect of the Displacement Current is quite considerable, and compensation for this is not easy. The Displacement Current is the flow of the bound charges residing on the receiver as a result of the changes of the prevailing potential gradient. The potential gradient, F, is related to the surface charge density, σ, of any conductor on which the lines of force terminate, by the relation:

$$F = - \frac{\sigma}{\epsilon}$$

THE SHIELDED RECEIVER

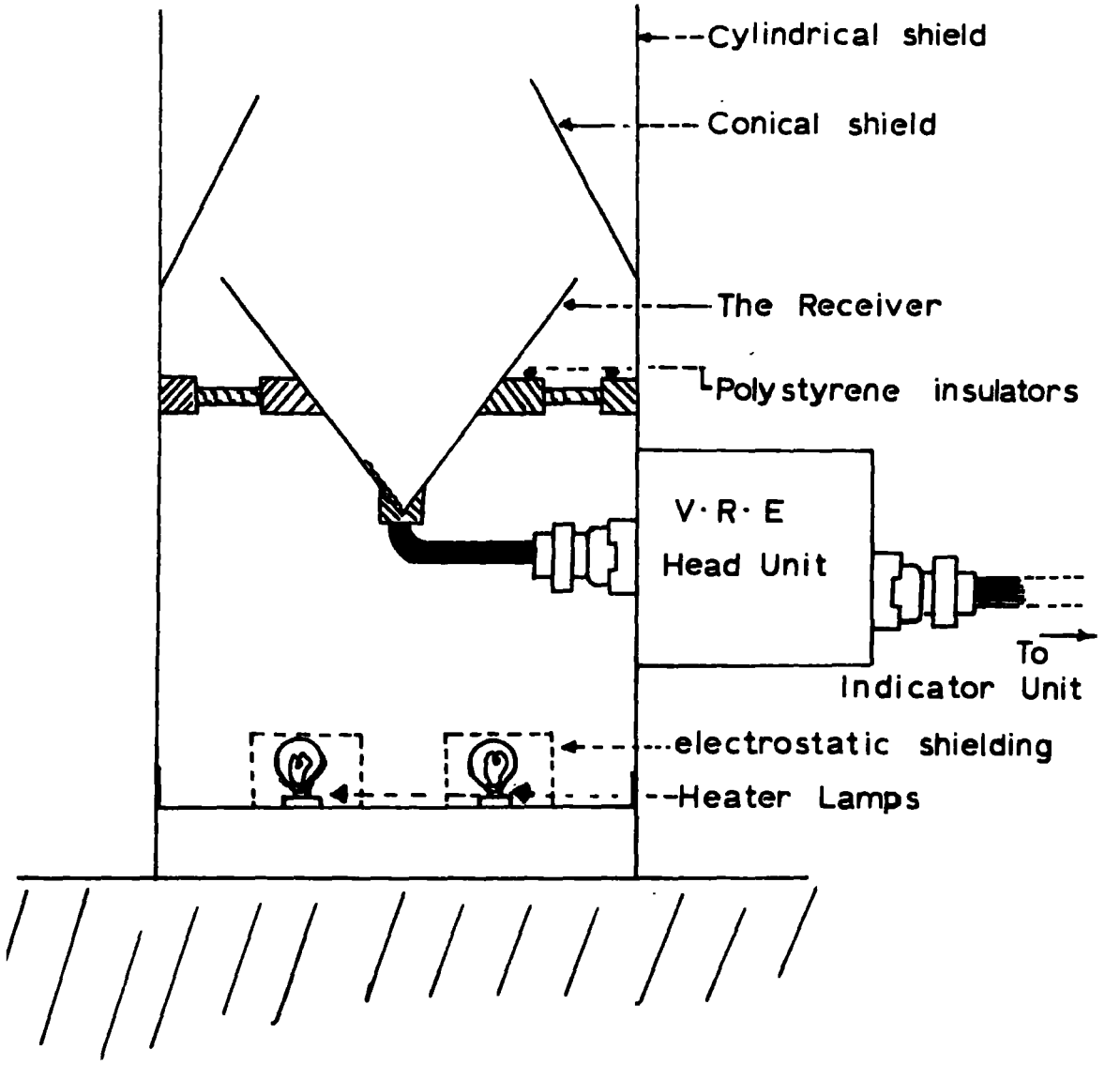

Fig. 3.

The Receiver

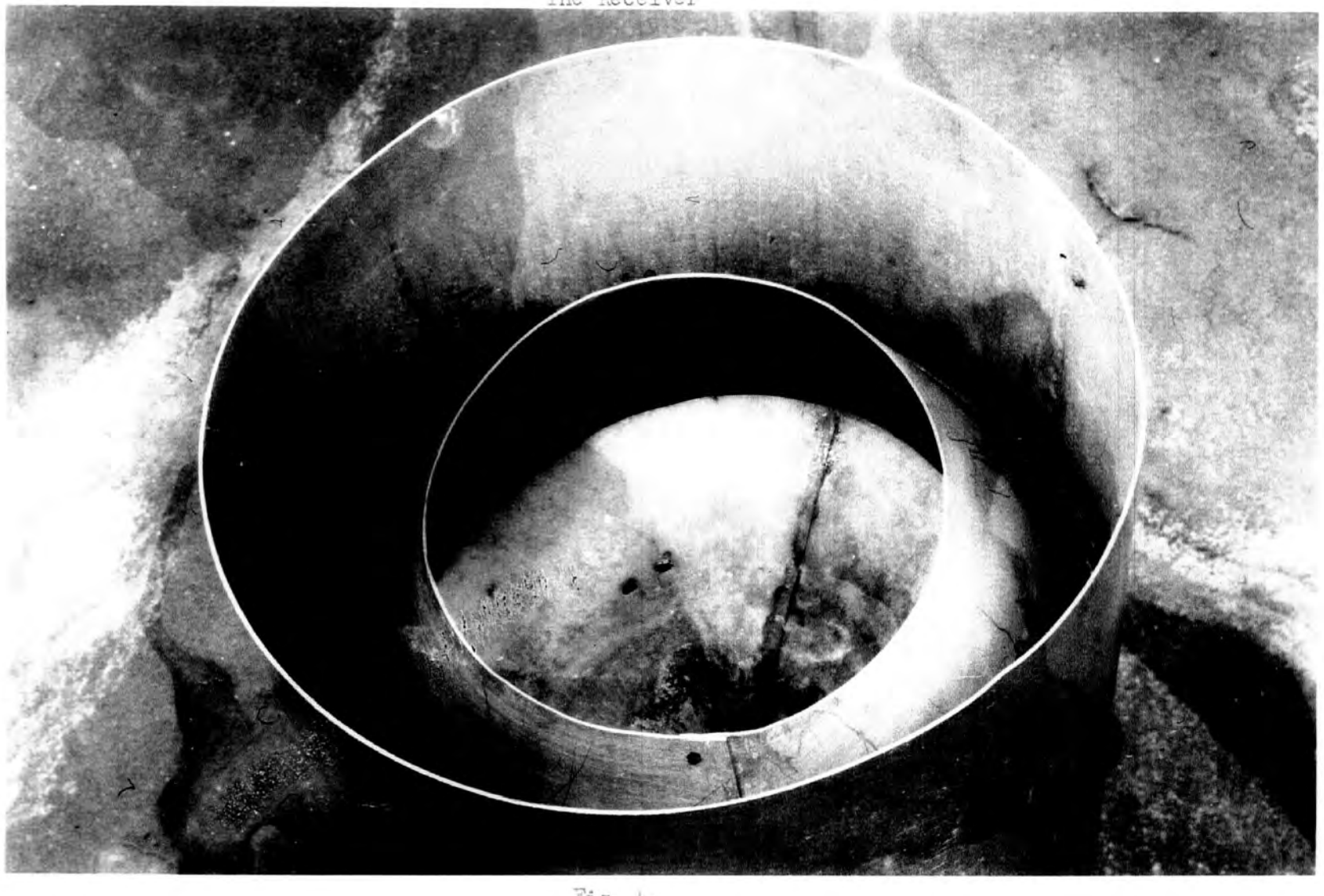

Fig. 4.

where ϵ is the permittivity of the medium; hence, the rate of change, $\frac{dF}{dt}$, of this potential gradient, gives rise to a displacement current, $-\frac{1}{\epsilon}\frac{d\sigma}{dt}$, which is comparable with the precipitation current being measured by an exposed receiver. However, the exposed receiver has the advantage over the shielded one, of the fact that all of the rain current is collected, whereas, shielded receivers do tend to miss some of the raindrops, especially the smaller drops and especially under windy conditions. Shielded receivers, on the other hand eliminate, or at least, reduce considerably, the displacement current. The fact that shielded receivers do not collect all the rain drops does not seem a serious factor in an experiment designed to compare the currents reaching two such identical receivers; hence the present worker decided to use shielded receivers.

The construction of the shielded receiver was in accordance with the model and dimensions of those already used by earlier workers for this purpose, the original design of which was suggested by Scrase (1938). A schematic diagram of the receiver is as shown (Fig. 3). The receiver was well supported by three pairs of polystyrene blocks, each pair connected by a short length of screwed brass rod. One of these blocks could be seen in Fig. 4, which shows, in perspective, the relative positions of the receiver, the conical and cylindrical shields; the full view of the whole system, with the head-unit of the V.R.E. fixed on to the cylindrical shield, could also be seen in Fig. 1. The resistance to earth of the receiver was stipulated to be about 10, or better still, 100 times the value

of the input resistance of the V.R.E. The highest value of the three input resistors of the V.R.E. was 10^{12} ohms, indicating that the resistance to earth of the receiver should be of the order of 10^{14} ohms. When the receivers were finally in good working conditions, this condition was satisfied, but, as will be discussed later, difficulties due to insulation break-down occurred at some stage of the work.

One of the precautions taken to keep up the insulation was the insertion, at the bottom of the receiver, of two 40-watt electric bulbs, connected in series and permanently switched on. This was to keep the polystyrene insulators dry, and keep off spiders whose webs could do a lot of havoc (Ramsay, 1959). The bulbs were connected in series so as to make them run at lower power and so prolong their life-time. They were also shielded electrostatically with perforated aluminium boxes which were also connected to the earthed cylindrical shield of the receiver. The cable connecting the V.R.E. head-unit to the receiver was a short and thick coaxial cable. It was rigid, so that the complication which might have been introduced due to its vibration, if the cable had been long and flexible, as experienced by earlier workers, was averted. Both the conical, and cylindrical shields were properly earthed through the earth-wire of the mains supply used for the heaters. This prevented the interference of the displacement current already explained, since none, or very few if any, of the lines of force would reach the actual receiver.

2.3 Potential Gradient Measurement

2.3.1 The Field Mill

Chalmers (1957) has described the two broad types of instruments that could be used to measure the earth's potential gradient. The first type concerns methods of measuring potential difference between two points at different heights one of which usually is at the earth's surface, and the potential is found by some form of potential equalizer. In the second type, the bound charge on a portion of the earth's surface, or on an earth-connected body is measured. The field mill, described later, falls into this category. For the discussions on the relative merits and demerits of these methods, the reader is referred to the various publications (e.g. Chalmers, 1957; Groom, 1963).

The author found it quite convenient to construct a field mill, first because the members of the Atmospheric Electricity research group of the Durham University have been quite conversant with it and most of the various problems relating to its proper functioning were well known. Secondly, the various components used for earlier instruments were readily available. For a description, a brief summary of the essential points need be given.

The basic principle is that a metallic plate, mounted on an insulator, is connected, through a high resistance and capacitance in parallel, to earth, and an earthed cover alternately shields this plate from, and exposes it to, the atmospheric potential gradient.

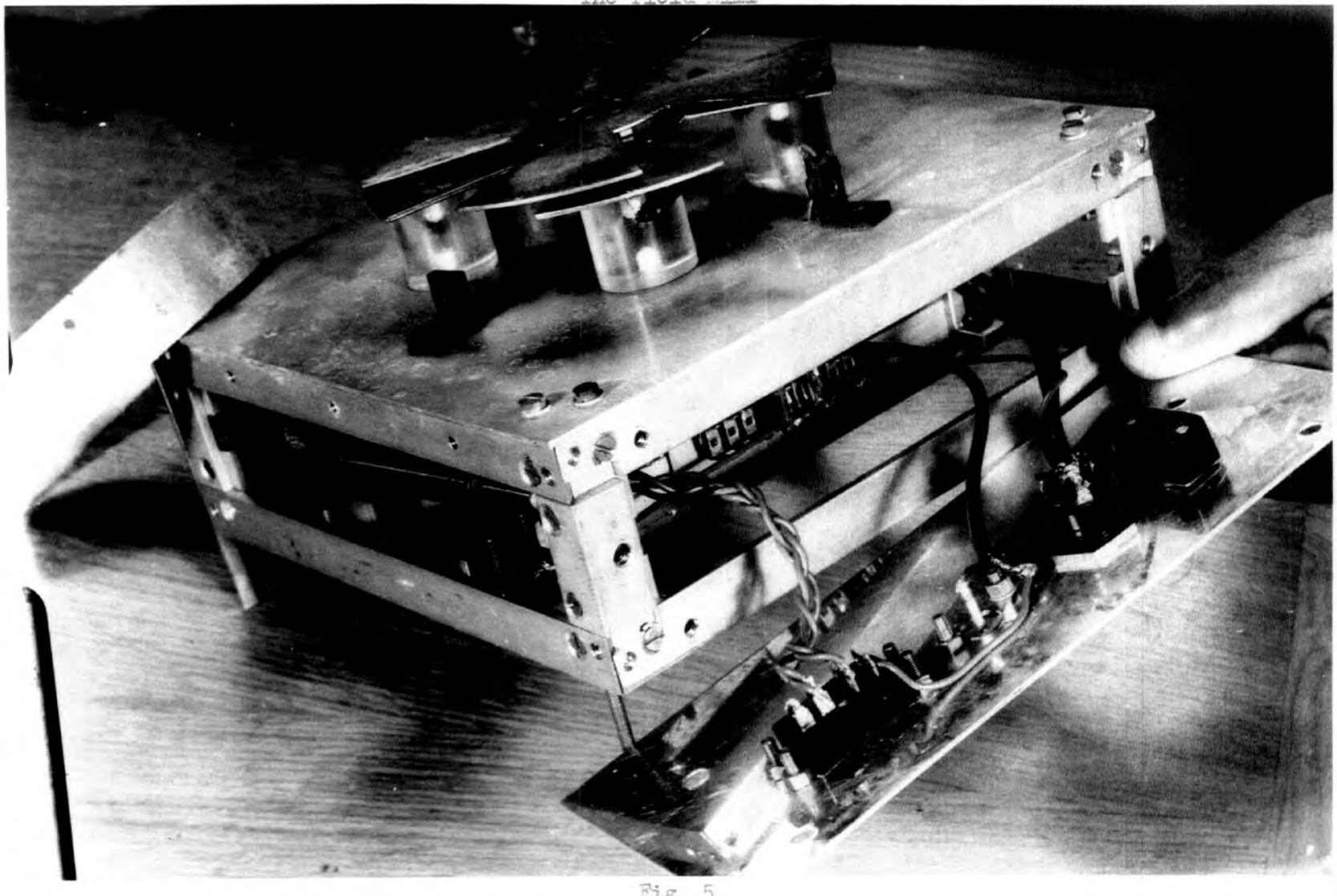

Fig. 5.

When the plate is exposed, lines of force end on the bound charges on the plate; these charges leak to earth through the high resistor and develops a voltage across it, when the plate is covered; the charges flow back to the plate from earth, again through the resistor, when the plate is re-exposed. The entire process of covering and uncovering gives rise to an alternating current, the magnitude of which is proportional to the potential gradient. This could be amplified, rectified and measured. However, the alternating nature of the current prevents one from knowing the sign of the potential gradient unless modifications are made specially for this. The method of sign discrimination used by the author will be described later.

Two circular brass plates, each cut into four equal segments in the shape of the Maltese Cross, were chromium plated and mounted coaxially one on top of the other with a separation of about 5 mm (Fig. 5). The lower plate was mounted on four one-inch long cylindrical polystyrene blocks, and the upper plate was rigidly attached to the spindle of a $\frac{1}{4}$ h.p., a.c., synchronous motor whose speed was 3000 revs. per minute. This plate (called the rotor) was earthed through a carbon brush whilst the lower plate (stator) was connected through a microphone cable, to a resistor of 10^8 ohms and a capacitor of 100 pf. in parallel, then to earth. To prevent the stator from driving rain and also to minimise the edge effect of the lines of force between the two plates, a cylindrical guard-ring was used to surround the plates. This guard-ring was mounted on four right-angled tufnol insulators (as seen in Fig. 5), for the purpose of

THE CATHODE FOLLOWER

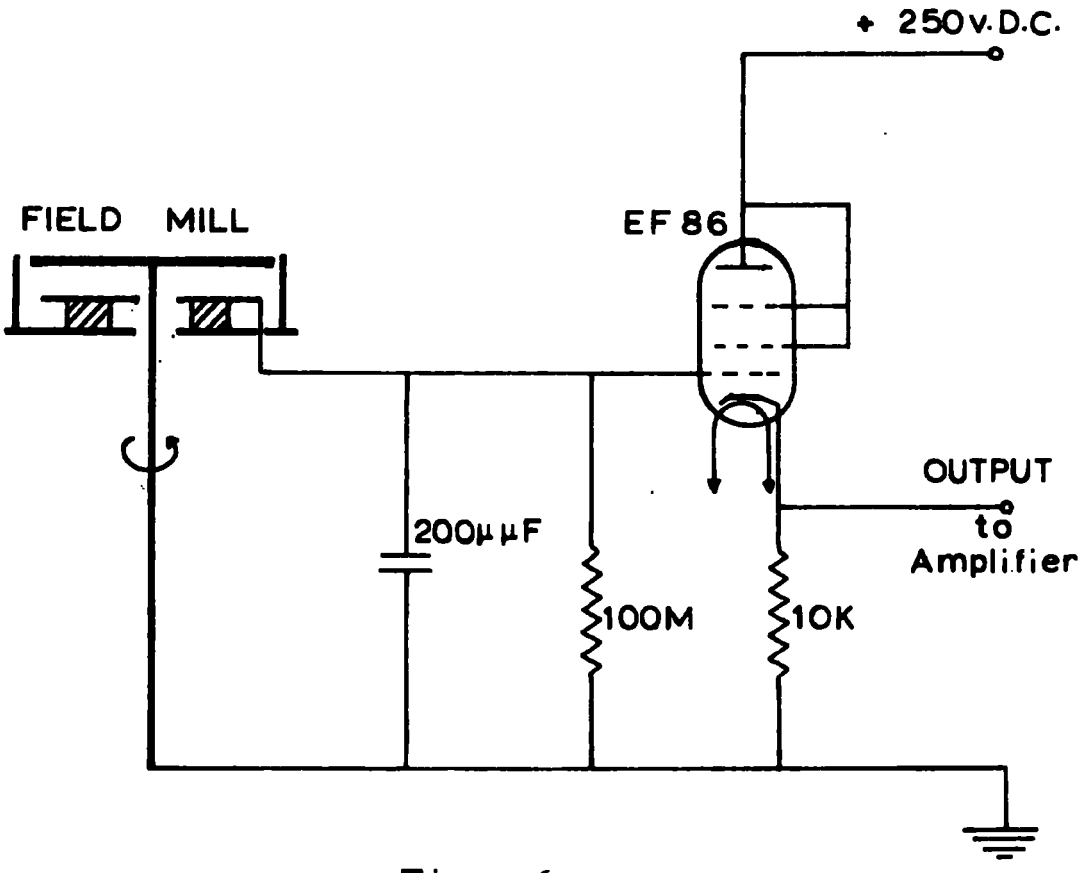

Fig. 6.

sign discrimination of the potential gradient, discussed later; but the ring was earthed all the time except for the one second in every half-minute for which voltage pulses were applied to it.

The alternating voltage appearing across the resistor was fed directly to the grid of a cathode-follower valve, EF 86 (Fig. 6). This was essential because the cathode-follower is a suitable impedance transformer, matching the high input impedance to the low value of impedance presented by the long length of cable carrying the signal to the amplifier and recording systems indoors. The cathode-follower gives no amplification, but its output voltage is not unduly reduced by the connection to it of the lower impedance of the cable.

For the first field mill constructed by the author, a 24 volt d.c. motor was used, and because he was not, by that time, yet aware of the various complications resulting from the commutator sparking of such motors, and of inadequate shielding of electronic components, considerable difficulty was encountered with the "grassy" signal output of the mill. This field mill had to be discarded later on and a new field mill constructed, using an a.c. synchronous motor to drive the rotor and making sure that the motor was adequately shielded electrostatically, and that microphone cables were used for the electronic parts. To ensure that the vibration of the entire framework of the field mill was not transmitted to the valve, the latter was suspended by rubber bands as an anti-vibration device.

THE POWER SUPPLY

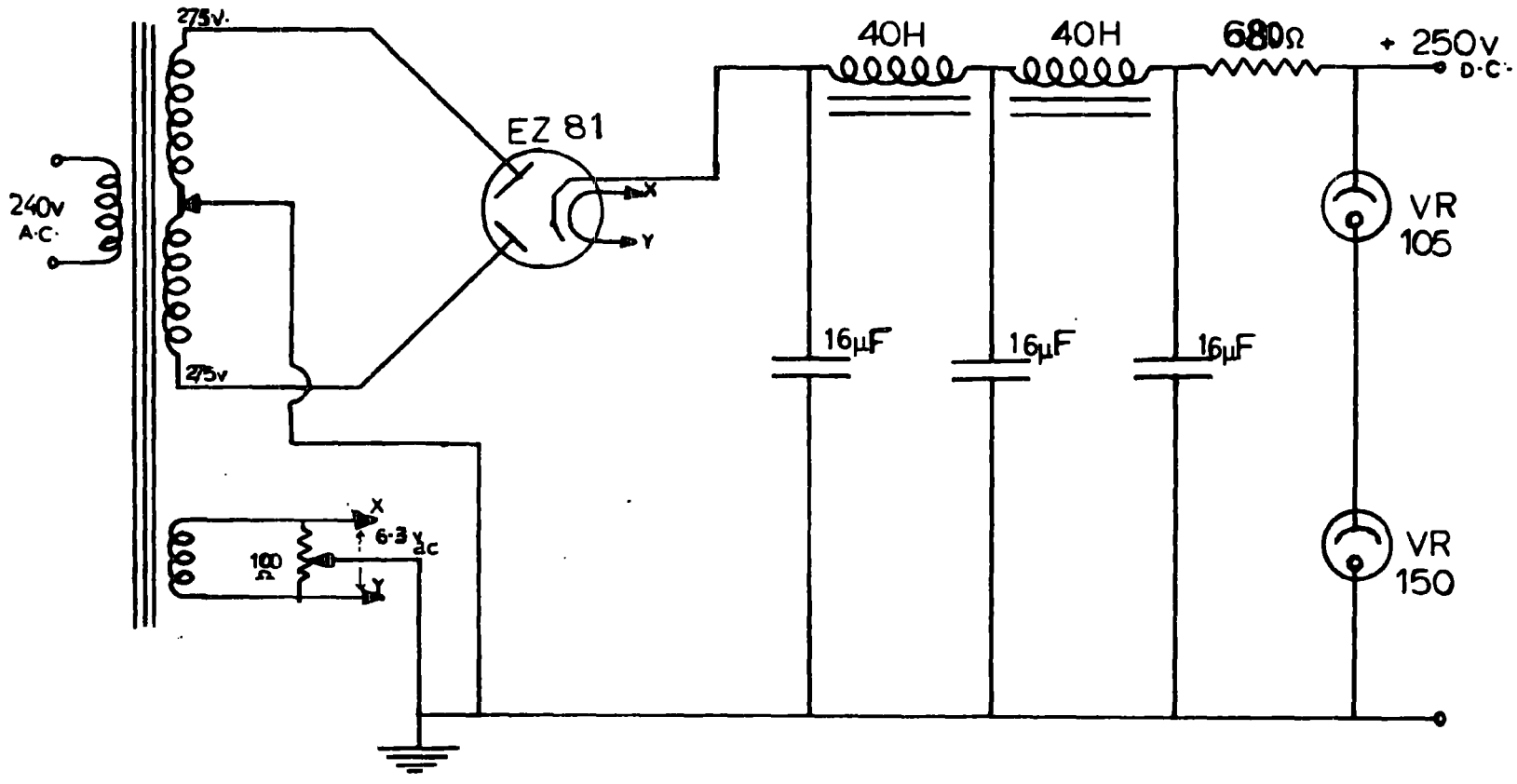

Fig. 7

In its working position, the mill was mounted, with the vanes up-side-down, on a rigidly supported handy-angle stand, one metre off the floor (as shown in Fig. 1). The purpose of running the mill upside down was to prevent the vanes from the rain. This, of course, reduced the number of lines of force terminating on the vanes. On the other hand, the handy-angle support increased this number. These two effects were found to be just about equal and opposite, by running the field mill standing on the surrounding floor, with the vanes the rightway up, and also in its mounted position. Hence, the Exposure Factor (explained later) of the mill in its mounted position was the same as that of the flat roof itself.

2.3.2 The Power Supply

The conventional method of using a double-wound transformer to provide 6.3 volts a.c. for the valve heaters, and the full-wave rectification to give an H.T. line of 250 volts was employed to supply the necessary power to thecathode-follower and amplifier valves. The circuit diagram is as shown (Fig. 7). This provided a stable voltage of 250 volts d.c. and 25 m.a. current, for which purpose the use of the stabilising tubes VR 105 and VR 150 is highly recommended. Use was made, also, of the 'hum-dinger' principle to repress the effect of the magnetic field generated when a cathode is heated by an a.c. current. This was done simply by connecting a 100-ohm potentiometer across the 6.3 v a.c. supply and connecting the centre of this potentiometer to earth, as against the usual method of earthing one end of the heater supply directly.

THE AMPLIFIER

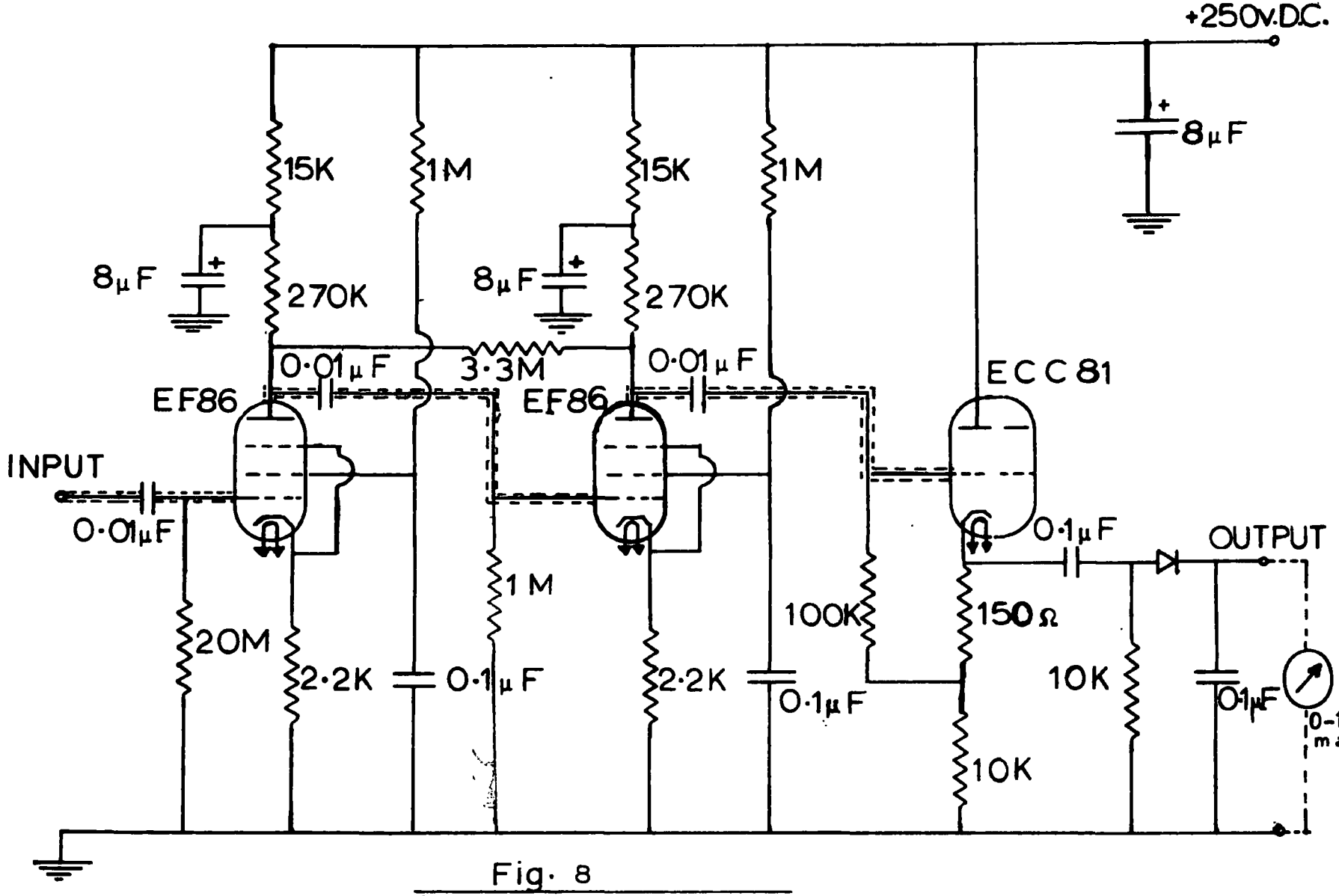

Fig. 8

2.3.3 The Amplifier

The design of the amplifier that the author used was different from that which earlier workers used only as regards the values of the electronic components and the method of application of the feed-back system. It was otherwise essentially the same. Since the field mill output signal was to be recorded on a milliamp recorder, thus requiring a current of about three orders of magnitude greater than that needed for a photographic method of recording, a high-gain amplifier was needed. The circuit diagram of the amplifier constructed is as shown in Fig. 8. It was essentially a two-stage R-C coupled amplifier, using low-noise pentode valves, EF 86, in the first and second stages, with screen-grid decoupling in both stages. The output stage was a cathode-follower, valve ECC 81. Suitable negative feed-back was applied at various points in the circuit, such as through the non-bypassed cathode resistors of the three valves, and across the 3.3 M resistor joining the anodes of the first two valves. The overall voltage amplification, even after the feed-back, was about 500. This gave a current of 1 m.a. for a potential gradient of about 1,000 V/m as shown by the calibration curve (Fig. 16). The gain could, however, be adjusted by altering the value of the resistor joining the anodes. Without this resistor, the amplifier was found to be quite susceptible to instability whenever the input voltage exceeded a certain, rather low, value.

SIGN DISCRIMINATION DEVICE for

POTENTIAL GRADIENT

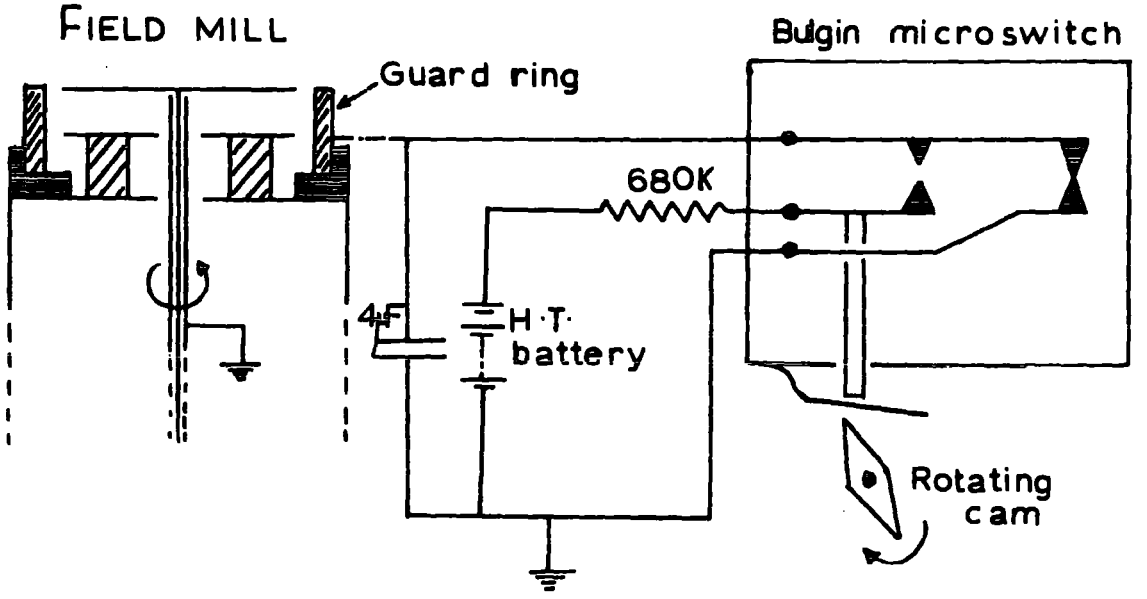

Fig· 9.

Sign-discrimination device for the Potential Gradient

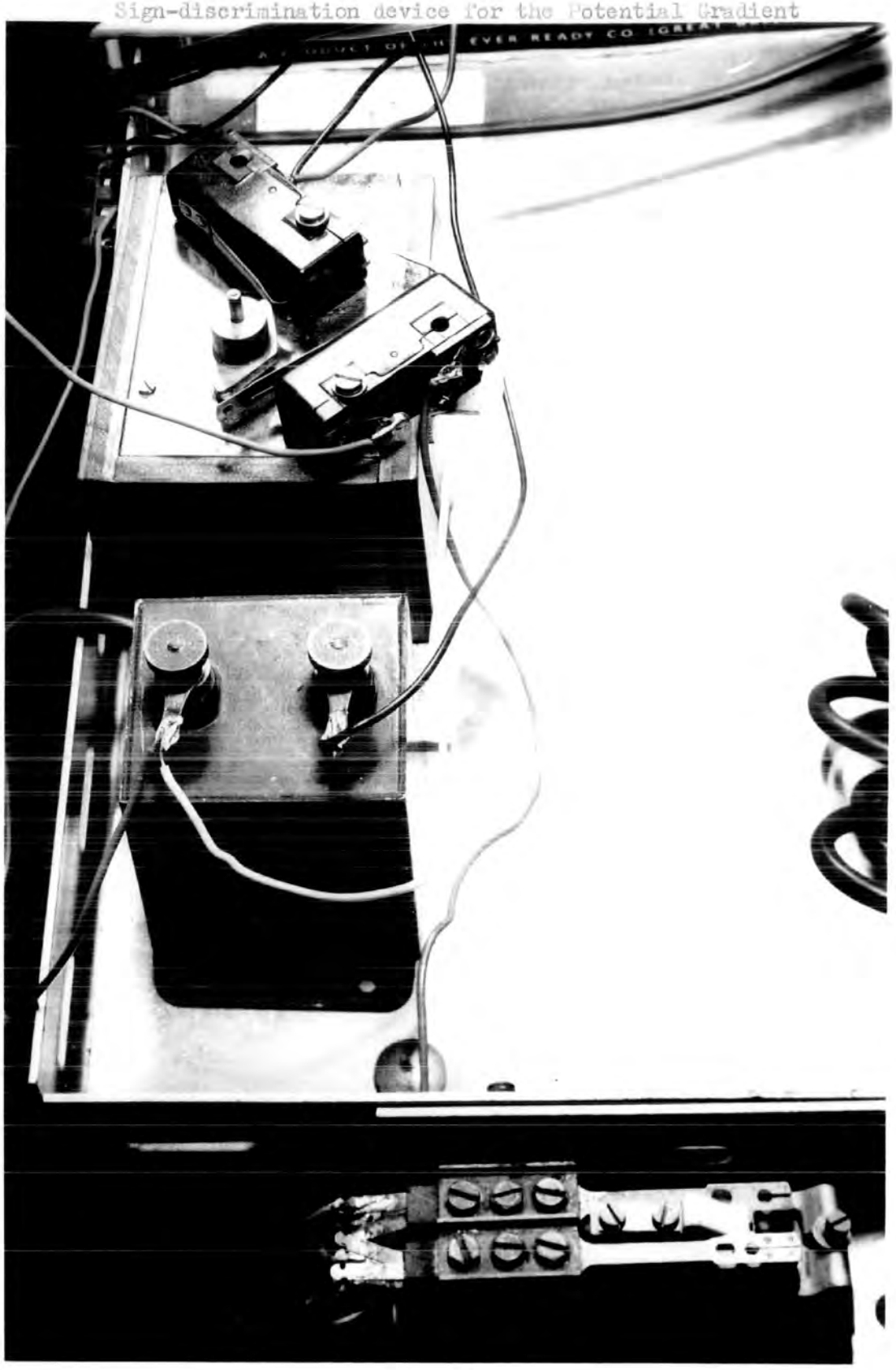

Fig. 10.

2.3.4 Sign Discrimination Device for the Potential Gradient

As mentioned above, the alternating nature of the output signal from the field mill gave rise, after rectification, to a unidirectional current whether or not the potential gradient was positive or negative. To discriminate between the signs of the potential gradient, therefore, various methods had been applied by various workers. For instance, Adamson (1960) used a mechanical commutator on the same shaft as the rotor, Mapleson and Whitlock (1955) used a phase-sensitive detector by running a reference-signal generator on the field mill shaft. A zero-displacement method had been used by Rangs (1942), and von Kilinski (1950), by applying a large synchronous signal of constant amplitude andphase tothe output, thus displacing the zero by an amount corresponding to more than the largest potential gradient value to be measured. These methods, of course, imply that the reference signals must be very stable.

A comparatively very simple method of sign discrimination had been designed by Collin (1962). A slight variant of this method was used by the present worker. The guard-ring was mounted on four small pieces of tufnol, as insulators, and a simple C-R circuit (Fig. 9) was made to supply a saw-tooth pulse from an H.T. battery each time a contact was made. The contact was by means of a cam-operated microswitch (Fig. 10). The cam was turned by a synchronous clock motor such that the C-R circuit was closed for one second once every half-minute, during which the condenser was charged up

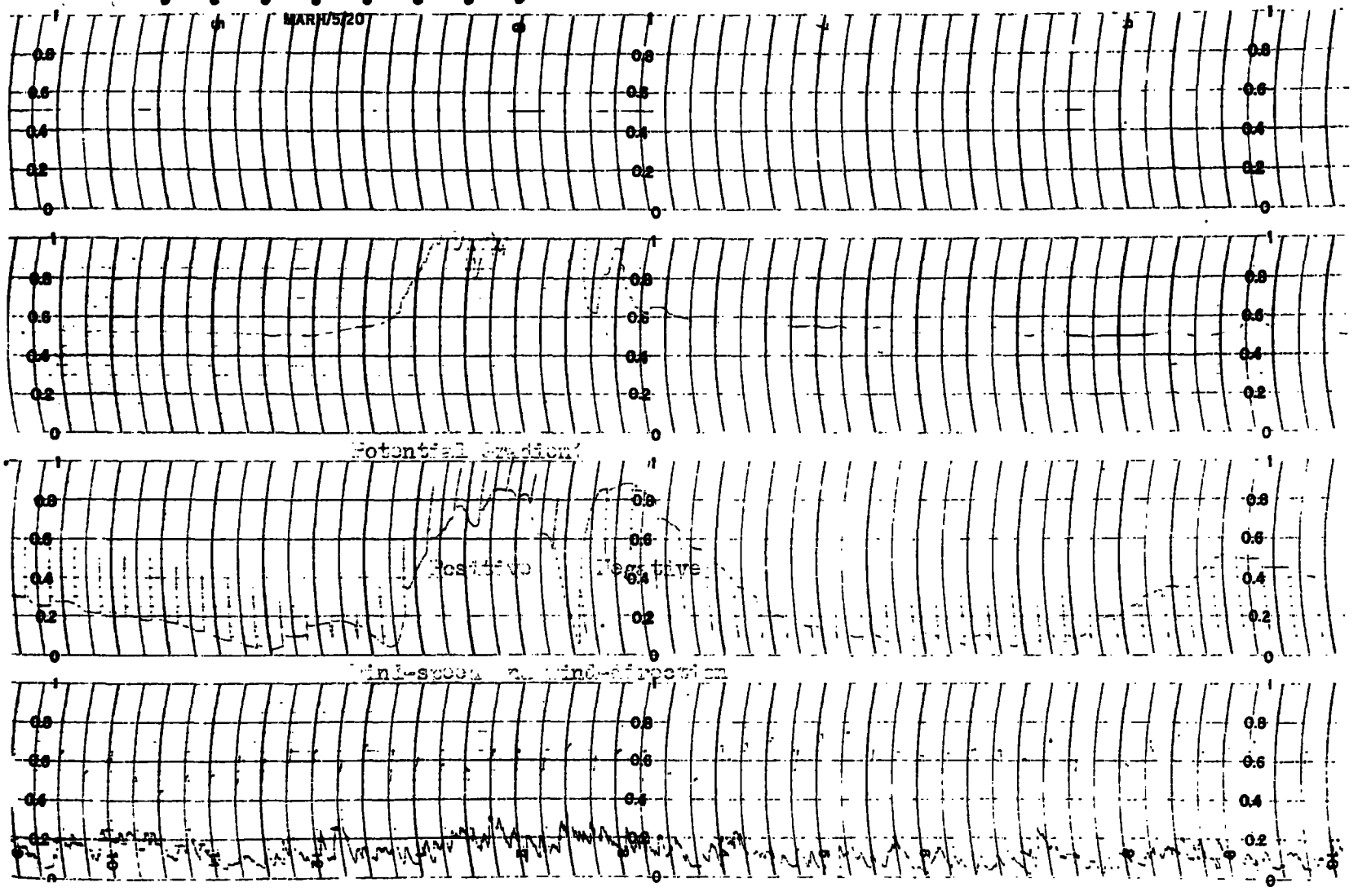
MARH/5/20
0.8
0.6
0.4
0.2
0
Potential gradient
positive
negative
Wind-speed
Wind-direction

linearly with time and the pulse was applied to the guard-ring. Whenever the circuit was broken, the guard-ring would be earthed immediately. The time constant of the C-R circuit was 2.7 secs., so that the one second for which the pulse was applied made it possible to use the linear portion of the rising voltage, and small, triangular pulses, as shown on actual records, resulted. If the potential gradient was positive when the pulse was applied, a spike in the positive direction was superimposed on the record, whereas if it had been negative, the application of such a positive pulse would tend to reduce the magnitude of the negative potential gradient just for one second and the spike would be a triangular dip on the record (Fig. 11). This slight modification of applying the pulse to the guard-ring had the advantage that the values chosen for the condenser and resistor had nothing to do with the proper earthing of the rotor, whilst still retaining the simplicity of Collin's method.

2.4 Wind-speed Measurement

2.4.1 The Anemometer

The anemometer used by the author was a three-cup, a.c. generator type. In principle, it was a small magnet fitted on to the spindle on which three moulded plastic cups were attached. This magnet was made to rotate inside a coil, thus generating an a.c. voltage, the magnitude of which was dependent on the rate of revolution of the magnet, hence on the wind-speed. This simple set-up could generate a voltage of the order of microvolts which, without further amplification, could be made to

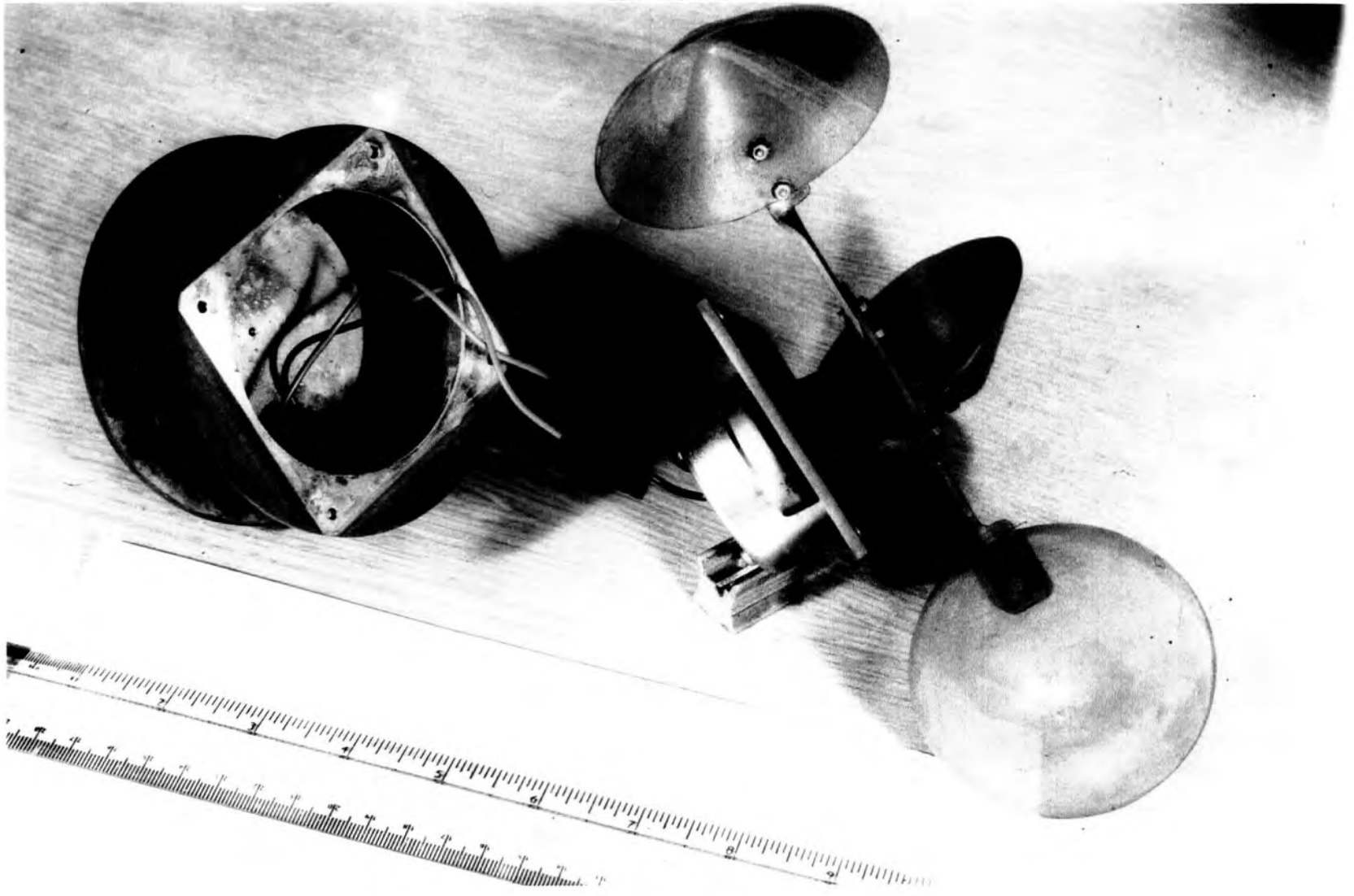

Fig. 12.

operate a mirror galvanometer for a photographic method of recording. To operate a milliamp recorder, however, the signal would need to be amplified a million times, since voltages of the order of 1 volt would be required for the pen-recorder. A suitable amplifier to handle such a low frequency signal and of this magnitude is not an easy proposition if only for the inherent noise of the amplifier itself. The author therefore used an a.c. synchronous motor, attaching the three cups on to the spindle of the motor (Fig. 12). This motor did generate a much greater voltage than the simple magnet type. Even then, this signal still had to be amplified in order to operate a pen-recorder. An amplifier was built for this purpose.

The anemometer was supported on a thick steel tube some two metres above the flat roof of the building (as in Fig. 1). The choice of this height and the positioning of the mast, were purely arbitrary, but care was taken to see that the cups projected above the surrounding walls so as to reduce the effects of eddy currents.

To find out to what extent the exposure of the anemometer had been affected by the surroundings, comparison of the anemometer record was made, at suitable periods, with the well-exposed anemometer on the top of the Durham University Observatory. It was found that for reasonably low winds, less than 10 m/s., say, there was no difference between the records, but disagreements occurred for the gale-force type of winds. This was due to the insensitivity of the author's anemometer to very high gusts of wind and also to the nature

Anemometer Signal Generator Amplifier

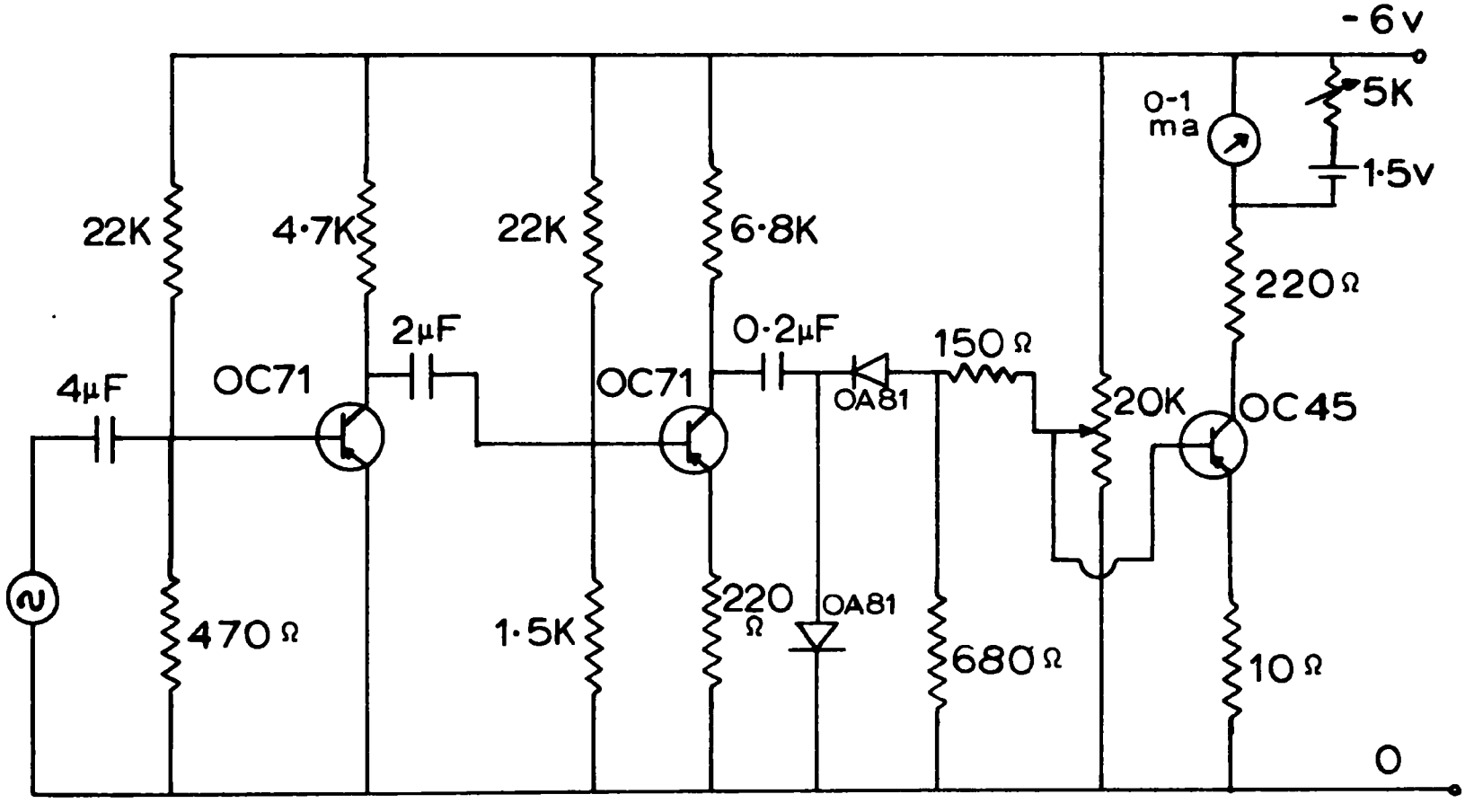

Fig. 13

of the characteristics of the variable frequency amplifier used, which was not very sensitive to high frequencies.

2.4.2 Anemometer Signal Generator Amplifier

Since the magnitude of the output signal from the anemometer motor depends on its frequency, hence on wind-speed, a three-transistor, variable input frequency, amplifier was constructed. The circuit diagram is as shown (Fig. 13). For the first two stages, OC 71 transistors were used and an OC 45 for the output stage, the reason being that the OC 45 characteristic is steeper, i.e. more sensitive than OC 71.

The variable input was first amplified and squared by the first two stages, integrated by diodes OA 81 and applied to the biased output stage. The meter was backed off by a separate cell of 1.5 v and a 5K potentiometer in series. The 20K potentiometer was pre-set for maximum sensitivity during calibration and thereafter left untouched.

2.5 The Wind-Vane

A simple potentiometer circuit was designed for the measurement of the wind-direction. As shown in the circuit diagram, Fig. 14, P is a rotary potentiometer, a high accuracy precision wire-wound potentiometer, supplied by the firm of Colvern Ltd. The potentiometer wire was housed in a mineral-filled moulded case, and the effective resistance angle was adjusted accurately by means of internal trimmers.

WIND-VANE CIRCUIT

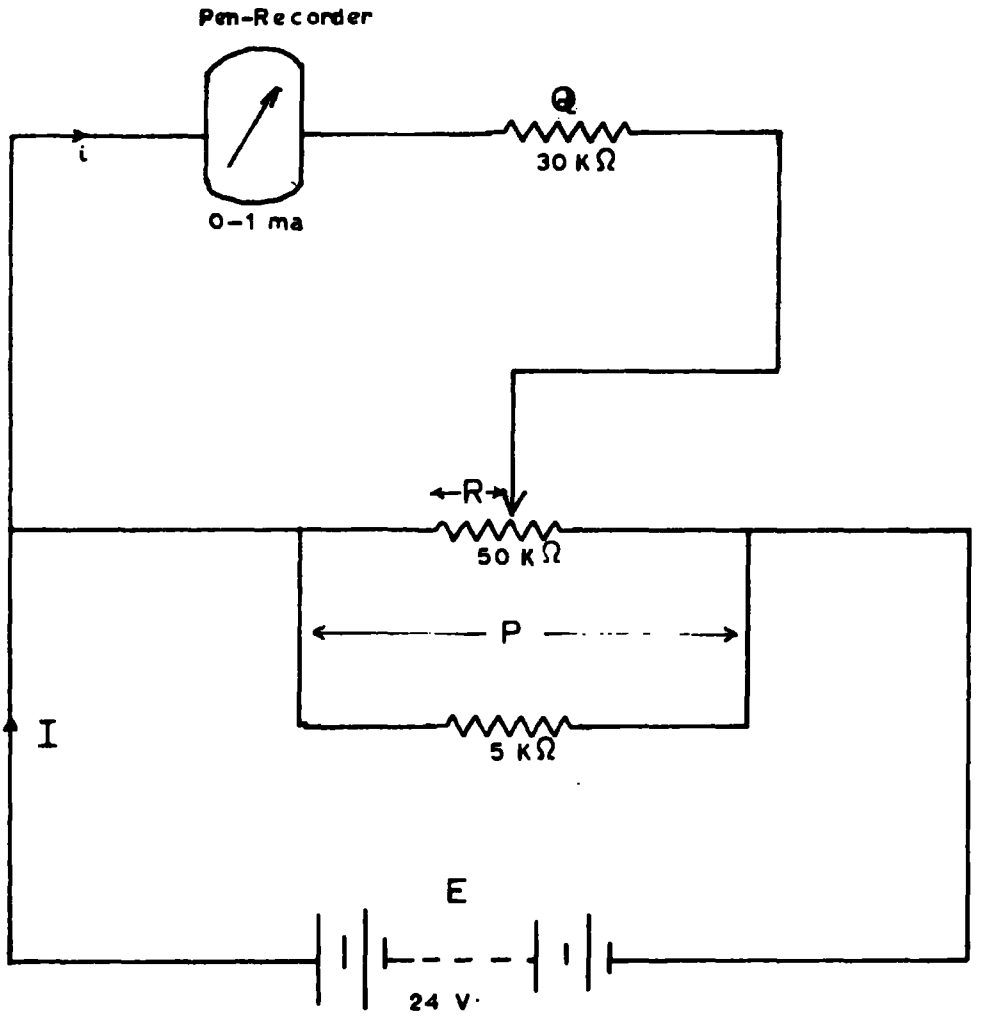

Fig. 14.

The centre tap gave a linear accuracy of resistance to within $\pm$ 0.1%, whilst the 50K type used had a $\pm$5% tolerance. The spindle was mounted in ball races, thus reducing the torque and increasing its sensitivity. The major defect of the potentiometer was the fact that the effective angle of resistance was 305°. The mechanical set-up could not be improved upon without altering the calibration. The ideal potentiometer should be one or two degrees short of 360°; but this could not be obtained. It was therefore decided to make the break-region of this available potentiometer the North-direction, this being a direction at right angles to the line of the receivers; and also a direction from which the prevailing wind in Durham does not usually blow.

From the circuit diagram:

$$I = \frac{E}{P} \qquad (\text{if } Q \gg P)$$

$$i = \frac{RI}{Q} = \frac{R}{Q} \times \frac{E}{P}$$

i.e. $i \propto R$.

$$i = i_{max}, \quad \text{when } R_{max} = P$$

$$i_{max} = \frac{R_{max}}{Q} \cdot \frac{E}{P}$$

$$= \frac{E}{Q} \quad (\text{independent of } P.)$$

Using a 24 v d.c. source therefore, the value Q = 30K gave a maximum current of 0.8 m.a.

The 50K wire-wound potentiometer was used because it was readily obtainable, and it was of a robust size enough to carry the vane. This had to be shunted with a 5K resistor in order to satisfy the

CHANGE–OVER CIRCUIT for recording WIND-SPEED and WIND-DIRECTION

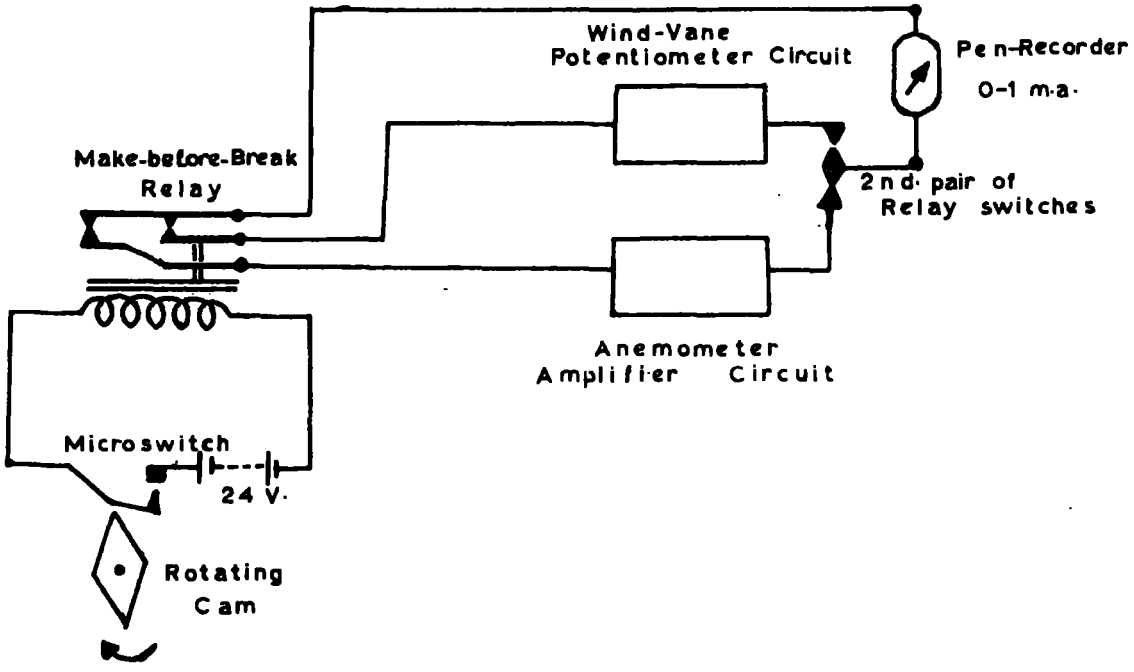

Fig. 15.

requirement stated above, for otherwise, either E or Q would have to be unduly increased. The combination was still a potentiometer but of maximum value 5K.

2.6 Method of recording the Wind-speed and direction

It was stated earlier that the author was in possession of a 4-channel pen-recorder whereas five parameters needed to be recorded simultaneously. The problem of how to use one of these pens to record two of the parameters therefore arose. As a solution, it was decided to use a single pen for the wind-speed and direction.

The same synchronous motor-operated cam that was used for the field-mill sign-discrimination device was also used for the present purpose. It was arranged such that the cam operated on a microswitch which in turn closed a relay-circuit, once every half minute (Fig. 15). Thus for about 5 seconds in every half minute, the pen-recorder was switched off from the anemometer circuit on to the wind-direction circuit. The wind-direction trace then appeared as rectangular pulses on the wind-speed record as can be seen on the actual records.

2.7 Recording Method

Photographic method of recording was first contemplated and for this, a dark box, already used by an earlier worker, was re-designed to house four Tinsley mirror galvanometers and an electric motor-worked rotating-drum camera, because the recording room could not be converted into a dark room very easily. The idea was later abandoned in favour of a pen-recorder, the advantages of which are quite obvious.

2.7.1 The pen-recorder

The pen-recorder used was a commercial instrument supplied by the firm of Everett Edgcumbe and Co. Ltd. It consisted of four writing pens, this being the maximum number of movements that could be fitted into one recorder. If more than four parameters were to be recorded, it would be necessary to have, say, two Triplex recorders. This was thought undesirable because of the unjustified increase in cost, and because it might be troublesome trying to synchronise two such instruments, hence the author had to devise the means of using one of the pens to record both the wind-speed and direction, as already explained.

All the four writing pen systems were entirely independent units, and were mounted apart from, and immediately behind, the chart driving mechanism. Each unit was essentially a moving coil d.c. milliammeter of high sensitivity, 1 ma. f.s.d. (this coincided with the V.R.E. full scale range), with galvanometer response time of 0.5 sec. However, since both positive and negative rain currents were to be measured, the appropriate pens were centre-zeroed (i.e. $\pm$0.5 ma. full scale); this means only half full-scale deflection on the V.R.E. was utilised. This did not lead to much loss of sensitivity; it, in fact, was desirable since the V.R.E. readings had been found not to be linear at the upper range of its scale for negative currents (Ramsay, 1959). The driving mechanism was a synchronous motor, working off the mains, and the chart speed was 3 inches (or 75 mm) per minute. By changing the driving cog-wheels

the speed of recording could be altered to $\frac{1}{2}$ inch per minute, thus allowing for the investigation of slowly varying parameters (cf. Fig. 19, 3 inches/minute, and Fig. 11, $\frac{1}{2}$ inch/minute).

An indicating scale was provided and so arranged that the writing pen, acting as a pointer, gave an instantaneous indication of the current being measured, thus combining the advantages of both a recording and indicating instrument. The author could therefore sit at a reasonable distance and watch these pointers. As soon as it started to rain, the V.R.E. needle and the recording pen would deflect, and the worker would set the recording chart in motion by switching on the mains and the record would thus be taken.

2.7.2 Recording

Records were taken only when the present worker was present to operate on the switches whenever there was precipitation. It was found impracticable to make the systems work automatically, first because the manipulation of the range switches of the V.R.E. could only be done manually; secondly, because some visual observations of the prevailing weather conditions were thought desirable and also because the recording speed was so fast that any automatic recording could lead to a collossal waste of the recording paper if there was any delay in switching off after the precipitation had stopped even for only about 15 minutes. It would be recalled that a 15-minute delay amounts to a run of some 45 inches of the recording paper!

Fortunately, the present worker lived at a short walking distance to the recording room and by listening to the weather forecast on his wireless (and these were more often than not accurate!) he made sure he was present to take a considerable number of records (except in the dead of night) under various types of weather conditions.

However, an attempt was made to devise an automatic recording system that might by-pass the difficulties listed. This proved unsuccessful.

Since the movements of the recording pens were quite visible there was no difficulty to note where exactly, on the record, any change of scale on the V.R.E. had taken place. This was a major advantage over the photographic method, where an accurate log of monitoring operations had to be kept.

As soon as the recording was stopped, the paper was removed, labelled, and kept for analysis at any suitable time thereafter. Analysis consisted of taking readings of any interesting section of the record directly off the paper, using the calibration curves and scales, at suitable time intervals, of the rain-currents (amps/metre^2), potential gradient (volts/metre), wind-speed (m/s) and wind-direction (degrees, measured from East-West direction as zero, thisbeing the direction along which the receivers were always displaced).

Statistical analysis of the data, and the results obtained, are discussed in the appropriate sections of this thesis.

Computation of results was made much easier by the use of the Elliott 803 digital computer purchased by the University of Durham just in time for the author to use it.

CHAPTER III

CALIBRATION AND PERFORMANCE OF APPARATUS

3.1 The Receivers

The display meter on the indicator unit of the V.R.E. used with each receiver had been calibrated in terms of the voltage in millivolts, developed across the input resistor; hence it was quite easy to convert this voltage to the direct current flowing through this resistor by merely dividing the voltage by the resistance. This gave the instantaneous values of the current received by the receiver. The effective area of the receiving cone was taken as the receiving area of the shielding cone. This was 1/30 of a square metre. The current density in amp/m^2 was thus obtained by multiplying the current above by 30. Further simplification of the calibration of the recording chart was provided by the fact that the V.R.E. gave a current output of 1 ma. f.s.d. on any of the ranges of millivolt scale on the panel meter and the pen-recorder was also a 1 ma milliammeter. A simple conversion table of the number of divisions on the recorder chart corresponding to the current density to the receiver was drawn up and it was quite possible to observe the pen deflections and convert these to the current density almost instantaneously even during the process of recording.

For the whole of the first year that the receivers were left in the open there was not any fault with them except occasionally after a heavy rain when the V.R.E. was observed to deflect steadily negative. It usually came back to normal only if the receiver was brought indoors and kept dry. As time went on, this steady negative zero-drift was no longer limited to heavy rains, it was observed to occur even during light rain. This was discovered by covering up the receiver whenever it was raining, with the hope that the V.R.E. would come to zero. Instead, it always deflected negative, but when switched to the 'set-zero' position, it would come to zero. This indicated that the trouble was that of insulation break-down. The trouble was finally completely eliminated by covering the input plessey plug completely in silicone compound - a moisture-proof, non-melting, greasy stuff.

3.2 The V.R.E.

On the front panel of the V.R.E. a socket for a standard tip and sleeve jack-plug was provided. Aknown D.C. voltage from a direct reading potentiometer circuit was inserted through this socket, and the calibration of each range of the instrument was checked and adjusted accordingly. There was also provision for setting the potentiometer in the meter circuit of the indication unit in order to match any external milliammeter used. This was also done.

FIELD–MILL CALIBRATION

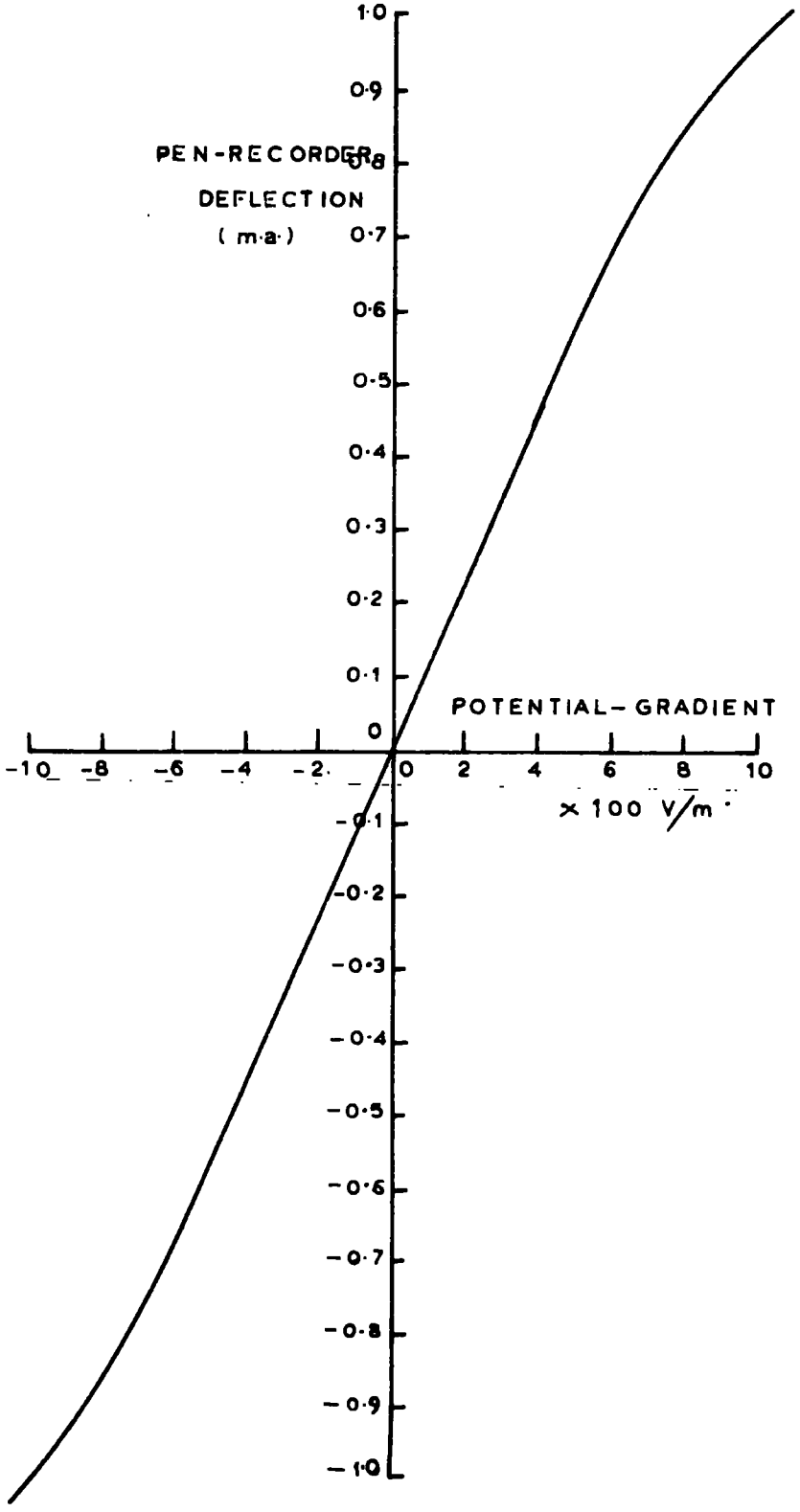

Fig. 16.

The instrument was left switched on throughout the period of the author's work. This was essential for its maximum zero stability. Day to day stability was given by the manufacturers as 1 mv. and short term stability was considered even better than this. However, the earlier experiences of the author with the performance of the V.R.E. were not very pleasant because of the erratic nature of the zero drifts and the large negative deflection occurring after heavy rains, already mentioned. Having discovered that insulation break-down was the major trouble, much of the headache was relieved. By constantly changing and drying the desiccator supplied to keep the reed and anvil surfaces free from moisture, the trouble with the instrument was brought to a minimum.

3.3 The Field Mill

The calibration of the field mill consisted of setting the field mill between two parallel metal plates, with the vanes mounted inside a circular hole through the lower plate, flush with plate. The upper plate was mounted on four cylindrical wooden blocks, each of length 10 cm. A known potential, from H.T. batteries, was applied to the upper plate whilst the lower one was earthed. The deflection on the pen-recorder was noted for each value of potential, and hence field, applied. The calibration curve drawn up is as shown in Fig. 16.

To make sure that the lines of force landing on the stationary vanes of the mill were reasonably vertical, thus ensuring that edge effects were insignificant, the parallel plates were made large (0.6 m^2) compared with the vanes.

The mill was then mounted in the position in which it was to be used, on a handy-angle stand, with the vanes facing downwards to prevent them from the rain. In a position such as this, and the fact that the whole set-up was on the flat roof of the physics building, 12 metres above the surrounding ground, the natural lines of force were bound to be distorted, and magnified by a certain factor - the Exposure Factor. This factor was determined by comparing the record as given by the field mill with another record taken at the same time at the observatory, some 900 metres away, due West, on a day when the weather was such that it could be assumed that there would not be much difference between the potential gradients at the two places. This proposition is a bit far-fetched, however, since it rests on the assumption of the absence of space charges within the space separating the two places. The comparison with the observatory records was therefore done from time to time in order to keep a check on any significant differences between the values of the exposure factors thus calculated.

The field mill at the observatory was itself calibrated against an ideal one which was mounted flush with the ground level on an open grass field at the observatory.

Anemometer Calibration

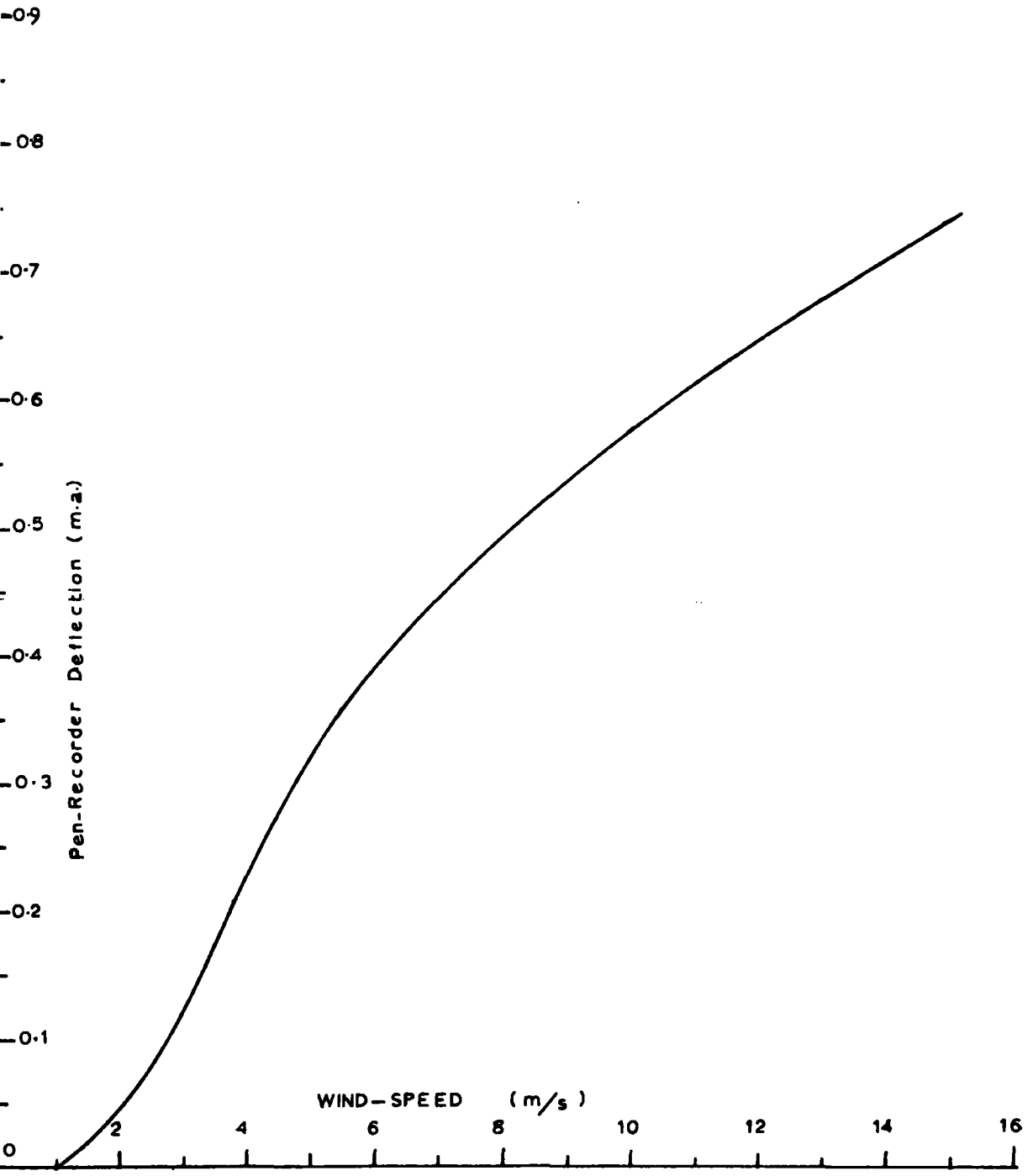

Fig. 17.

Throughout the period of use, the field mill gave no trouble whatever, this being due to the fact that suitable precautions were taken during its construction, as already discussed under paragraph 2.3 of this thesis.

3.4 The Anemometer

The anemometer was calibrated in the wind-tunnel of the National Coal Board, Scientific Division, Benton, Newcastle-upon-Tyne. It, with the amplifier, was calibrated against the AVO meter using its 0-1 ma range because the pen-recorder was much too bulky to carry to the wind-tunnel. The pen-recorder was in turn, calibrated against the AVO. This second calibration was found necessary because, even though both were 0-1 milliammeter, the resistances of their moving coils were not the same, with the result that they gave different readings when inserted, in turn, in the same circuit. The readings were in fact, inversely proportional to their respective resistances.

The calibration curve is as shown in Fig. 17, the shape of which is due partly to the nature of the a.c. voltage generated by the motor with the frequency of rotation of the cups and partly to the characteristics of the transistor amplifier.

The anemometer was insensitive to wind-speeds less than 1 m/s, but very sensitive to wind-speeds between 2 and 10 m/s - this being the range of values of interest to the present worker.

The anemometer gave no trouble whatsoever except once or twice when the gale-force wind blew the cups off the support and had them shattered, resulting in the moulding of new plastic cups and a re-calibration of anemometer! It was thereafter realised that if the cups were rotated clockwise (instead of anti-clockwise) the fixing screw would tend to be tightened more and more as the wind became stronger and stronger and so the cups could no more be loosened off, unless the whole support was knocked over. This was safe-guarded, however, by fixing the stand rigidly with a couple of sand-bags as seen in Fig. 1.

A constant check on the calibration was kept by a second anemometer used by an earlier worker, mounted on the same stand, one foot below the author's. This other anemometer had previously been calibrated against a scalamp galvanometer, and no amplification of the generated signal was necessary. By making a visual observation of the scalamp deflection, mounted as in Fig. 2, the author could detect if there was any loss of sensitivity due to the flattening of the batteries used for the amplifier or not.

3.5 The Wind-Direction

The break-region in the rotary potentiometer used for the wind-direction measurement was set due North, using an ordinary laboratory compass. The potentiometer was so arranged that a maximum current of 0.8 ma flowed through the recording milliammeter when the potentiometer was at zero resistance, and zero current for maximum resistance of the potentiometer, thus a linear scale on the record

chart was obtained with the North position at these 0 and 0.8 ma part of the record chart. For the East, South, and West directions, the record read 0.2, 0.4 and 0.6 ma respectively. Intermediate directions were correspondingly obtainable. However the accuracy was not much better than about 5°. This was not a serious drawback since the rain-current receivers were always separated in the East West direction only.

The wind-direction was recorded for only 5 secs. in every half-minute as already explained. This trace could be seen as rectangular pulses on the actual record. No confusion with the wind-speed trace occurred since these rectangular pulses were at regular distances apart.

CHAPTER IV

STATISTICAL PROCEDURE OF ANALYSIS OF RESULTS

4.1 Straight line of best fit to observational data

Suppose we have a set of n pairs of values of 2 related variates, (x_1, y_1), (x_2, y_2), ..., (x_i, y_i), ..., (x_n, y_n), which are assumed to be plotted as points on a scatter diagram. The equation to the straight line to be fitted to the points is given by

$$y = ax + b, \quad \text{where a and b are constants.}$$

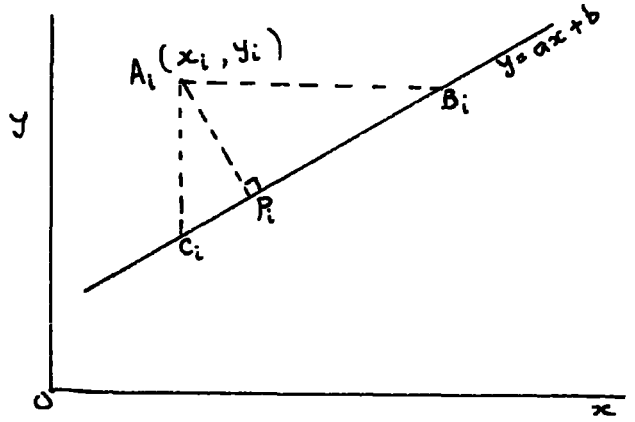

As shown in the diagram above, let A_i represent the point (x_i, y_i). A_iB_i, A_iC_i, are drawn parallel to the x- and y-axes respectively. A_iP_i is drawn perpendicular to the straight line. The departure of the point A_i from the line $y = ax + b$ can be measured in various ways, e.g., distances such as A_iB_i, A_iC_i, A_iP_i or B_iC_i. These departures, in terms of x_i, y_i, a and b are $(y_i-ax_i-b)/a$; (y_i-ax_i-b); $(y_i-ax_i-b)/(a^2+1)^{\frac{1}{2}}$; and $(y_i-ax_i-b)(a^2+1)^{\frac{1}{2}}/a$, respectively. These are all particular cases of the general form

$$(y_i-ax_i-b)\theta(a), \quad \text{where } \theta = f(a).$$

Applying method of least squares, a and b are determined by minimizing the expression

$$\sum_{i=1}^{n} (y_i - ax_i - b)^2 \; \theta^2(a), \text{ or}$$

$$\sum_{i=1}^{n} (y_i - ax_i - b)^2 \; \phi(a), \text{ where } \phi(a) = \theta^2(a).$$

The mean, $\bar{x}$, $\bar{y}$, of x and y variables respectively are

$$\bar{x} = \left(\sum_{i=1}^{n} x_i \right) / n$$

$$\bar{y} = \left(\sum_{i=1}^{n} y_i \right) / n$$

The standard deviations, s_x, s_y, of x and y respectively are

$$s_x = \left[\sum_{i=1}^{n} (x_i - \bar{x})^2 / n \right]^{1/2}$$

$$s_y = \left[\sum_{i=1}^{n} (y_i - \bar{y})^2 / n \right]^{1/2}$$

The correlation coefficient, r, between the set of pairs of variables is

$$r = \left[\sum_{i=1}^{n} (x_i - \bar{x})(y_i - \bar{y}) \right] / n s_x s_y.$$

For the fitted line to give consistent results whatever the scale adopted, the slope, a, of the line should vary directly with the related scales of measurement of the variates. The values s_x, s_y,

vary directly with the respective scales of measurement of the variates, so that 'a' should vary directly with s_y/s_x.

Morgan (1960) showed that the only expression for $\phi(a)$ which produces consistent results with change of unit is

$$\phi(a) = \text{constant}.a^k,$$

where k depends on the relative errors e_x, e_y, of x and y respectively, i.e.

$$e_x = \delta x/s_x, \quad e_y = \delta y/s_y.$$

The straight line of best fit, when both variates are subject to error, therefore, is

$$(y - \bar{y})/s_y = c(x - \bar{x})/s_x, \quad \text{where c is obtained from}$$

$$(k + 2)c^2 - 2(k + 1)\,rc + k = 0.$$

$$k = -e_x/e_y \text{ when } 0 \leq e_x/e_y \leq 1$$

$$k = -e_y/e_x - 2 \text{ when } 1 \leq e_x/e_y \leq \infty$$

$$c = \left[(k+1)r \pm [1 - (k+1)^2\,(1-r^2)]^{\frac{1}{2}}\right]/(k+2), \text{ when } k \neq -2,$$

where the sign of the radical is the same as that of r.

c = r, when k = 0. This gives the line of best fit as the regression line of y on x, i.e. when x is assumed free from error.

c = 1/r, when k = -2, giving the line of best fit as the regression line of x on y, i.e. y ~~from~~ free from error.

c = 1 when k = -1 (for r positive),

c = -1 when k = -1 (for r negative), where both x and y are subject to equal errors; the line of best fit then has a slope equal to the geometric mean of the slopes of the two regression lines.

The various values of c corresponding to other values of k in the range 0 to -2 for various values of the correlation coefficient, r, when both variates are subject to unequal errors, have been drawn up by Morgan, and this modification was applied by the present worker, wherever desirable, in drawing the straight lines of best fit.

4.2 Correlation Coefficients with time-lags between Variates

Whenever there was physical justification for assuming that the correlation between any two variates was dependent upon a certain process in motion, such as in the measurements of the potential gradients or the precipitation currents at two different places horizontally displaced, the former depending on the space-charge in motion, and the latter on precipitation cloud in motion, the above procedure of calculating the correlation coefficient was often repeated, allowing for various time lags between the variates. Curves of the correlation coefficient against the time-lag of one variate on the other were drawn, as well as the scatter diagrams corresponding to incidents of maximum or significant correlations. The slope of the graph giving the maximum, and significant, correlation coefficient was then taken as the best estimate of the regression coefficient between the variates.

4.3 Significance Test of Correlation Coefficient

The word 'significant' as used in this context should be explained. The value of the correlation coefficient, r, found between a pair of variables, should be considered on the basis of the number, n, of paired observations in the sample, i.e. the number of degrees of freedom. If the number is small, r may appear high even when there is little or no correlation at all. An extreme example is afforded when n = 2, which gives r = 1 (perfect correlation!). Hence, for small samples, it is important to test the significance of the calculated value of r by determining the probability that such a value (or a larger value) could arise as a result of random sampling from an uncorrelated population. If this probability is low, say 0.5%, the value of r is said to be significant to this level. The levels of significance for r can be obtained by referring to the appropriate tables of statistics (e.g. Biometrika Tables by Pearson and Hartley).

In all the graphs drawn in this thesis, relating the various values of r with time-lags between any pair of variables, the dotted horizontal lines drawn at r indicate the levels above (if positive) or below (if negative) which there is a probability of 0.5% that the calculated value of the correlation coefficient could result by chance from an uncorrelated pair of variables.

4.4 Trivariate Correlation

The theory of correlation and linear regression can be extended to more than two variables. If there is a correlation between two variables x, y, and also a correlation between y and another variable z, then this latter correlation will affect that between x and y; for if the value of y is to some extent dependent on that of z, then the apparent dependence of x on y may be regarded as partly representing the dependence of x on z. To eliminate the effect of z, we need to measure the correlation between x and y, when z is constant. A partial correlation coefficient, $r_{xy.z}$, may therefore be defined, the suffix after the dot denoting that the variate z is constant, and this can be regarded as the average dependence of x on y at constant z.

If we have total correlation coefficients, r_{12}, r_{13}, and r_{23} between variables 1 and 2, 1 and 3, and 2 and 3 respectively, then the partial correlation coefficient $r_{12.3}$ between 1 and 2 at constant 3 is given by

$$r_{12.3} = (r_{12} - r_{13}\, r_{23})/[(1 - r_{13}^2)(1 - r_{23}^2)]^{\frac{1}{2}},$$

the sign of $r_{12.3}$ being the same as that of the numerator.

Similarly, if there are four variables, the partial correlation coefficient between 1 and 2, the effects of 3 and 4 being eliminated is

$$r_{12.34} = (r_{12.4} - r_{13.4}\, r_{23.4})/[(1 - r_{13.4}^2)(1 - r_{23.4}^2)]^{\frac{1}{2}}.$$

Correlation should not, however, be confused with causation. An apparent relationship between two variables might merely express the

fact that both depend on a third.

4.5 Comparison of Correlation Coefficients

In order to compare correlation coefficients, a useful transformation due to R.A. Fisher may be used. This is

$$Z = \tfrac{1}{2}\left[\log_e(1 + r) - \log_e(1 - r)\right]$$

which is very nearly normally distributed, with standard deviation $1/(n-3)^{\frac{1}{2}}$. This transformation enables us to calculate approximate confidence limits for r and for a difference between correlation coefficients, and also to combine correlation coefficients from two or more samples. Tables of z for various values of r can also be obtained from the Biometrika Tables.

4.6 The Computer Programme

The author drew up an Algol programme for the Elliott 803 computer which then performed all the relevant statistical computations (See the Appendix for the actual Algol Programme). Feeding in two sets of data, x_1, x_2, x_3 .... x_i, ... x_n; y_1, y_2, y_3 .... y_i ..... y_n, the computer calculated the means $\bar{x}$, $\bar{y}$, the standard deviations s_x, s_y, of the variables x and y respectively. The constant, a_{yx}, and regression coefficient, b_{yx}, in the regression equation $y = a_{yx} + b_{yx}x$ were calculated, and also a_{xy}, b_{xy} in the regression equation $x = a_{xy} + b_{xy}y$, as well as the errors in a and b. The computer next calculated the geometric mean of the regression coefficients, giving the correlation coefficient, r. Finally, the geometric mean ~~of the slopes~~ of the slopes of the two regression

TABLE 1

S T	MY	MX	CX	ECX	RX	ERX	
	CY	ECY	RY	ERY	STX	STY	R
			GMR				
1 0	0·574	0·511	0·167	0·251	0·797	0·085	
	0·113	0·235	0·693	0·074	2·925	3·136	0·743
			1·072				
2 0	0·584	0·496	0·212	0·272	0·748	0·091	
	0·117	0·254	0·650	0·079	2·943	3·156	0·698
			1·073				
3 0	0·592	0·478	0·239	0·280	0·737	0·093	
	0·100	0·262	0·639	0·081	2·959	3·177	0·686
			1·074				
4 0	0·596	0·428	0·313	0·309	0·660	0·104	
	0·094	0·287	0·561	0·088	2·949	3·199	0·603
			1·085				
5 0	0·601	0·418	0·363	0·336	0·569	0·112	
	0·127	0·312	0·483	0·095	2·969	3·222	0·525
			1·085				
6 0	0·614	0·408	0·427	0·362	0·460	0·120	
	0·168	0·337	0·391	0·102	2·989	3·243	0·424
			1·085				
0 0	0·562	0·516	0·068	0·167	0·957	0·057	
	0·049	0·156	0·832	0·049	2·906	3·117	0·892
			1·072				
0 1	0·558	0·525	0·166	0·270	0·745	0·091	
	0·164	0·252	0·647	0·079	2·925	3·137	0·694
			1·073				
0 2	0·547	0·534	0·200	0·303	0·650	0·101	
	0·225	0·282	0·565	0·088	2·944	3·157	0·606
			1·073				
0 3	0·517	0·541	0·200	0·322	0·586	0·107	
	0·276	0·300	0·512	0·094	2·963	3·169	0·548
			1·069				
0 4	0·473	0·542	0·174	0·332	0·551	0·109	
	0·311	0·311	0·488	0·097	2·984	3·170	0·519
			1·062				
0 5	0·467	0·546	0·219	0·355	0·456	0·116	
	0·357	0·333	0·404	0·103	3·005	3·192	0·429
			1·062				
0 6	0·445	0·556	0·219	0·368	0·405	0·120	
	0·396	0·345	0·360	0·106	3·026	3·209	0·382
			1·061				

lines (with respect to y-x co-ordinate) was calculated, giving the slope of the straight line of best fit of the scatter diagram. In all, fourteen quantities were calculated in each operation.

The above procedure was repeated for $x(i+S)$ against y_i, where S is the lag of parameter x on y, i.e., if S = 4, then x_5, x_6, x_7, etc. would be compared with y_1, y_2, y_3, etc., respectively; similarly for x_i against $y\ (i + T)$ where, for T = 4, say, x_1, x_2, x_3, etc., would be compared with y_5, y_6, y_7, etc., respectively.

On the value of the correlation coefficient calculated, the significance test was performed, as already explained. If r was significant, the scatter diagram and the line of best fit would be drawn for the two sets of variables. If r was not significant, then it was thought unwise to draw up the scatter diagram at all, since small or insignificant value of r indicated that the idea of having a straight line representation would be unjustified.

A typical result sheet is as shown in Table 1, where the parameters are

y ≡ Precipitation current to first receiver,

x ≡ " " " second "

and the following notations had been adopted for easier programming:

S, T ..... Units of time lags between variables, as explained above.

MY, MX ..... $\bar{y}$, $\bar{x}$ respectively.

CX, ECX .... a_{yx}, and error in a_{yx} respectively.

RX, ERX .... b_{yx}, " " " b_{yx} "

CY, ECY .... a_{xy}, " " " a_{xy} "

RY, ERY .... b_{xy}, and error in b_{xy} respectively.

STX, STY ... s_x, x_y "

GMR ..... slope of the straight line of best fit.

R ..... Correlation Coefficient, r.

The two receivers were stood side by side when the record of Table 1 was taken. S(0), T(0), were the instantaneous records of the currents to the two receivers. The correlation coefficient, 0.89, between the currents, and the slope, 1.07, of the straight line of best fit to their scatter diagram, indicate to what extent the current measured by the two receivers, when placed close together, agreed. Each unit of time-lag shown in Table 1 represents 10-sec. lag of one parameter on the other, and 75, 10-sec. averages of the currents were taken.

4.7 Variations of wind velocity with height

In the layers of the atmosphere at levels of 500 m or more, the actual wind velocity at each level approaches very nearly the theoretical geostrophic value consistent with the pressure distribution at that level. From the earth's surface to this height, however, in a stable atmosphere, there are changes in the speed and direction of the air currents because of pressure distribution, which in most cases tend to decrease the westerly component of the motion and because of ground-friction. Under normal conditions, variations in wind velocity with height are rather complex. Near

WIND VELOCITY RATIO , V_h/V_{10} , against HEIGHT, h

after A·C· BEST

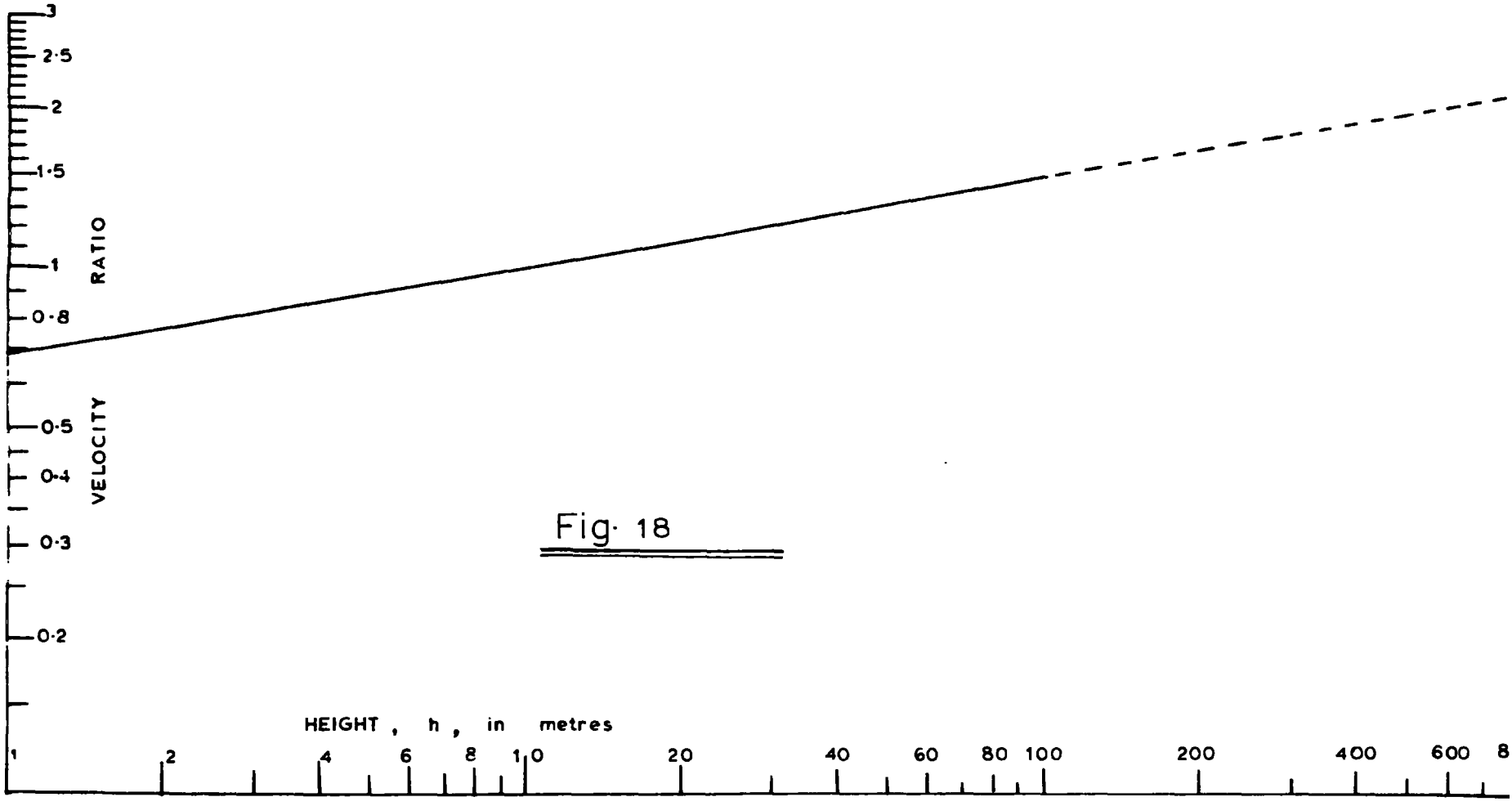

Fig· 18

the earth's surface, stream-line motion is of rare occurrence and there is a 'mixing-up' of velocities at different levels dependent upon the amount of turbulence in the intervening layers of air, which in turn, depends upon relative air temperature. Thus any law giving wind velocity as a function of height can apply rigidly only to one particular locality, and to one specified temperature gradient.

Most writers assume the form $V = kh^{\alpha}$ for the relation of mean wind velocity, v, to height, h. The index α does vary under different conditions, the variations depending principally on the temperature gradient and the type of ground surface over which observations are made. It is, therefore, impossible to lay down a rigid law for estimating the change of mean velocity with height. The power law form quoted above is the simplest. An examination of the results of A.C. Best (1935), M.A. Giblett (1932) and J.S. Dines (1912) suggests the use of $\alpha = 0.17$ for all heights up to at least 30 m. This value is that given by A.C. Best for zero temperature gradient with moderate winds and corresponds also to the modal value of Giblett's ratio V_{150}/V_{50}. The graph in Fig. 18 shows on log scales the variation of velocity with height from 1 to 100 m according to data by A.C. Best and extrapolated from 100 m to 800 m. The ordinate is the mean velocity at a given height compared with that at 10 m.

CHAPTER V

GENERAL RESULTS

5.1 Qualitative Description of Results

The apparatus described in the earlier chapters were assembled and in proper working order for almost two of the three years of this research. The earlier records taken with the photographic method were excluded from the analysis because the speed of recording was generally too slow for any definite resolution of the precipitation current records. Useful results obtained, therefore, began when the pen-recorder was in use, from June 1963 to June 1964. Opportunities were afforded, during this one year period, of taking some records in the summer of 1963, the winter of 1963-64, and in the spring of 1964. No attempt was made to analyse a lot of these records quantitatively, because a cursory inspection of them suggested no useful purpose would be served by so doing. Moreover, it was not the intention of the author to repeat what had been done by earlier workers by finding definite functional relationships between precipitation current and the potential gradient. As explained in other parts of this thesis, a better method of calibrating the field mill would be desirable to get anything near the absolute values of the potential gradient. The very few records subjected to quantitative analysis to determine correlation coefficients between any pair of the parameters measured, as well as the time-lags between corresponding points on the records, are presented under various headings

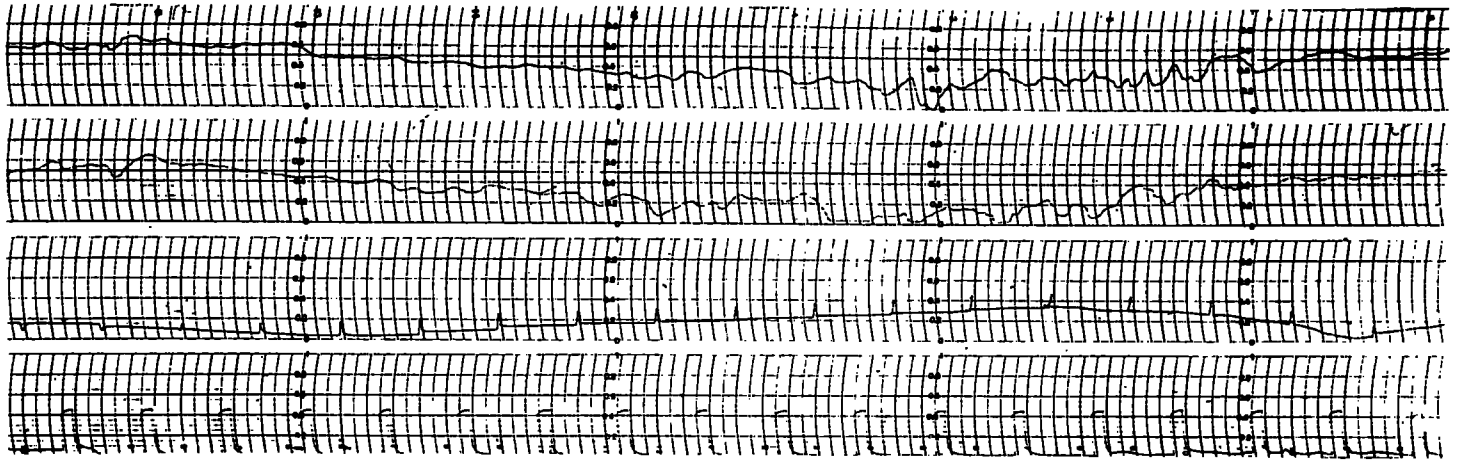

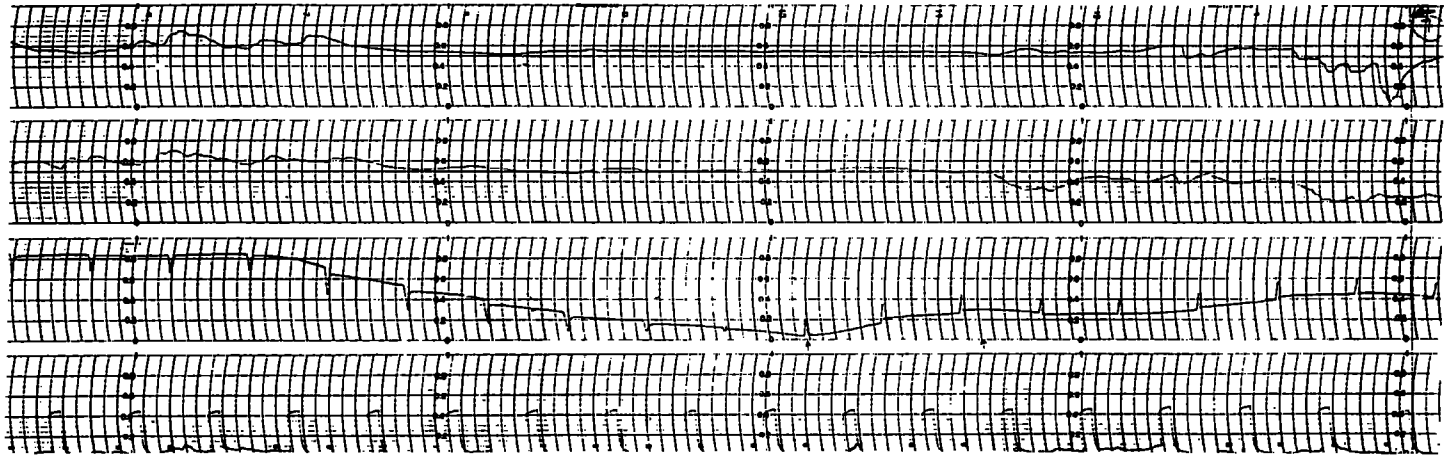

later on. Qualitative conclusions that could be made on the other records are as follows:

a. Continuous rainfall - Light and Heavy

Strong support is lent to other workers' findings about the general inverse relation between the precipitation current and the potential gradient. In quiet, continuous rainfall, the rain current was observed to be mostly positively charged whilst the potential gradient was negative. These often changed signs, the current sometimes before and sometimes after the potential gradient, but with only short time differences. Some of the actual records obtained are shown in Figs. 19 (a & b), 20 (a & b). The traces for the currents to the first and second receivers, the potential gradient, wind-speed and wind-direction on the photographs of the actual records shown in Figs. 19 to 24 and Fig. 38, are as labelled in Figs. 11 and 19.

The Summer results showed that the time lags between current and potential gradient were of the order of minutes, sometimes two or three minutes, whilst the lags were much shorter in Winter (cf. Figs. 19 & 20). Some of the results obtained during heavy rainfall did show very rapid variations of both the current and the potential gradient. The variations were so rapid that the monitoring of the recording instruments could hardly cope with them, and so, most often the records of the current and the potential gradient would be off-scale even on the largest scales of measurement, thus making quantitative analysis of continuous variations impossible. But generally,

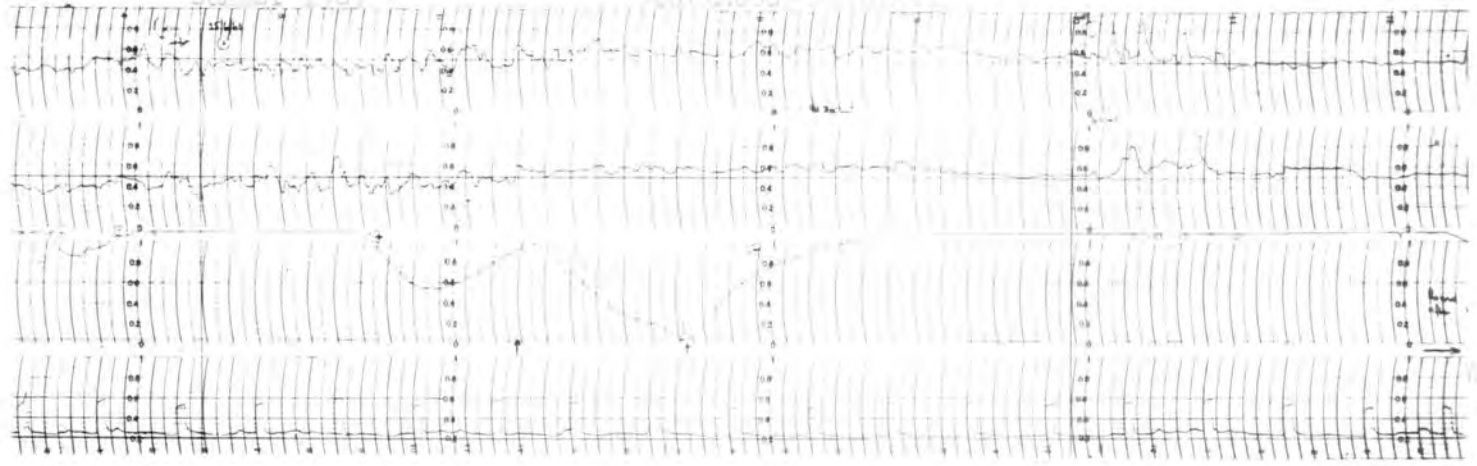

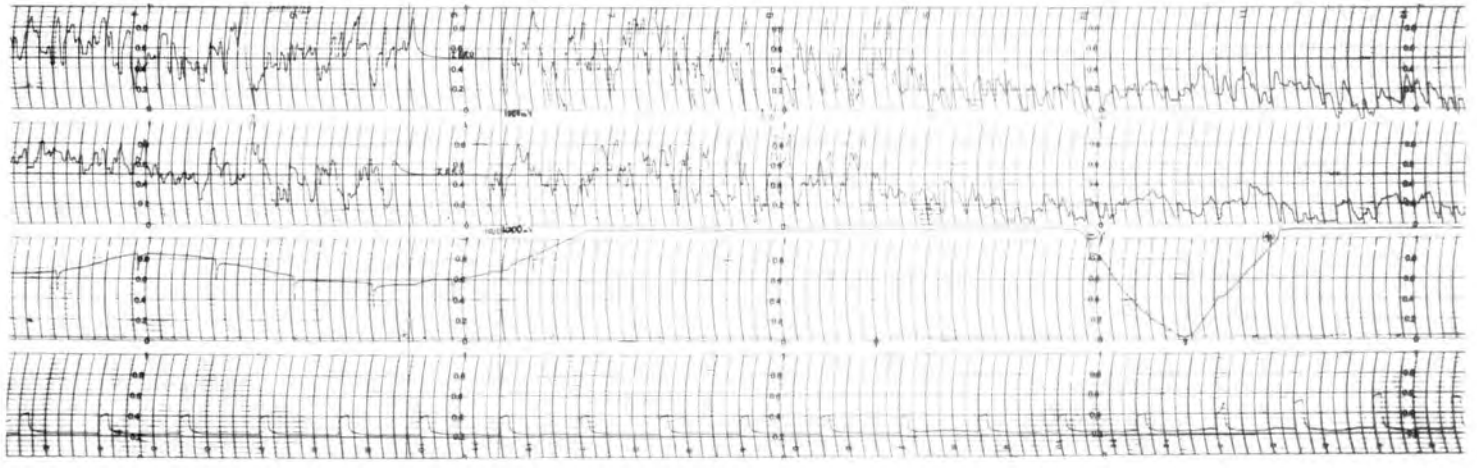

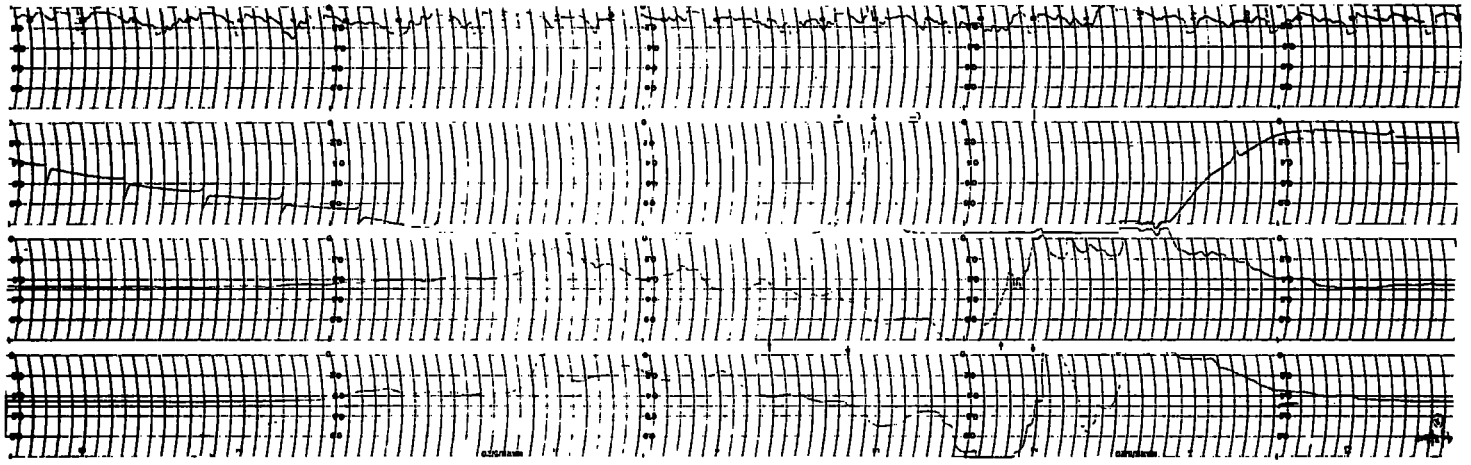

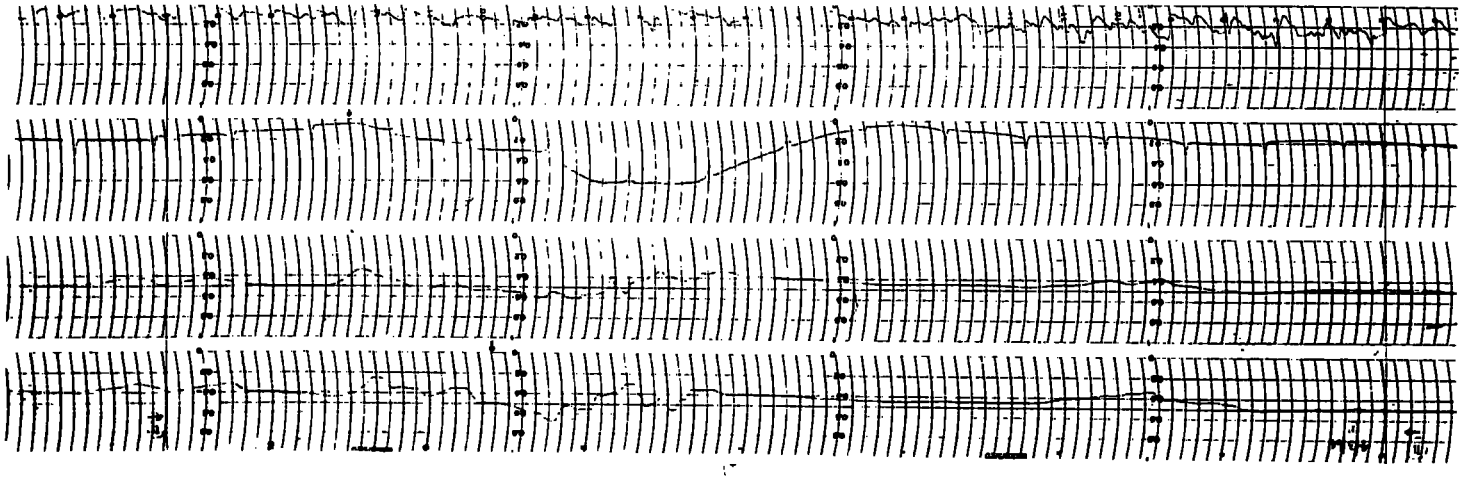

even under such turbulent conditions, the inverse relations were still observable (see Figs. 19a & 21b). The change of sign of the potential gradient was sometimes of the order of seconds, that is, one moment the potential gradient might be large and negative (>1000 V/m) and in the next five or ten seconds, it would have changed sign to a large positive value, or vice-versa (see Fig. 21b). The rain current sign changes were equally rapid under these turbulent conditions, but due to the rapid speed of recording, these sign changes were hardly simultaneous. The speed of recording, 75 mm per minute (or 1.25 mm in 1 sec.), is quite a good degree of time resolution. Lags of various times ranging from, say, 5 secs. to minutes were observable on most of the records; but whenever there were very rapid fluctuations, it became very difficult to say whether the current lagged behind the potential gradient or vice-versa. Earlier workers reported several occasions when the current and the potential gradient changed signs simultaneously. The recording of their observations were such that the time lags of less than a minute could easily be missed due either to the time constant of the recording instrument or the speed of movement of the recording chart.

Prior to the change of sign of the potential gradient, which was always a definite event, (since, apart from the sign-discrimination device, it had to go through zero to change sign) the rain current often had small positive and negative excursions about the zero-line. It was therefore difficult to decide the exact moment at which the

current changed sign. The places indicated by arrows in Figs. 19, 20, and 21, could be regarded as incidents of sign changes since the current traces were definitely to one side of the zero-line.

b. Showers

Records were obtained of rain showers lasting for about five minutes or so on several occasions. Typical records are shown in Figs. 21 to 24. Attention is here drawn to the behaviour of the potential gradient just before appreciable precipitation current was recorded. Fig. 21(a) shows an occasion when the potential gradient, previously of low positive value of about 150 V/m, changed sign to negative at the approach of a shower which initially brought down excess of negative charge. The potential gradient rose to a maximum (negative) of about-500 V/m in about a minute before the current changed sign to positive. With the arrival of the positive current, the negative potential gradient decreased in magnitude to zero, again in about a minute, changed sign and finally got back to the original steady, positive value of about 150 V/m. This shower lasted for just two minutes. A heavier shower lasting for about five minutes followed the first one, Fig. 21(b), seven minutes later. Again, with the approach of the negatively charged shower, the potential gradient became negative, and rose to over -1000 V/m in less than a minute. The current changed sign to positive, and the potential gradient too changed sign a minute later to positive.

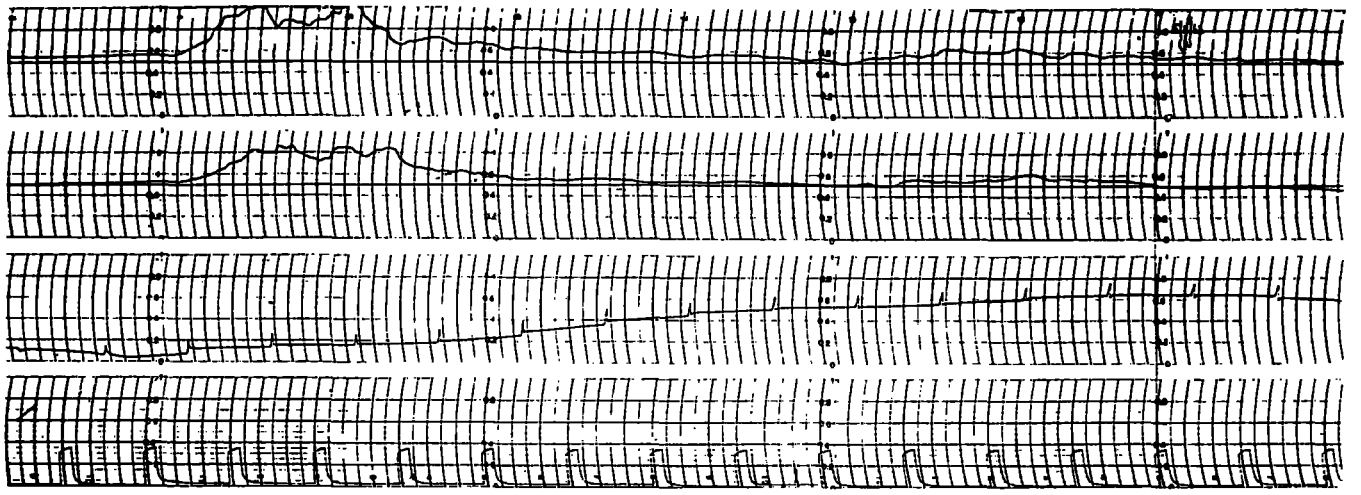

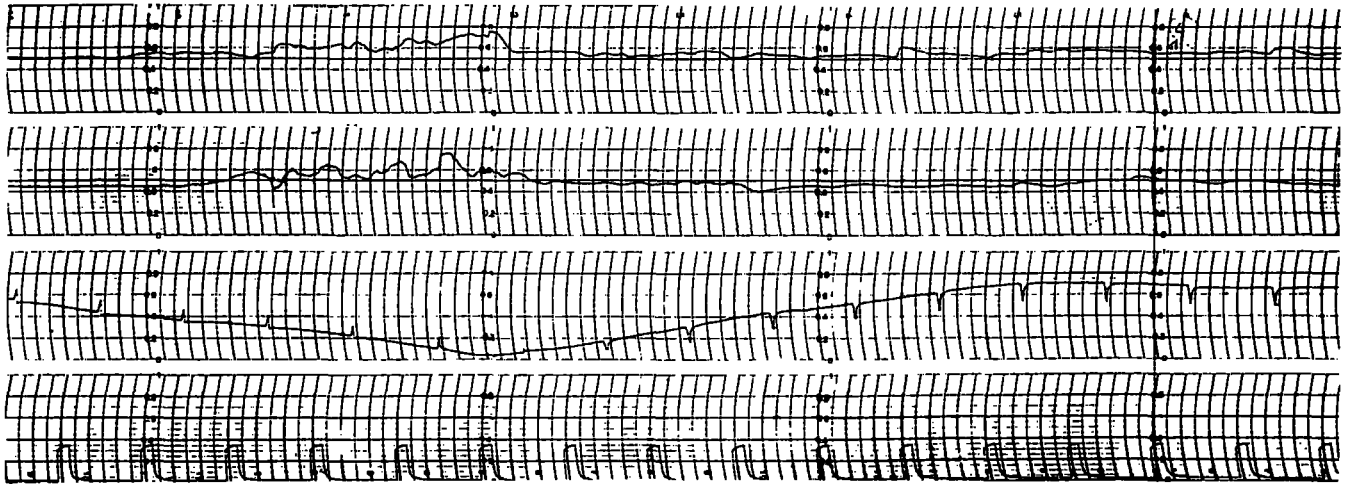

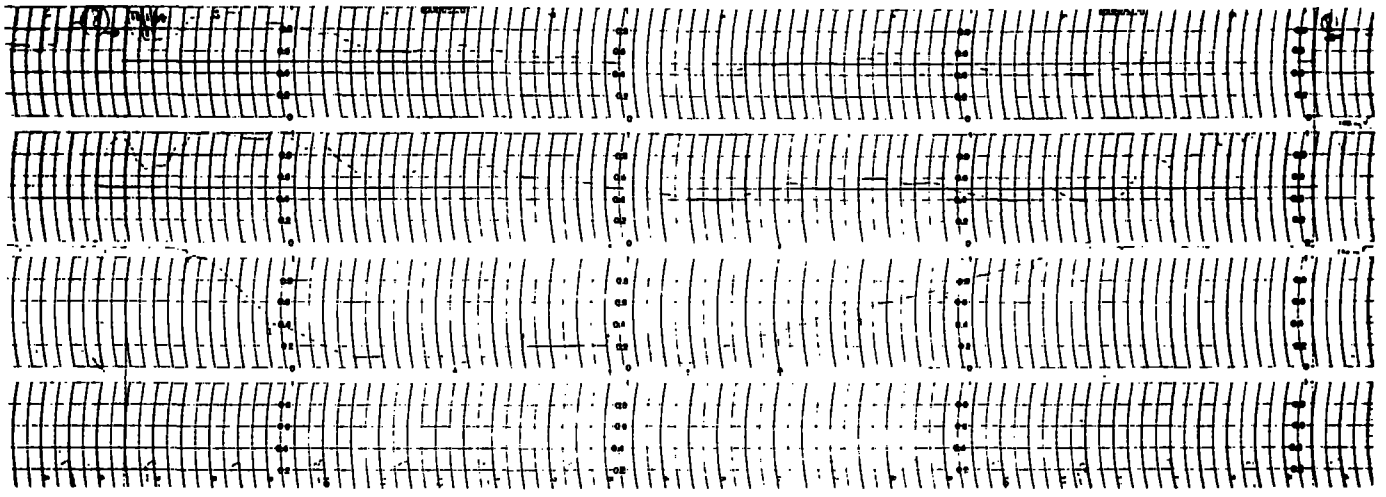

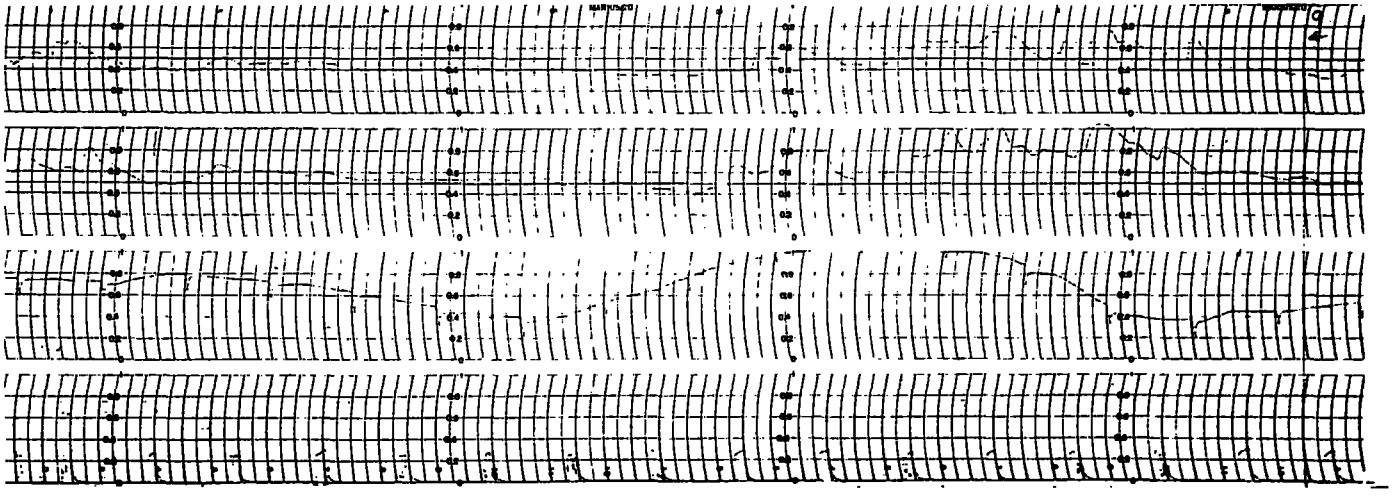

This sort of behaviour occurred on several occasions when showers were recorded. Fig. 22(a) is another example, but Fig. 22(b), which is a continuation of Fig. 22 (a) gave a slightly different picture in that the potential gradient, though positive, was already decreasing before the arrival of the shower. The inverse relation between current and potential gradient was more marked in continuous rainfall than in shower type. Figs. 23, 24 were occasions when the relation held for shower-type rains however.

c. Correlation between currents measured by two receivers displaced 30 metres apart

The principal aim of this investigation is to find out how far apart two identical rain-current receivers could be displaced horizontally before a break-down of the correlation between the currents measured occurred. The two receivers placed on the flat roof of the Physics building were capable of being separated horizontally to about 30 metres. An examination of the records obtained showed clearly that at 30 m separation, under continuous, steady precipitation from a widespread cloud, such as that from the Nimbostratus cloud, the currents had a somewhat similar general trend. That is, over a period of, say, 5 mins., both currents could be observed to go either progressively positive or negative. Due to the fast speed of recording, however, an examination of the records within a period of seconds might show quite a poor correlation. A typical record taken with the receivers close together, and later-on separated by

about 30 m, during a continuous rainfall, gave values of correlation coefficients of 0.90 and 0.84, respectively. Both records were averaged at 10-sec. time intervals over a period of 10 mins. These two values of correlation coefficients are not significantly different, that is, we cannot refer to them statistically as being samples from two different parent populations. A much shorter time interval analysis of the correlation coefficient (5-secs. averages of three 2-min. sections of the same record), gave the values 0.57, 0.39, and 0.39, for the case when the two receivers were 30 m apart. Only the first one of these is significantly different from zero statistically.

Much more interesting records were obtained in conditions of rain and snow showers. Very few records were obtained of the very beginning of these showers since the recording was not automatic. Sometimes, after a period of a shower, the record was left on if a possibility of occurrence of another shower was suspected. Figs. 21 and 22 are examples of such. The lower records in eachcase are continuations of the upper ones, but in the case of Fig. 21, the two records were separated by 7 minutes when there was no precipitation, and in Fig. 22, the lower record is a direct continuation of the upper one. Even under these shower conditions, it was rather difficult to say precisely if one rain receiver collected some raindrops at a definite time before the other, even when the wind was blowing in the direction of the receivers, as was the case in Fig. 21. The

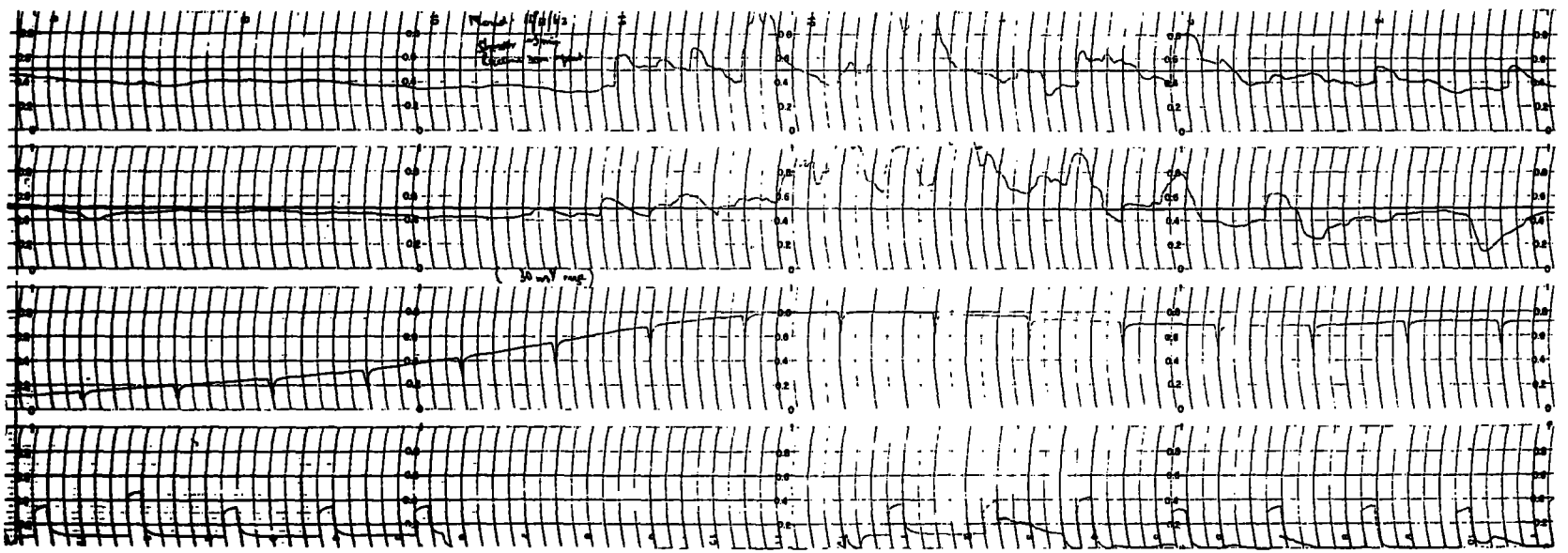

reason for this is that the onset of rain was usually not instantaneous. A few drops usually fell here and there, and the rain-current traces could be observed to traverse the zero-line up and down, but keeping rather close to the line.

Fig. 24 shows a typical rain shower lasting for some 6 minutes. The receivers were separated 30 m apart. The correlation coefficient between the two currents over the 6-min. period was found to be 0.46, averaging at 5-sec. intervals. The values of 0.68, 0.20, and 0.55, were obtained when the record was divided into 3 sections, each of about 2 minutes duration. The first value (0.46), is more significant than the other three because a greater number of pairs of readings was involved. Nevertheless, this value is still poorer than that obtained (0.84) for continuous rainfall.

The results shown in tables 2 to 6 are the values of the correlation coefficients between the currents to the two receivers I and II for various time lags (and leads) of the current to receiver I on that to receiver II. Results shown in table 2 were obtained for a rain-shower lasting for some fifteen minutes, and the receivers were placed side by side. The other results in tables 3 to 6 were for steady, continuous rainfall, with the receivers separated by 30 metres. The readings were averaged at 10-sec. time intervals.

Tables 2 to 6 are tables of correlation coefficients, r, between the rain currents to receivers I and II against time-lags (and leads) of the current to receiver I on that to receiver II.

Table 2

Receivers placed side by side: Rain-shower 4.10.63

	Time lag							Time lead →					
Time (secs)	60	50	40	30	20	10	0	10	20	30	40	50	60
$r \times 10^{-3}$	293	414	575	682	807	848	926	854	818	759	646	544	414

10-secs. averages of 15-min rain-shower.

n = 100; 0.5% significance level for r for n = 100 is 0.25

$r \times 10^{-3}$	-526	-425	-441	133	9	348	880	229	29	44	-524	-424	-337
	166	-111	-39	-227	142	176	748	261	542	412	218	-102	-26
	-60	156	447	611	765	836	917	853	829	845	680	625	346
	-228	318	699	860	933	898	970	832	793	504	377	95	-133

Pooled value of r, using the z-transformation = 0.90; 0.5% significance level of r is 0.5.

The last 4 rows above are for 4 equal sections of the same record.

Table 3

Receivers 30 metres apart: continuous rainfall 7.11.63

	Time lag							Time lead →					
Time (secs)	60	50	40	30	20	10	0	10	20	30	40	50	60
$r \times 10^{-3}$	131	72	78	210	389	496	486	371	266	181	261	387	385

10-sec. averages of a 20-min. section of the record.

n = 120; 0.5% significance level of r for n = 120 is 0.25.

$r \times 10^{-3}$	542	313	187	371	578	570	556	516	363	336	457	436	355
	-45	-278	-362	-233	51	344	243	-41	-108	-89	120	521	617
	144	-125	-411	-233	186	463	566	421	202	-62	62	149	-154
	474	167	71	9	-27	-41	220	88	-66	-360	-404	-134	19

The last 4 rows above are for 4 equal sections of the same record.

n = 30; 0.5% significance level of r for n = 30 is 0.5.

Table 4

Receivers 30 metres apart: Continuous rainfall 15.11.63

	Time lag							Time lead →					
Time (secs)	60	50	40	30	20	10	0	10	20	30	40	50	60
$r \times 10^{-3}$	823	834	855	881	893	896	893	875	869	855	824	795	775

10-sec. averages of 10-min. section of the record.

n = 60; 0.5% significance level of r is 0.35

$r \times 10^{-3}$	389	401	391	429	484	520	545	623	616	590	603	549	464

10-sec. averages of another 20-min. section of the same record.

n = 120; 0.5% significance level of r is 0.25

Table 5

Receivers 30 metres apart: Continuous rainfall 21.11.63

Time (secs)	60	50	40	30	20	10	0	10	20	30	40	50	60
$r \times 10^{-3}$	612	610	629	645	665	758	895	793	663	647	589	509	511

10-sec. averages of a 12-min. section of the record.

n = 72; 0.5% significance level of r is 0.30

Table 6

Receivers 30 metres apart: Continuous rainfall 19.11.63

	Time lag							Time lead →					
Time (secs)	60	50	40	30	20	10	0	10	20	30	40	50	60
$r \times 10^{-3}$	754	793	833	882	919	943	954	956	936	910	878	827	804

10-sec. averages of a 12-min. section of the record.

n = 72; 0.5% significance level of r is 0.30

$r \times 10^{-3}$	578	635	733	807	852	883	934	919	926	929	880	815	765
	-42	77	21	263	466	556	653	733	643	492	231	-247	-397
	475	499	613	711	799	879	897	862	752	639	583	414	405

Pooled value of r for the instantaneous readings of the current, using the z-transformation is 0.864.

n = 24; 0.5% significance level of r is 0.5.

The values of the correlation coefficients between the instantaneous readings of the currents were in all cases significant to 0.5% level. As the time lag between the currents was increased, these values of correlation coefficients fell steadily from their maxima which, in nearly every case, occurred for the instantaneous readings. Where the maximum is not for the instantaneous readings, as in table 3 (1st, 2nd, and 3rd rows), table 4 (1st row) and table 6 (1st and 3rd rows), the respective values were found not significantly different statistically from the values for instantaneous readings of the currents.

In table 4, results for two different sections of the same record are shown, these being the steady portions of the record. The pooled value of the correlation coefficients, determined by the Z-transformation method, was 0.77.

The last 4 rows in tables 2 and 3 respectively and the last 3 rows in table 5 are for much smaller periods of time than those shown in the first row of each table. Even for such short periods of time, the correlation still remained strong when the receivers were placed side by side, (table 2), but at 30 metres separation, it varied quite a lot.

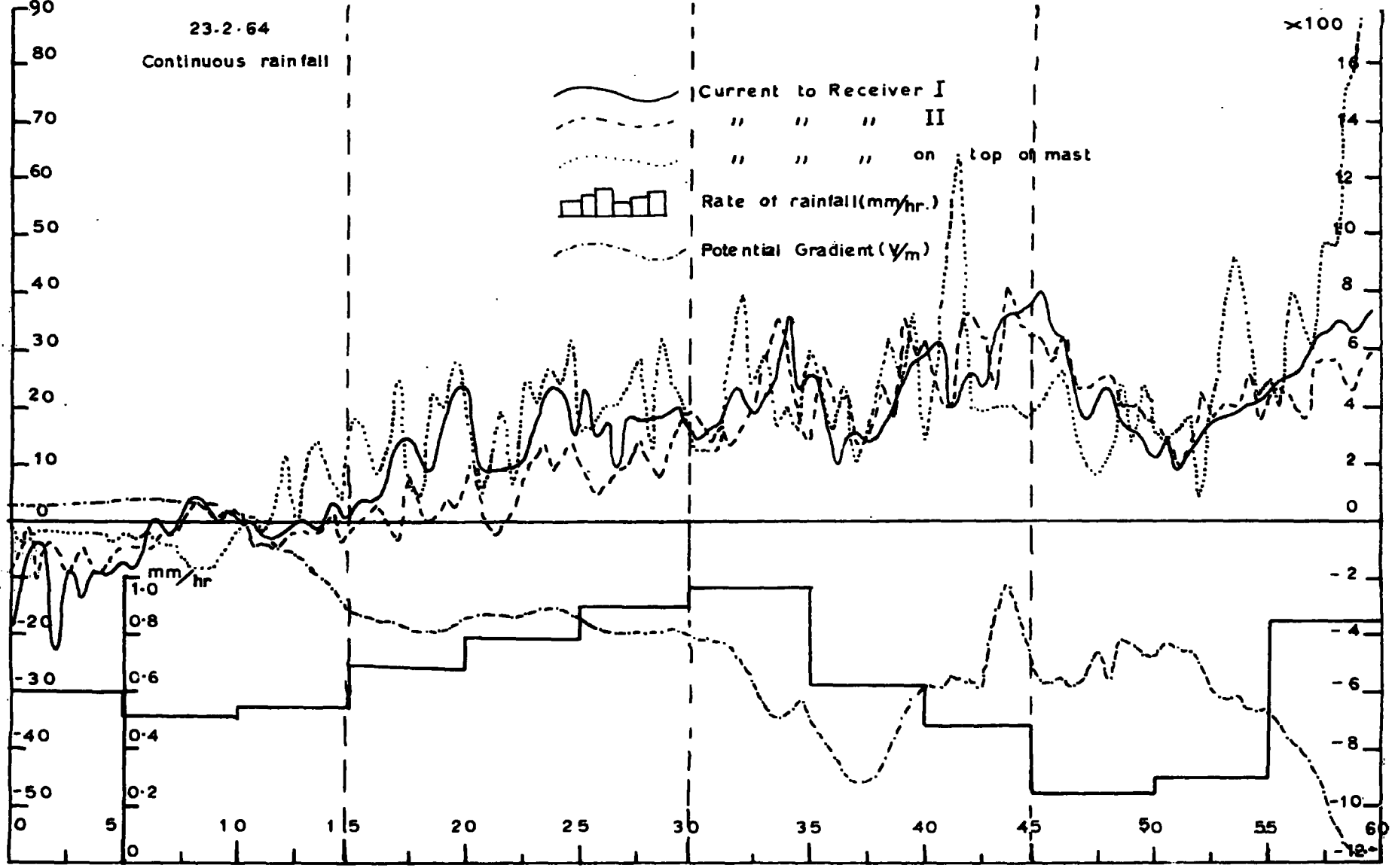
23.2.64
Continuous rainfall
Current to Receiver I
" " " II
" " " on top of mast
Rate of rainfall (mm/hr.)
Potential Gradient (V/m)
×100
mm/hr
mins

Fig. 25.

d. Correlation between currents measured by two receivers displaced 900 metres apart

In view of the above observations, the author's attention was diverted to comparing the records as measured at the Science Laboratory with those measured at the University Observatory by a colleague of his, H.L. Collin. To do this, the speed of recording at the laboratory had to be geared down to $\frac{1}{2}$ inch per minute (or 12.5 mm/min). The two places were 900 metres apart in an East-West direction. It was also an easy matter to synchronise the times of recording.

Some of the records taken at these two places could not be analysed quantitatively, too, because of the very rapid variations of the parameters. However, two interesting records were analysed. The first one, taken on 23rd February, 1964, under continuous rainfall, and the other, taken on 19th March, 1964, when there was a five-hour continuous recording of snow current, are discussed below.

5.2 Continuous rainfall

On 23rd February, 1964, an hour's record was taken of the rain currents to the two receivers at the laboratory, displaced 30 metres apart in an E-W direction, rain current to the receiver on top of the 25 metre mast at the observatory, the potential gradient on top of the mast and the rate of rainfall. Fig. 25 is

Figs. 26, 27: Graphs of correlation coefficients, r_{xy}, against time-lag (or lead) of x on y.

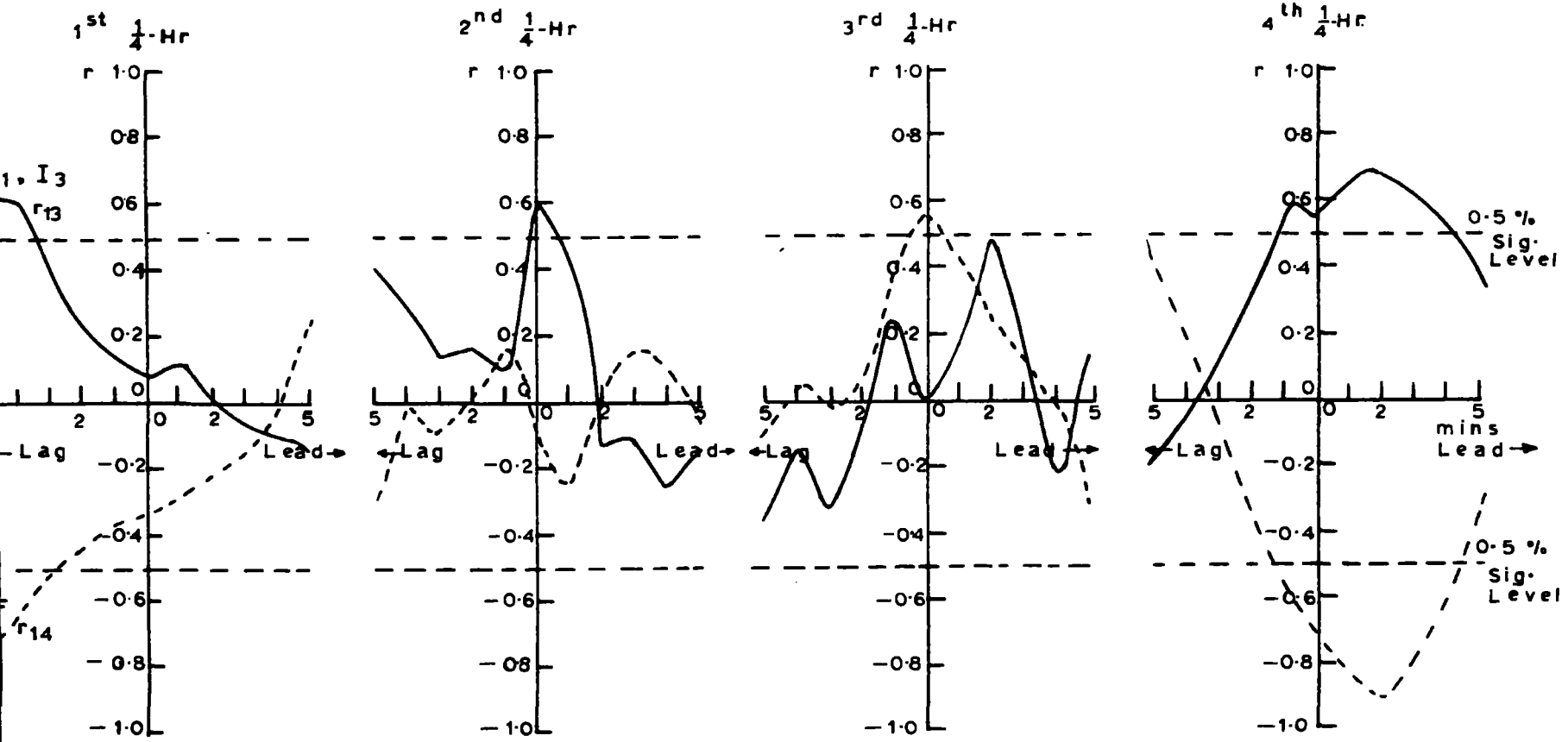

Fig. 26.

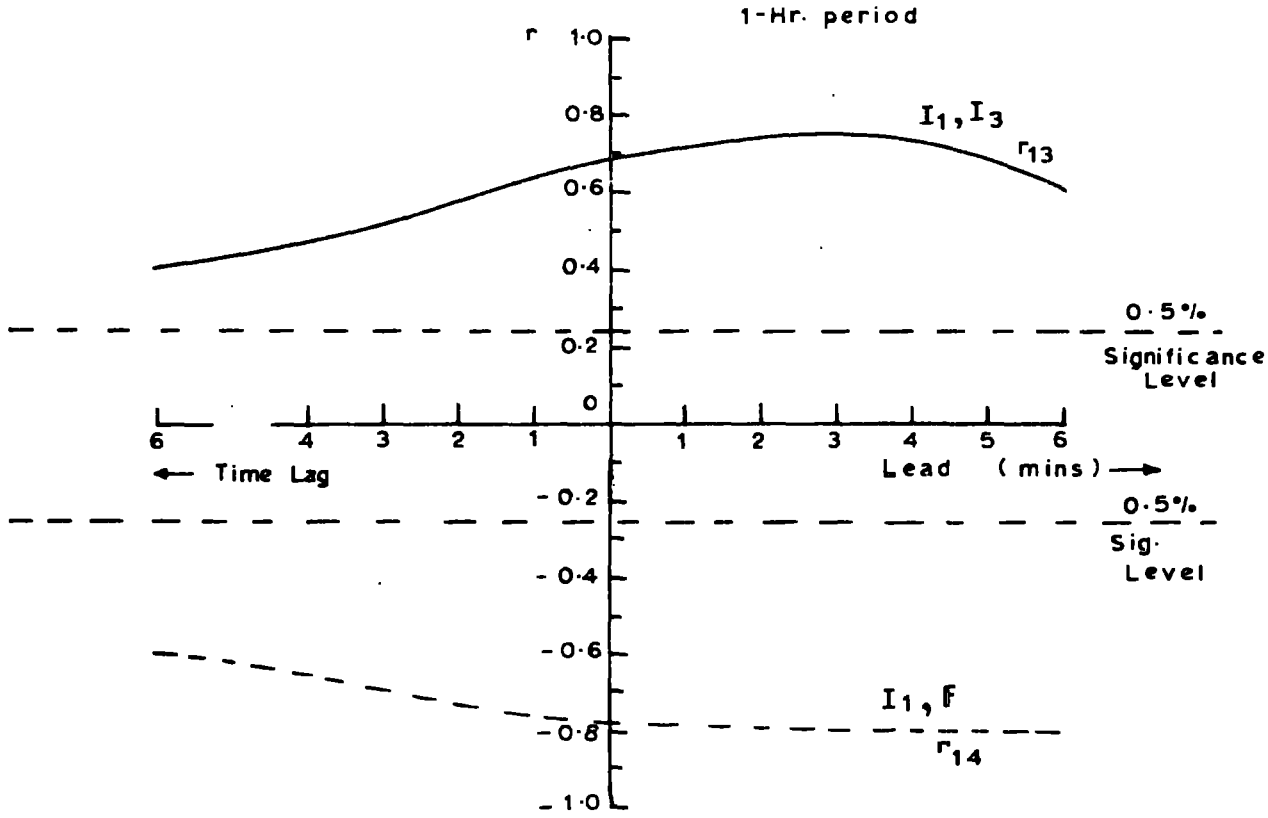
1-Hr. period
r
1·0
0·8
0·6
0·4
0·2
0
-0·2
-0·4
-0·6
-0·8
-1·0
I_1, I_3
r_{13}
0·5% Significance Level
0·5% Sig. Level
I_1, F
r_{14}
6
4
3
2
1
1
2
3
4
5
6
← Time Lag
Lead (mins) →

Fig. 27.

a plot of half-minute averages of these parameters. It can be seen that there is a good correlation between the three rain currents even at such distances apart as 30 m and 900 m! A record of the wind speed showed that there was very little wind, mostly below the lower limit of measurement (1 m/s). The wind direction was constant at S.E. The record of the current on top of the mast showed some individual sharp peaks, which had been interpreted by Collin as due to splashing of raindrops in the high potential gradient on the mast. These peaks are more pronounced on the latter half of the record where the potential gradient is much higher than the earlier part.

Numbering these parameters as 1, 2, 3, 4, to stand for the rain currents at the laboratory (1 & 2), rain current on top of the mast (3), and the potential gradient (4), the following values were obtained for the correlation coefficients between each pair of parameters over the whole one-hour period:

$r_{12} = 0.86$ $r_{13} = 0.69$ $r_{14} = -0.77$ $r_{34} = -0.78$ $r_{13.4} = 0.03$

(the correlation coefficient between the two rain currents measured at 900 m apart, at constant value of the potential gradient).

The record was divided into four quarter-hour sections and the correlation coefficients r_{13}, r_{14}, determined for various time-lags between 1 & 3, and 1 & 4 respectively. The curves obtained are as depicted in Fig. 26, which shows that for simultaneous recordings of

TABLE 7

	1st $\frac{1}{4}$-hr.	2nd $\frac{1}{4}$-hr.	3rd $\frac{1}{4}$-hr.	4th $\frac{1}{4}$-hr.	Whole hour
n =	30	30	30	30	120
Mean current I_1 x10^{-12} a.m^{-2}	-4.1±1.1	14.4±1.1	22.8±1.4	23.0±0.1	14.0±1.2
Mean current I_3 (at Obs.) x10^{-12} a.m^{-2}	-0.7±1.0	18.5±1.4	23.3±2.0	30.2±3.9	17.8±1.6
Mean Potential Gradient F(at Obs.) V/m	2.5±18.7	-354±5.1	-601±32.5	-660±40.4	-403±27.5
Mean rate of rainfall mm/hr.	0.55	0.79	0.69	0.46	0.62
r_{13} (Simultaneous readings)	0.08	0.58	0.00	0.55	0.69
r_{14} (Corr. Coeff. between I_1 & $F_{Obs.}$)	-0.36	-0.10	0.54	-0.73	-0.77
r_{34} (Corr. Coeff. between $I_{Obs.}$ & $F_{Obs.}$)	-0.79	-0.02	0.02	-0.88	-0.78
$r_{13.4}$ (Corr. Coeff. between I_1 & $I_{Obs.}$ at const. F)	-0.08	0.51	-0.02	-0.02	0.03

Main currents to two receivers, 30m. apart.

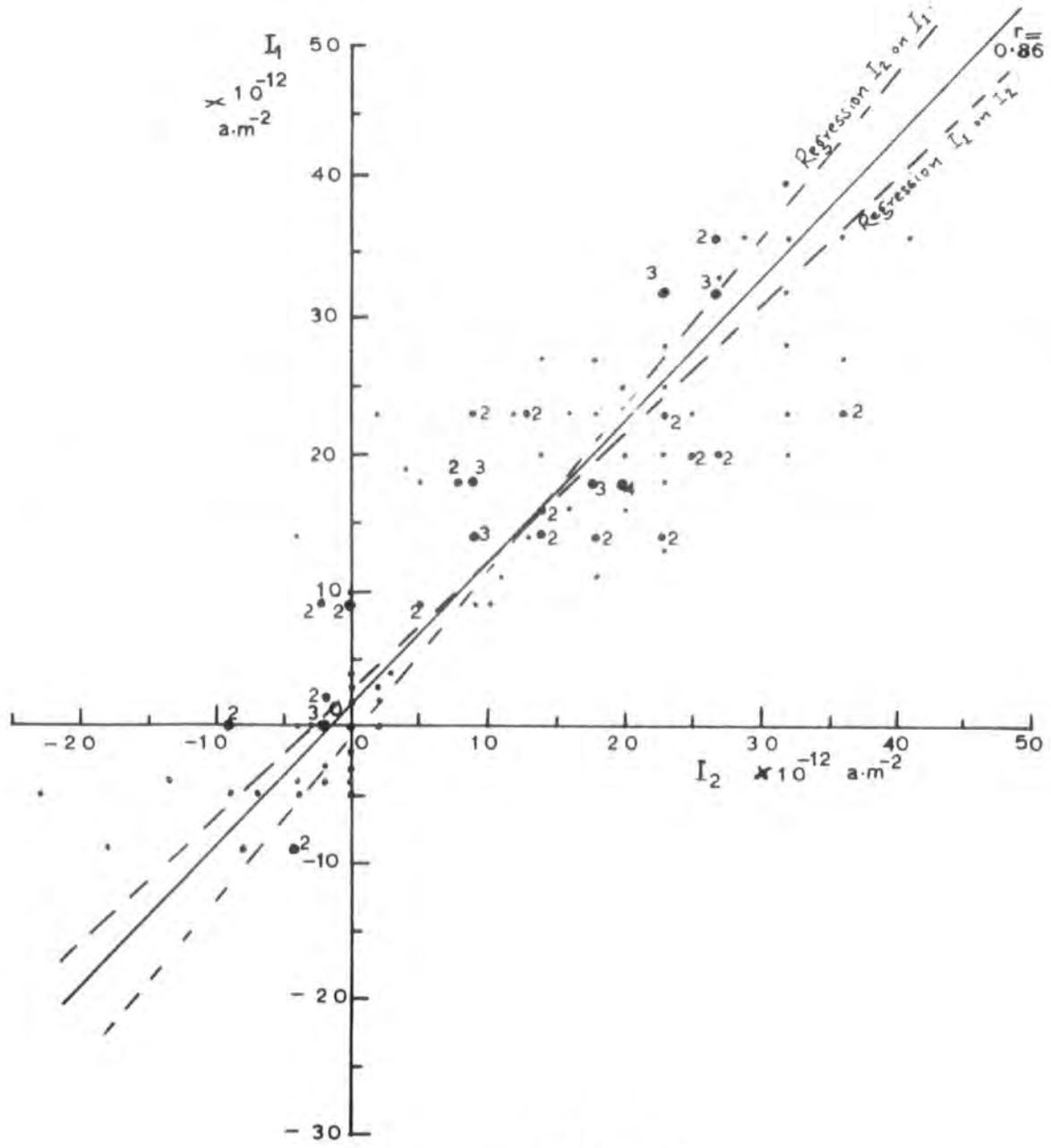

Fig. 28.

Main currents in two receivers, 900m. apart.

(I_3 at top of grid)

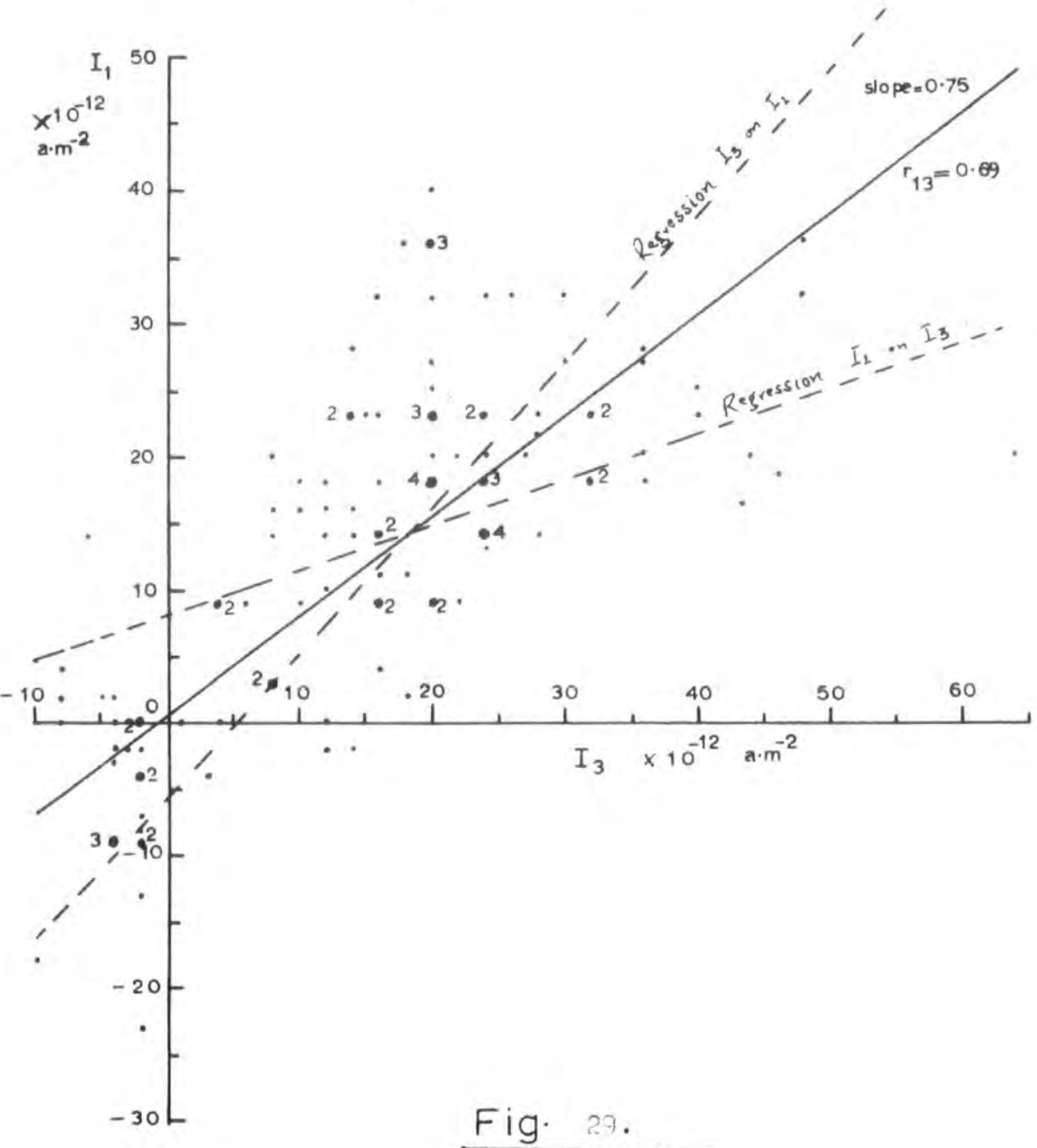

Fig. 29.

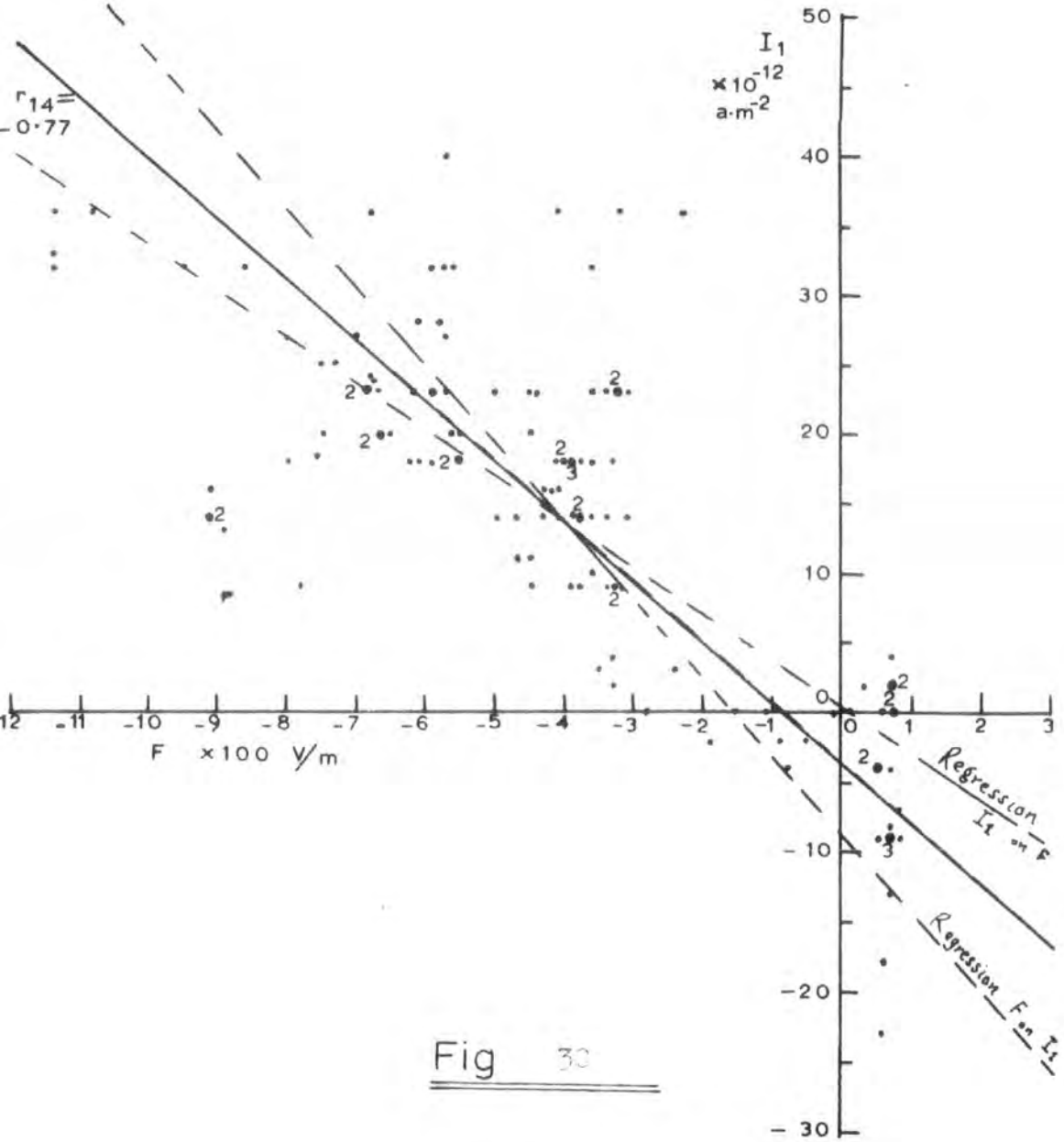

Fig 30

/ Scatter diagram : Continuous rainfall.

the currents, various values can be obtained for the correlation coefficients over short intervals of time. In this case, the first and third quarter-hour periods gave values which were not significantly different from zero, whilst the second and fourth quarter-hour periods gave values of 0.58, 0.55 respectively, which are significant. On the other hand, the correlation coefficient obtained taking the whole hour together, as shown in Fig. 27 indicates quite a good correlation coefficient of 0.69 between the two currents. This lends support to the idea that when two receivers are displaced some distance apart, the short-term variations of the currents may not be correlated, but that over a longer period of time, some correlation may be found, especially if the rain is from a widespread layer cloud.

Table 7 gives the values of the mean currents, the mean potential gradient, mean rate of rainfall, and the correlation coefficients r_{13}, r_{14}, r_{34} and $r_{13.4}$ for the quarter-hour periods as well as for the whole hour.

The scatter diagrams between I_1 and I_2, I_1 and I_3, I_1 and F, are shown in Figs. 28, 29, 30, respectively.

From the histogram at the bottom of Fig. 25, depicting the rate of rainfall, it can be seen that the first half hour, when the potential gradient was between 0 and -400 V/m, the current increased with the rate of rainfall, but no such relation could be seen for the second half when the potential gradient was between -400 V/m and -1200 V/m.

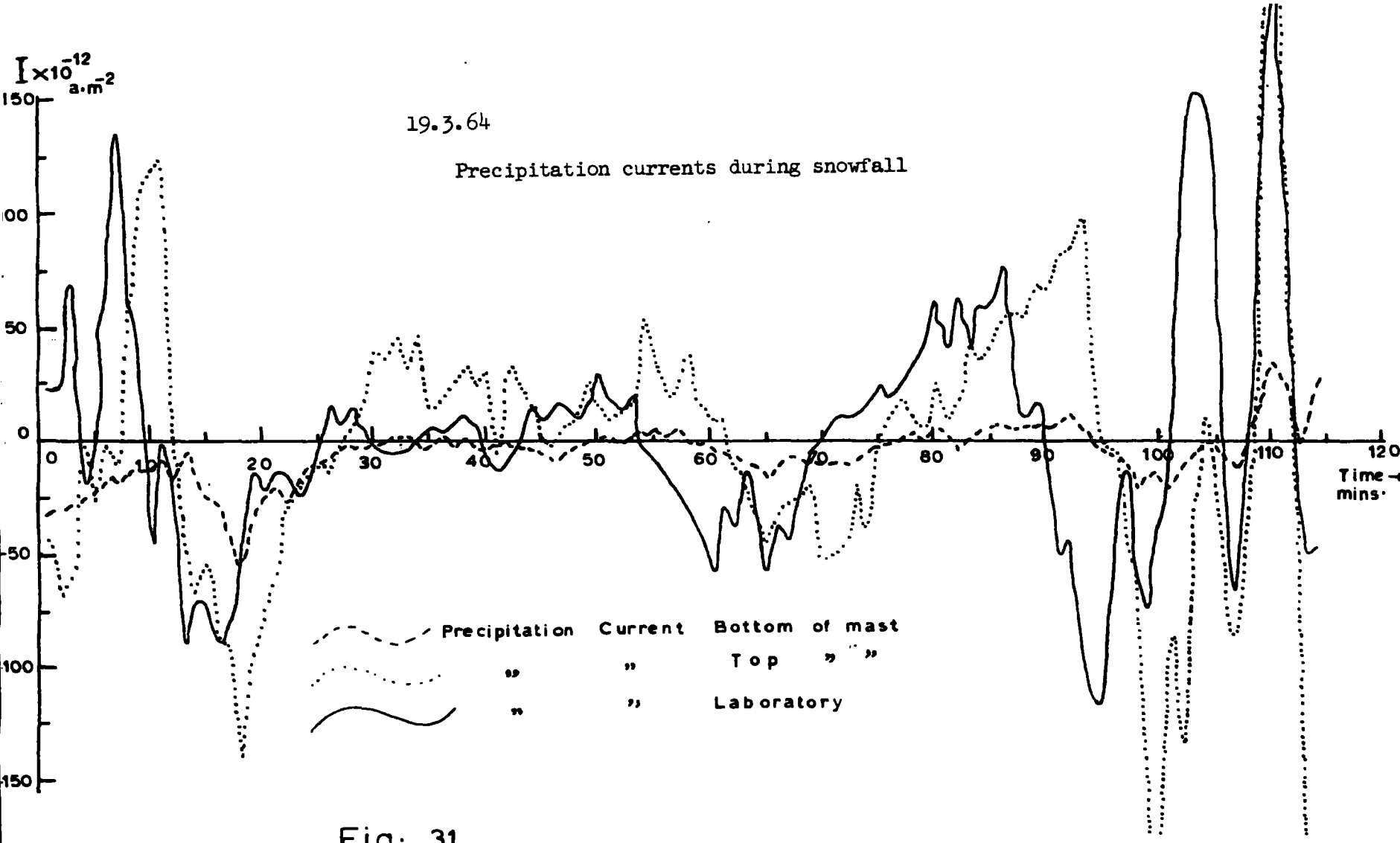
I×10⁻¹² a·m⁻²
19.3.64
Precipitation currents during snowfall
150
100
50
0
-50
-100
-150
0
10
20
30
40
50
60
70
80
90
100
110
120
Time - mins.
Precipitation Current Bottom of mast
" " Top " "
" " Laboratory

Fig. 31

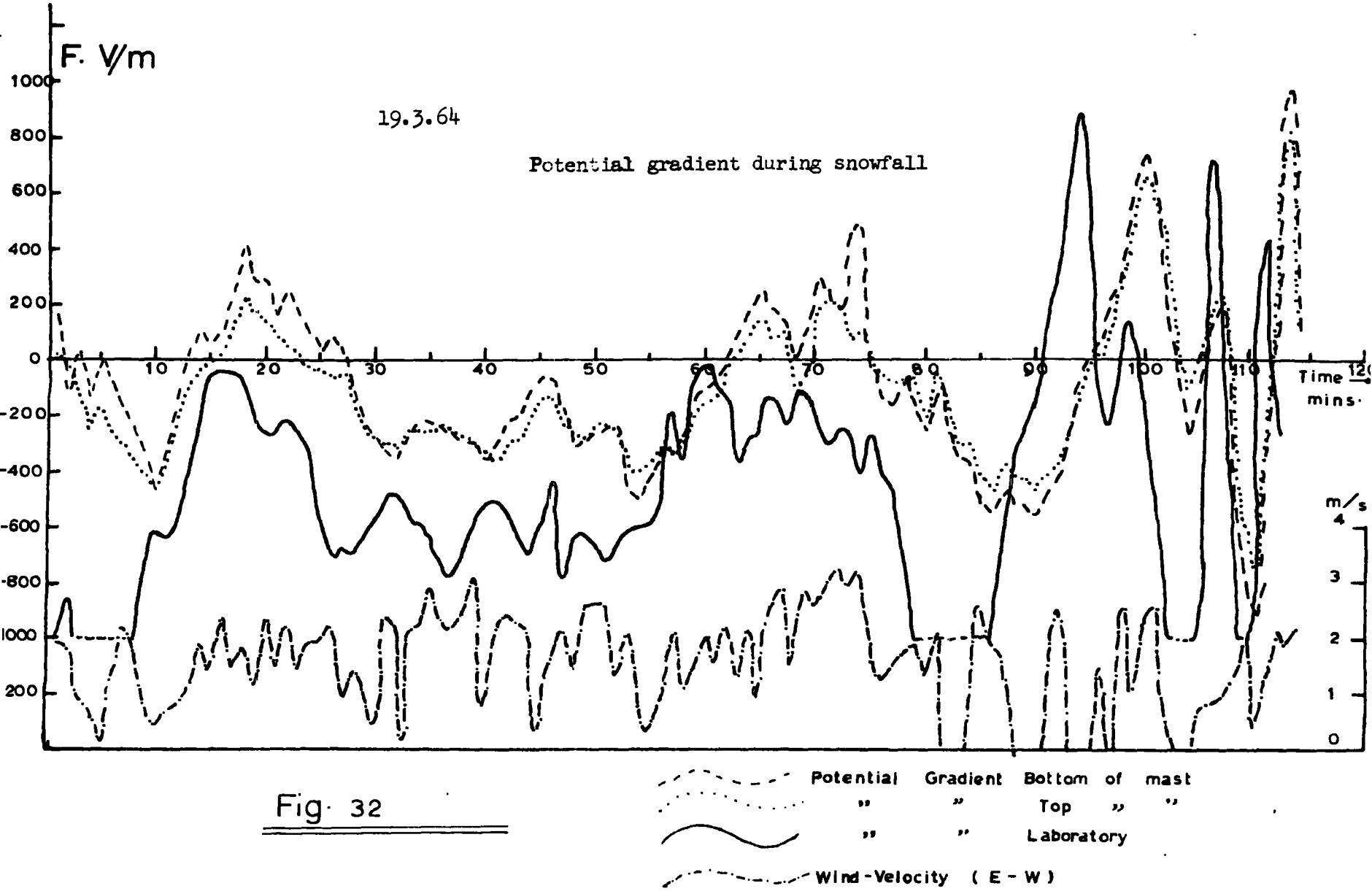
F. V/m
19.3.64
Potential gradient during snowfall
1000
800
600
400
200
0
-200
-400
-600
-800
1000
200
10
20
30
40
50
60
70
80
90
100
110
Time
mins.
m/s
4
3
2
1
0
Potential Gradient Bottom of mast
" " Top " "
" " Laboratory
Wind-Velocity (E - W)

Fig. 32

5.3 Snow

On 19th March, 1964, a belt of low pressure moved across the whole of the British Isles. Snow and Fog prevailed throughout the whole day. A continuous record lasting for about 5 hours was made of the current and the potential gradient at the laboratory as well as at the top and bottom of the mast at the observatory. A record of the wind speed and wind direction was also taken at the laboratory. Only two hours of the five-hour record gave fairly steady values. For the rest of the record, conditions were rather turbulent; the potential gradient was off-scale (i.e. >1100 V/m) and changing rapidly whilst the current was equally rapidly varying. Figs. 31 & 32 are plots of one-minute averages of these parameters.

From Fig. 31, it can be seen that the current on top of the mast at the observatory followed that at the laboratory quite faithfully, with a definite time-lag between them. This is also true of the potential gradients, (Fig. 32).

The two potential gradients at the top and bottom of the mast had corresponding peaks simultaneously, though the values were sometimes the same and sometimes not, indicating, perhaps, variations in the space charges between the top and bottom of the mast (see Collin and Raisbeck, 1962). Variations in the potential gradient were also identifiable with the variations in the wind speed measured at the laboratory, but there was no correlation between their magnitudes.

Simultaneous readings of Snow currents to two receivers, 900m. apart.

(I_1 at bottom of mast)

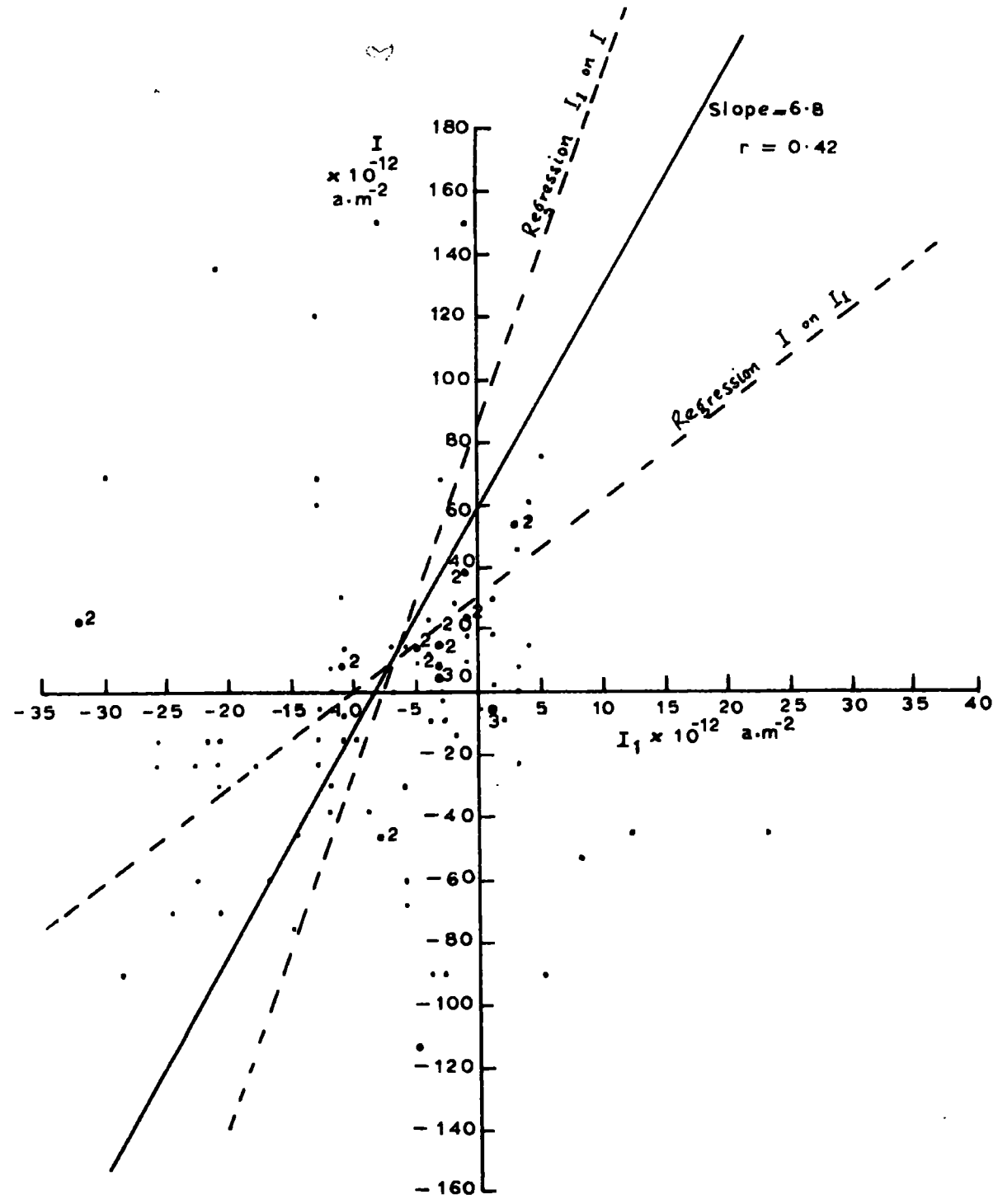

Fig. 33.

Simultaneous readings of snow currents to two receivers, 900 m. apart.

(I_2 at top of mast).

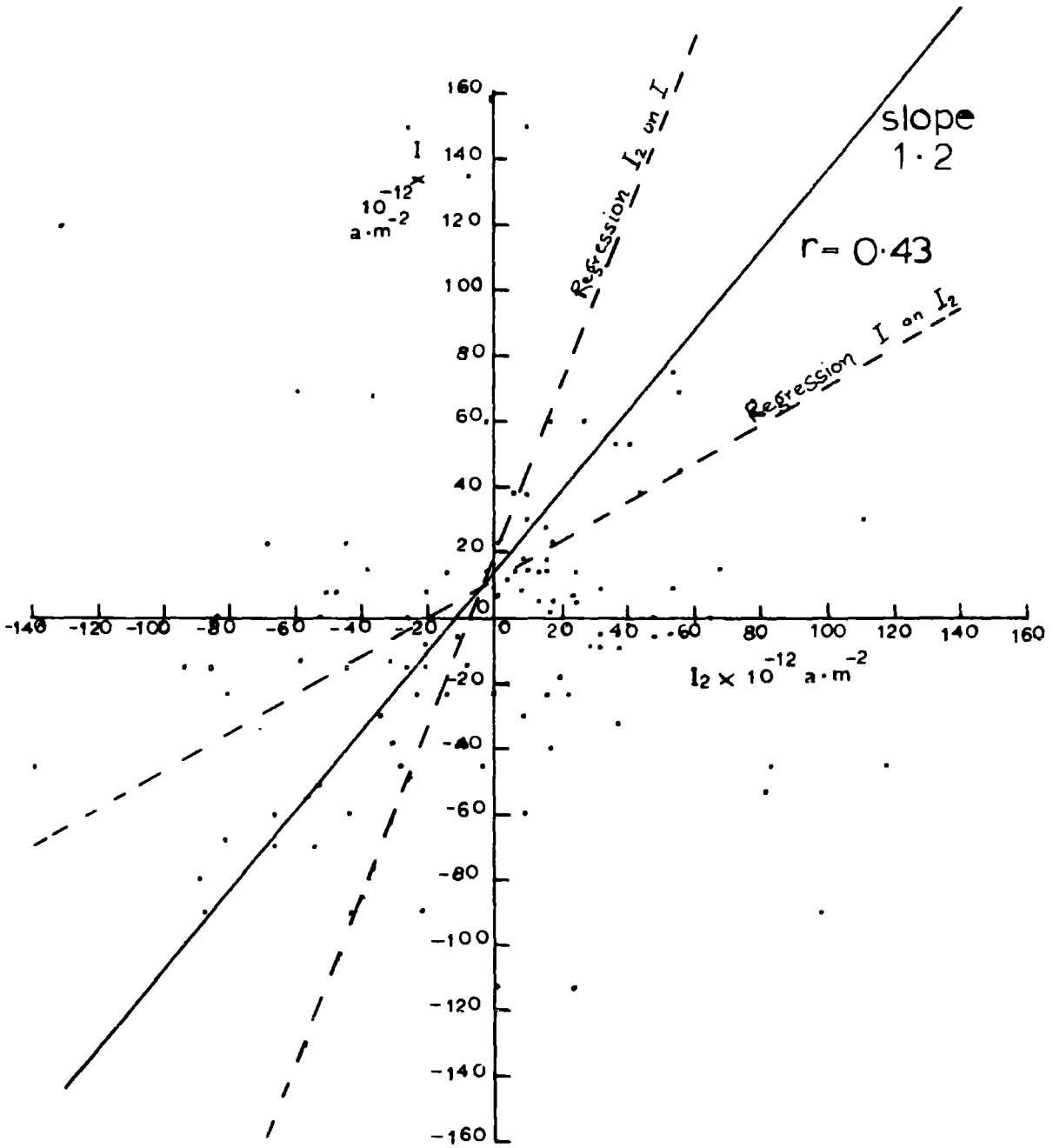

Fig. 34 (a).

Snow currents to two receivers, 900 m. apart:

7 mins. time-lag of I_2 (at top of mast) on I.

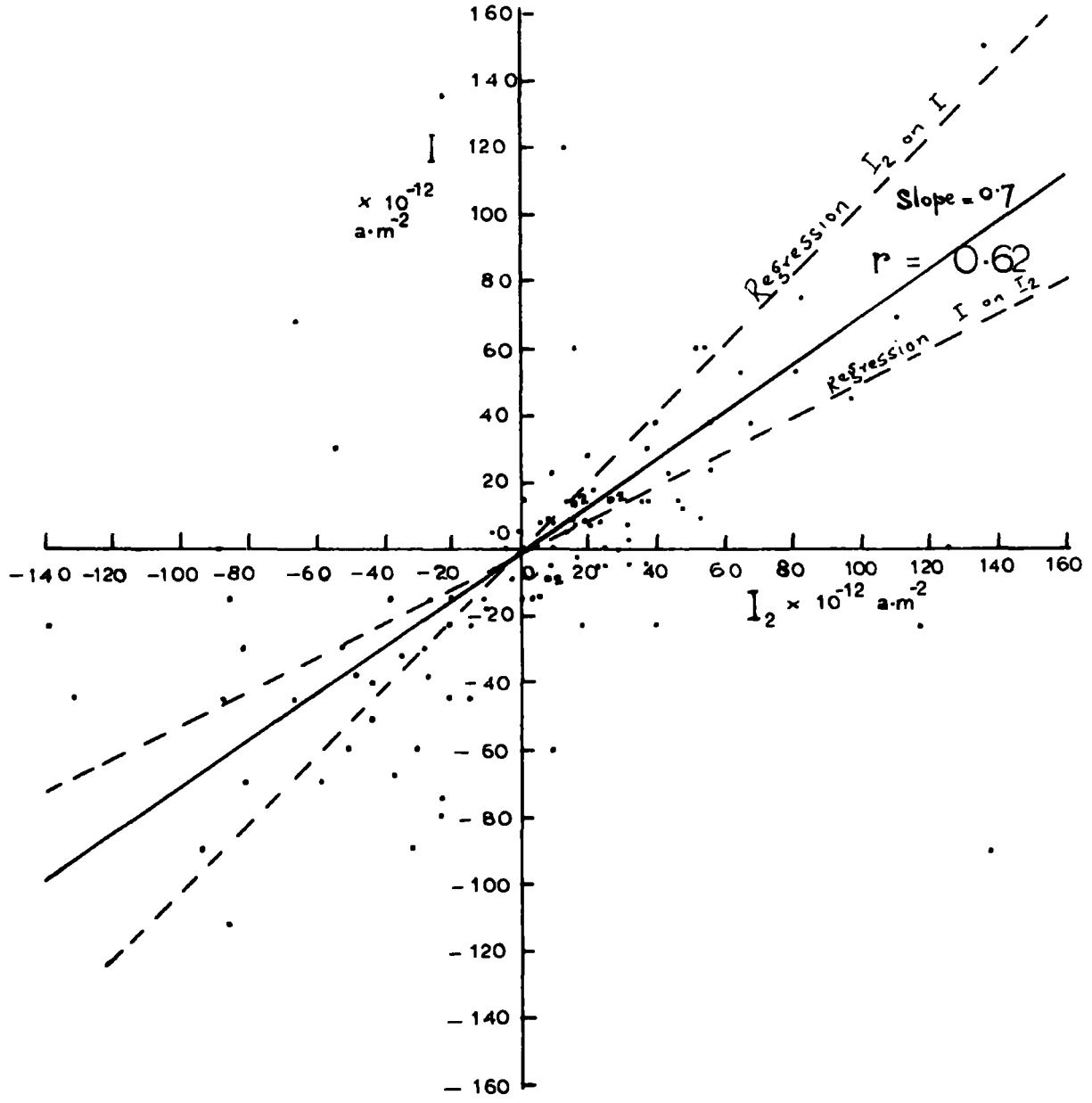

Fig. 34 (b).

19.3.64

I/F Scatter diagram: SNOW

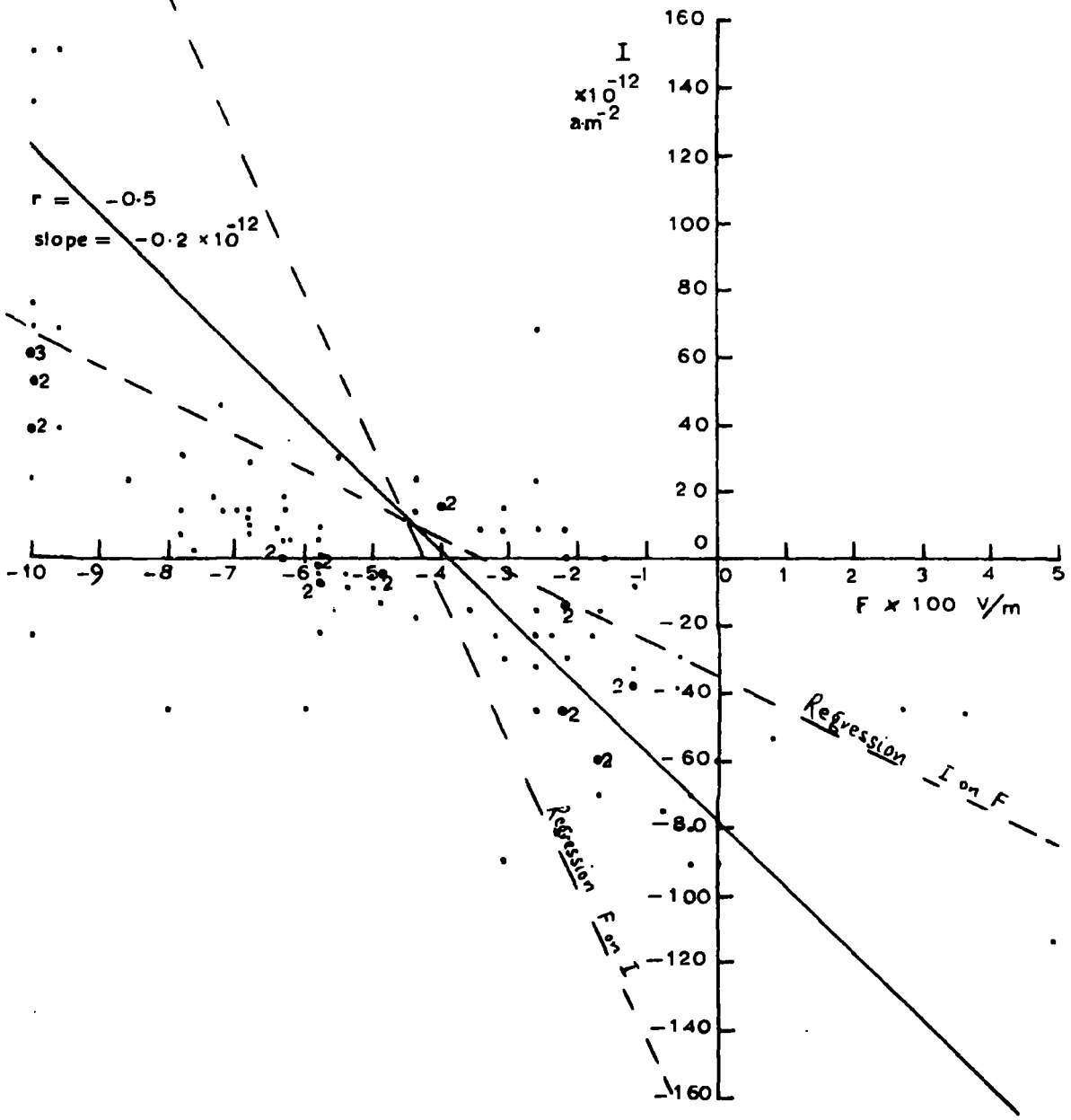

Fig. 35.

Fig. 33 shows the scatter diagram between the currents as measured at the laboratory (I) and at the bottom of the mast (I_1). Figs. (34a & b) were drawn for the instantaneous recordings of the currents (34a) as well as for the incidence of maximum correlation (34b). I_2 was measured on top of the mast.

Fig. 34a gives a poorer correlation than Fig. 34b. The values 0.43 and 0.62 obtained as the correlation coefficients between I and I_2 in Figs. 34a and 34b respectively, are significantly different. If I/F scatter diagram of Fig. 35 gives a correlation coefficient of -0.5 between I and F. It would appear from this scatter diagram that different straight lines would fit the positive current negative potential gradient values (2nd quadrant) and the negative current negative potential gradient (3rd quadrant) values better than the single line used for both quadrants. That is, a 'parabolic' sort of curve would give a better correlation between the two sets of values. This phenomenon was also observed by Ramsay (1959) although his 'parabolic' effect for rain was of opposite sense to this one being found out for snow. For rain, Ramsay found that the points lie above the I/F line for all positive and for high negative potential gradients and below for low negative values. Here, for snow, the points lie below the line for positive current and high negative potential gradient, and above for low negative values.

19.3.64

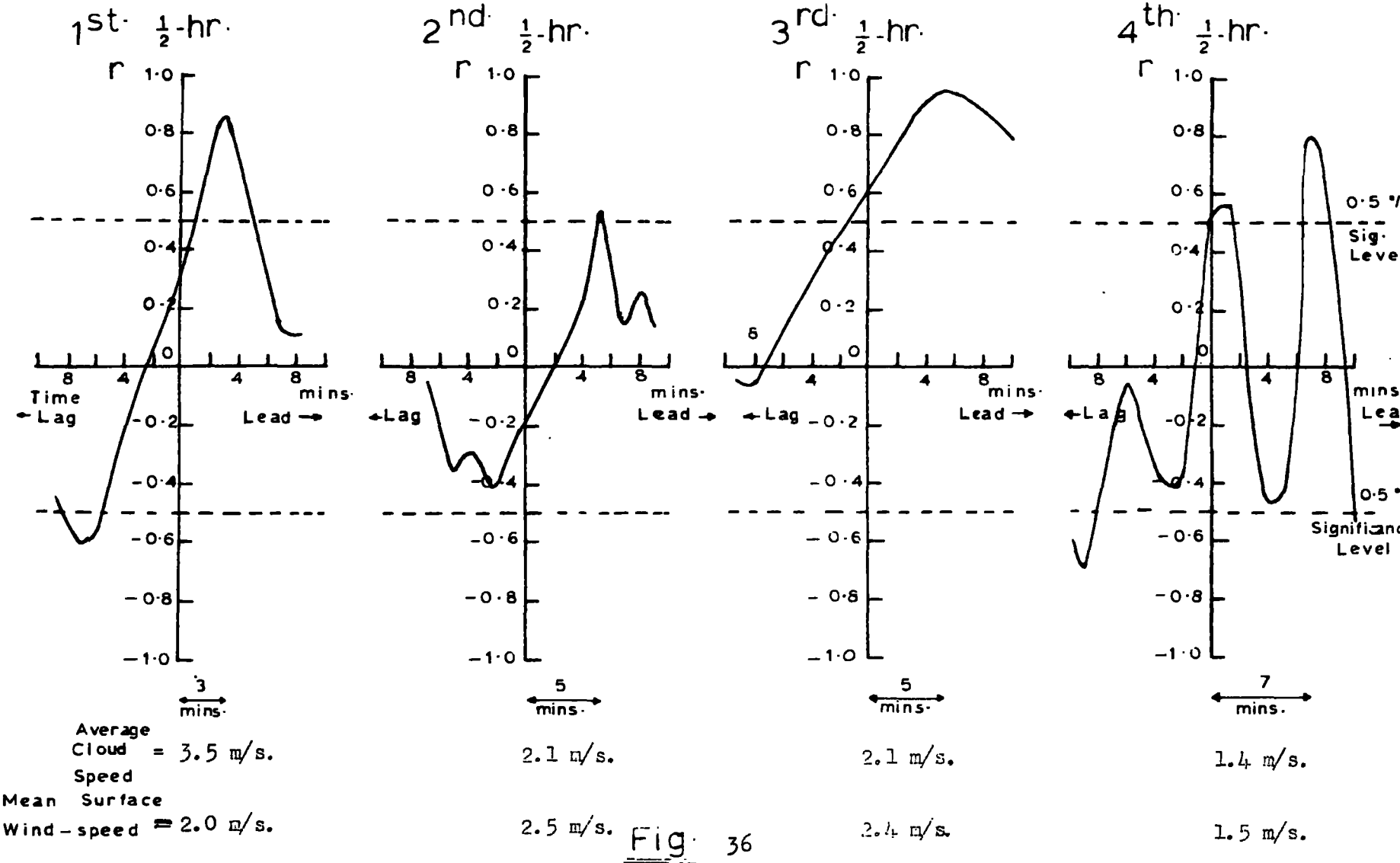

	1st ½-hr.	2nd ½-hr.	3rd ½-hr.	4th ½-hr.
Average Cloud Speed	= 3.5 m/s.	2.1 m/s.	2.1 m/s.	1.4 m/s.
Mean Surface Wind-speed	= 2.0 m/s.	2.5 m/s.	2.4 m/s.	1.5 m/s.

Fig. 36

Figs. 36, 37: Graphs of correlation coefficients between snow currents measured at the Laboratory and Observatory against time-lag (and lead) of the former on the latter.

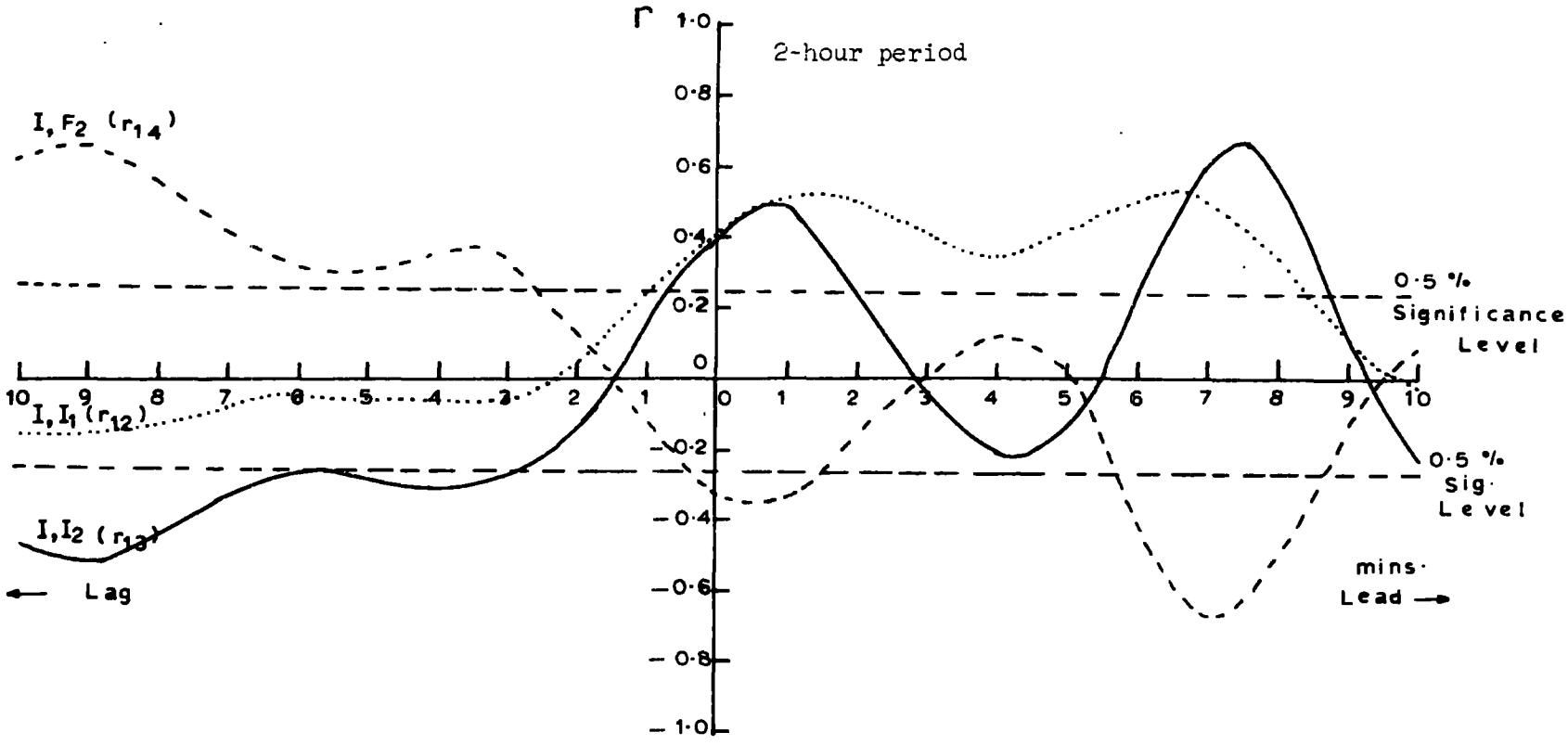

Fig. 37